

Characterization of Retinoic Acid Synthesis and Signalling in Vertebrate Eye Development

by

Caroline Sue Tracy Cheng

A thesis submitted in partial fulfillment of the requirements for
the degree of

Doctor of Philosophy

in

Molecular Biology and Genetics

Department of Biological Sciences

University of Alberta

© Caroline Sue Tracy Cheng, 2016

Abstract

Normal eye development requires a complex series of morphological movements and ocular patterning with aberrant eye development resulting in birth defects and retinal dystrophies. Eleven percent of paediatric blindness is caused by microphthalmia (small eyes), anophthalmia (no eyes) and coloboma (incomplete optic fissure closure), collectively known as MAC. The incidence of eye birth defects is higher in developing nations where vitamin A deficiency is more prevalent. Vitamin A plays an essential role in organ development, including ocular embryogenesis. The biologically active derivative of vitamin A, retinoic acid (RA), is required for proper brain formation and neurogenesis, but its precise role in eye development remains unclear.

Proper eye morphogenesis requires a tight coordination of complex morphogenetic movements and precise spatial and temporal gene expression. Mutations in RA synthesis enzyme, *aldehyde dehydrogenase 1a3 (aldh1a3)*, are associated with human MAC cases. We hypothesize that retinoic acid synthesized in the dorsal and ventral retina is required for proper eye morphology and proper optic fissure closure. To test this hypothesis, we used a combinatorial approach to block RA synthesizing enzymes thereby reducing endogenous levels of RA during embryogenesis. To achieve this, we depleted three RA synthesis enzymes that are expressed within dorsal and/or ventral domains of the retina: *aldehyde dehydrogenase 1a2 (aldh1a2)*, *aldehyde dehydrogenase 1a3 (aldh1a3)* and *cytochrome p450 1b1 (cyp1b1)*. We studied the function of RA using zebrafish, a genetically tractable model vertebrate

whose transparent embryogenesis and external fertilization enables observation of eye development. Our studies revealed that RA is required for the closure of the optic fissure and may be implicated in the regulation of eye size. However, RA signalling is not required for dorsoventral retinal patterning. Interestingly, we observed that RA synthesized within the ventral retina signals within the dorsal retina.

The vertebrate retina is a highly organized and laminar structure, the development of which is conserved among all vertebrates. Differentiation of retinal cell types from retinal progenitor cells is influenced by extrinsic and intrinsic factors. Previous studies have shown that sustained high levels of RA influences retinal cell fate decision. To better understand how RA synthesized in the retina is required for retinal neurogenesis, we used depleted RA synthesis enzymes to reduce endogenous RA levels. We observed a depletion of RA levels results in a reduction of rod photoreceptors. Further, we have obtained preliminary data that suggests that RA levels influence cone photoreceptor fate, biasing towards the differentiation of blue- and ultraviolet (UV)-sensitive cones. Taken together, we observed that RA plays a role both in eye morphogenesis as well as retinal neurogenesis. This analysis is paving the way to understanding how mutations in RA-synthesizing enzymes are causing ocular pathologies.

Preface

This thesis is an original work of Caroline S. T. Cheng. The study, of which this thesis is a part, has received research ethics approval from the University of Alberta Animal Policy and Welfare Committee. The author has met the Canadian Council on Animal Care (CCAC) mandatory training requirements for animal users on the Care and Use of Animals in Research Teaching and Testing.

A portion of Chapter 5 was published:

Laura M. Pillay, Lyndsay G. Selland, Valerie C. Fleisch, Patricia L. A. Leighton, Caroline S. Cheng, Jakub K. Famulski, R. Gary Ritzel, Lindsey D. March, Hao Wang, W. Ted Allison, and Andrew J. Waskiewicz. 2013. Evaluating the mutagenic activity of targeted endonuclease containing a *Sharkey* FokI cleavage domain variant in zebrafish. *Zebrafish*. 10(3):353-364.

Caroline S. Cheng performed experiments, analyzed data, edited manuscript and contributed diagrams. Valerie C. Fleisch generated the *prp2* ZFNs. R. Gary Ritzel generated the *crx* ZFNs. Lyndsay G. Selland is responsible for the construction of *hoxb1b* and *wwtr1* TALENs, and for performing zebrafish mutagenesis using TALENs. The data presented in Table 5.1 results from experiments performed in collaboration with Valerie C. Fleisch and Lindsey D. March. The data presented in Figure 5.3 results from the experiments performed in collaboration with Laura M. Pillay and Jakub K. Famulski. Figure 5.4 results from experiments performed by Laura Pillay and Lyndsay Selland. The data presented in Table 5.4 results from experiments performed by Lyndsay G. Selland. Laura M. Pillay wrote the manuscript. Lyndsay G. Selland, Valerie C. Fleisch, Patricia L.A. Leighton, Laura M. Pillay and Jakub K. Famulski helped to analyze data and edited the manuscript. Andrew J. Waskiewicz and W. Ted Allison were co-supervisory authors, analyzed data and edited this manuscript.

Unless otherwise specified, data presented in this thesis is the author's original work.

Acknowledgements

I would like to express my sincere gratitude to the following people:

To Dr. Andrew Waskiewicz. Thank you for your advice and mentorship that has helped me grow over the years.

To my committee members, Drs. Ted Allison and Heather McDermid for help and advice throughout the years.

To Aleah McCorry and Sophie Koch for fish care. There should be parades for the amount of hard work you both put in to keep the fish facility in running condition.

To past and present lab members for scientific and personal help and support, for general commiseration and for making the lab a friendly and enjoyable place to be.

To all of my dance family for being around for a hug, a dance or an encouraging word. You all did so much to destress me throughout grad school. Every cup of tea, every silly youtube video, every supportive message, every dance did not go unnoticed or unappreciated.

To Darcy. I'm so grateful to have you around. Admittedly, I haven't been a basket of puppies and rainbows in stressful times. I can't begin to describe how thankful I am for your patience, kindness, and love (and the freezer full of mini pizzas).

To my family for their endless love and support. Mom and Dad, you inspired me to keep learning and to dream big. You have taught me to be independent, kind, and generous and you have shown me that any dream worth having is worth 110% of my effort. Sis, you always make time for me and are always there to comfort and encourage me when the stress becomes overwhelming. Words cannot express how grateful I am to you for all of the sacrifices you've made for your support and encouragement is what sustained me through the tough times.

Table of Contents

1	<u>INTRODUCTION</u>	1
1.1	CONGENITAL EYE DISORDERS	2
1.1.1	MORPHOGENETIC DISORDERS – MICROPTHALMIA, ANOPHTHALMIA AND COLOBOMA	3
1.1.2	PHOTORECEPTOR DISEASES – LEBER CONGENITAL AMAUROSIS	4
1.2	ZEBRAFISH AS A MODEL TO STUDY EMBRYONIC EYE DEVELOPMENT	5
1.3	BIOLOGY OF ZEBRAFISH EYE DEVELOPMENT	7
1.3.1	EMBRYONIC EYE MORPHOGENESIS	7
1.3.2	VERTEBRATE DORSAL-VENTRAL RETINAL PATTERNING AND RETINOTECTAL MAPPING	8
1.3.3	NEURAL CREST CELLS IN OCULAR DEVELOPMENT	10
1.3.4	RETINAL NEUROGENESIS AND ORGANIZATION	10
1.3.5	CONE AND ROD PHOTORECEPTOR DEVELOPMENT	12
1.4	VITAMIN A METABOLISM AND RETINOIC ACID SIGNALLING	13
1.4.1	IMPORTANCE OF VITAMIN A IN THE HUMAN EYE	13
1.4.2	ANIMAL MODELS IN VITAMIN A DEFICIENCY	15
1.4.3	RETINOIC ACID SYNTHESIS	16
1.4.3.1	CANONICAL RA SYNTHESIS	17
1.4.3.2	NON-CANONICAL SIGNALLING	18
1.4.4	RA METABOLISM	19
1.4.5	RA GENE REGULATION	20
1.4.6	HUMAN GENETICS OF RETINOIC ACID AND CONGENITAL OCULAR DEFECTS	22
1.5	PURPOSE OF STUDY	24
2	<u>MATERIALS AND METHODS</u>	34
2.1	GENERAL ZEBRAFISH CARE	35
2.1.1	ZEBRAFISH LINES AND MAINTENANCE	35
2.1.2	FIN CLIPPING	37
2.2	EMBRYO MANIPULATION AND CARE	37
2.2.1	MORPHOLINO PREPARATION AND INJECTION	37
2.2.2	MRNA INJECTION	37
2.2.3	EMBRYO FIXATION	38
2.3	PCR AND CLONING	38
2.3.1	ISOLATION OF GENOMIC DNA	38
2.3.2	RNA EXTRACTION	38
2.3.3	ONE STEP REVERSE TRANSCRIPTION-PCR (RT-PCR)	39
2.3.4	POLYMERASE CHAIN REACTION (PCR)	40
2.3.5	TOPO CLONING AND TRANSFORMATION	40
2.3.6	ISOLATING AND PURIFYING LINEAR DNA	41
2.3.7	SEQUENCING	42
2.3.8	IN VITRO MRNA SYNTHESIS	43

2.4	WHOLE MOUNT IN SITU HYBRIDIZATION	44
2.4.1	DIGOXYGENIN-LABELED ANTI-SENSE RNA RIBOPROBE SYNTHESIS	44
2.4.2	WHOLE MOUNT mRNA IN SITU HYBRIDIZATION PROTOCOL (ISH)	44
2.4.3	MOUNTING AND PHOTOGRAPHY	46
2.5	EYE AREA MEASUREMENTS	46
2.6	ZINC FINGER NUCLEASE CONSTRUCTION	47
2.7	TRANSCRIPTION ACTIVATOR-LIKE EFFECTOR NUCLEASE (TALEN) CONSTRUCTION	48
2.7.1	GOLDEN GATE REACTION 1	49
2.7.2	GOLDEN GATE REACTION 2	50
2.8	TARGETED ENDONUCLEASE PROTEIN SYNTHESIS AND <i>IN VITRO</i> DNA CLEAVAGE ASSAY	51
2.9	ZEBRAFISH MUTAGENESIS	52
2.10	HIGH RESOLUTION MELT CURVE ANALYSIS	53
2.11	ANALYSES OF TARGETED ENDONUCLEASE TOXICITY	53
2.12	RNA SEQUENCING	54
2.13	STATISTICAL ANALYSIS	54
3	<u>RETINOIC ACID SYNTHESIS ENZYMES FUNCTION IN EARLY ZEBRAFISH EYE DEVELOPMENT</u>	60
3.1	INTRODUCTION	61
3.2	RESULTS	65
3.2.1	ALDH1A3 MUTANTS ARE STRONG HYPOMORPHS	65
3.2.2	ALDH1A3 MUTANTS HAVE REDUCTION OF RA SIGNALLING IN BOTH DORSAL AND VENTRAL RETINA.	65
3.2.3	ALDH1A3 MUTANTS HAVE NORMAL DORSOVENTRAL RETINAL PATTERNING.	66
3.2.4	ALDH1A3 MUTANTS DO NOT SHOW DETECTABLE DEFECTS IN MIGRATION OF PERIOCCULAR MESENCHYME.....	67
3.2.5	LOSS OF RA SYNTHESIS ENZYMES RESULT IN DECREASED EYE SIZE	67
3.2.6	LOSS OF RA SYNTHESIS ENZYMES ALDH1A3 AND ALDH1A2 RESULTS INCREASED INCIDENCE OF COLOBOMA	68
3.2.7	DEPLETION OF THREE RA SYNTHESIS ENZYMES GREATLY REDUCES RA SIGNALLING IN THE DORSAL AND VENTRAL RETINA	70
3.3	DISCUSSION	71
3.3.1	ALDH1A3 CONTRIBUTES TO RA SIGNALLING IN THE DORSAL AND VENTRAL RETINA.....	71
3.3.2	LOSS OF ALDH1A3 DOES NOT AFFECT DORSOVENTRAL PATTERNING	72
3.3.3	ALDH1A3 MAY NOT HAVE A ROLE IN POM MIGRATION.....	72
3.3.4	RETINOIC ACID PLAYS A ROLE IN REGULATING EYE SIZE.....	73
3.3.5	RA MEDIATES THE CLOSURE OF THE CHOROID FISSURE	74
3.3.6	REDUNDANCY OF RETINOIC ACID SYNTHESIS IN THE EYE	74
4	<u>A ROLE FOR RETINOIC ACID IN PHOTORECEPTOR DEVELOPMENT</u>	

4.1	INTRODUCTION	89
4.2	RESULTS.....	93
4.2.1	RA DEPLETION REDUCES UV- AND BLUE-SENSITIVE CONE PHOTORECEPTOR DIFFERENTIATION	93
4.2.2	RA DEPLETION REDUCES ROD PHOTORECEPTOR DIFFERENTIATION.....	96
4.2.3	RA SIGNALLING MAY ACT UPSTREAM OF FOXN4, A REGULATOR OF AMACRINE CELL FATE	96
4.3	DISCUSSION.....	97
4.3.1	RA IN THE PHOTORECEPTOR DIFFERENTIATION	97
4.3.2	RA AND THE REGULATION OF FOXN4.....	99
5	<u>EVALUATING THE MUTAGENIC ACTIVITY OF TARGETED ENDONUCLEASES CONTAINING A <i>SHARKEY</i> FOKI CLEAVAGE DOMAIN VARIANT IN ZEBRAFISH</u>	<u>117</u>
5.1	INTRODUCTION	118
5.2	RESULTS.....	122
5.2.1	INCREASED EFFICIENCY OF SHARKEY FOKI NUCLEASE-CONTAINING ZFNs IN VITRO.....	122
5.2.2	IN VIVO MUTAGENESIS BY SHARKEY FOKI NUCLEASE-CONTAINING ZFNs	123
5.2.3	TOXICITY OF SHARKEY FOKI NUCLEASE-CONTAINING ZFNs.....	124
5.2.4	CREATION OF BCMO1 AND BCO2A TALENS	124
5.2.5	DECREASED IN VIVO MUTAGENESIS BY SHARKEY FOKI NUCLEASE-CONTAINING TALENS	125
5.3	DISCUSSION.....	126
5.3.1	SHARKEY FOKI NUCLEASE INCREASES ZFN EFFICIENCY IN VITRO AND IN VIVO.....	126
5.3.2	TALENS MAY NOT CAUSE GERMLINE TRANSMITTED MUTATIONS.....	127
5.3.3	SHARKEY FOKI NUCLEASE DOES NOT INCREASE THE EFFICIENCY OF TALENS.....	128
6	<u>CONCLUSIONS AND FUTURE DIRECTIONS</u>	<u>141</u>
6.1	RA IN EYE MORPHOGENESIS	142
6.2	RA AND RETINAL NEUROGENESIS	148
6.3	ANALYSES OF TARGETED ENDONUCLEASES CONTAINING <i>SHARKEY</i> FOKI ...	151
	<u>REFERENCES.....</u>	<u>154</u>
	<u>APPENDIX 1: IDENTIFICATION OF RA-RESPONSIVE GENES IN THE ZEBRAFISH EYE</u>	<u>180</u>
A1.1	INTRODUCTION	181
A1.2	RESULTS AND DISCUSSION.....	181

List of Tables

2.1	Primers used for genotyping carriers of mutant alleles	56
2.2	Translation-blocking morpholino sequences and injected dosage	56
2.3	Primer sequences used for PCR-based RNA riboprobe synthesis	57
2.4	Plasmids used for RNA riboprobe synthesis	58
2.5	ZFN target sequence	58
2.6	Site-directed mutagenesis primers	58
2.7	TALEN target sequence	59
2.8	Primers for HRM analysis	59
3.1	Quantification of total eye area in 4 dpf Aldh1a2 MO injected <i>aldh1a3</i> ^{-/-} mutant embryos	84
3.2	Quantification of total eye area in 4 dpf Aldh1a2 MO and p53 MO injected <i>aldh1a3</i> ^{-/-} mutant embryos	85
3.3	Quantification of incidence of coloboma in 4 dpf Aldh1a2 MO injected <i>aldh1a3</i> ^{-/-} mutant embryos	86
3.4	Quantification of total eye area in 4 dpf Aldh1a2 MO and p53 MO injected <i>aldh1a3</i> ^{-/-} mutant embryos	87
5.1	Analyses of target-site specific mutations present in zebrafish embryos injected with control or <i>Sharkey</i> zinc finger nuclease (ZFN) mRNAs	137
5.2	Analyses of target-site specific mutations present in zebrafish embryos injected with <i>bcmo1</i> or <i>bco2a</i> transcription activator-like effector nuclease (TALEN) mRNAs	138
5.3	Analyses of target-site specific mutations present in progeny of P0 adults that had been injected with <i>bcmo1</i> or <i>bco2a</i> transcription activator-like effector nuclease (TALEN) mRNAs	139
5.4	Analyses of target-site specific mutations present in zebrafish embryos injected with control or <i>Sharkey</i> transcription activator-like effector nuclease (TALEN) mRNAs	140
A1.1	RNA-seq analysis of gene expression in zebrafish embryo heads at 48hpf	185
A1.2	Differential expression of eye, photoreceptor and extraocular tissues genes in dissected heads of <i>aldh1a3</i> ^{-/-} ; <i>cyp1b1</i> ^{-/-} zebrafish embryos at 48 hpf	186

List of Figures

1.1	Vertebrate eye morphogenesis	29
1.2	Sequences of eye development in zebrafish	30
1.3	The organized laminar structure of the vertebrate retina	31
1.4	Retinoic acid synthesis and signalling pathway	32
2.1	Diagrams of transgenes and mutations in zebrafish lines used	55
3.1	Expression of <i>aldh1a3</i> is reduced in <i>aldh1a3</i> mutants	76
3.2	<i>aldh1a3</i> mutant embryos exhibit reduced RA signalling	77
3.3	<i>aldh1a3</i> ^{-/-} mutants do not display overt defects in dorsoventral patterning	78
3.4	POM migration is not obviously affected in <i>aldh1a3</i> mutants	79
3.5	Total eye area is reduced in <i>Aldh1a2</i> ; <i>aldh1a3</i> morphomutants	80
3.6	Knockdown of RA synthesis enzymes delays choroid fissure closure	81
3.7	RA signalling is greatly reduced in <i>Aldh1a2</i> ; <i>aldh1a3</i> ^{-/-} ; <i>cyp1b1</i> ^{-/-} morphomutants	82
4.1	Loss of RA synthesis genes results in gaps of UV-sensitive photoreceptors	100
4.2	Diagram of box and whisker plot	102
4.3	Frequency and severity of gaps in <i>opn1sw1</i> expression increases with decrease in RA synthesis genes	103
4.4	Loss of RA synthesis genes results in gaps of blue-sensitive photoreceptors	105
4.5	Frequency and severity of gaps in <i>opn1sw2</i> expression increases with decrease in RA synthesis genes	107
4.6	Loss of RA synthesis genes does not strongly alter green-sensitive photoreceptor distribution	109
4.7	Frequency and severity of gaps in <i>opn1mw1</i> expression in unchanged with decrease in RA synthesis genes	111
4.8	Loss of RA synthesis genes reduces rhodopsin expression	113
4.9	Loss of RA synthesis genes results in the upregulation and expansion of <i>foxn4</i> expression	115
5.1	Zinc finger nuclease (ZFN) structure and target site recognition	129
5.2	Transcription Activator-Like Effector Nuclease (TALEN) structure and target-site recognition	130
5.3	<i>In vitro</i> comparison of target-site specific DNA cleavage activity between control and <i>Sharkey</i> ZFNs	131
5.4	Effects of injecting control and <i>Sharkey</i> zinc finger nuclease mRNA on embryonic morphology and mortality	132
5.5	The <i>bcmo1</i> TALEN binds DNA in coding sequence of the gene	133
5.6	The <i>bco2a</i> TALEN binds DNA in coding sequence of the gene	134
5.7	Comparison of control and <i>Sharkey</i> <i>wwtr1</i> TALENs	135

List of Common Abbreviations

°C	degrees Celsius
ANOVA	analysis of variance
BCIP	5-bromo-4-chloro-3-indolyl-phosphate
bp	basepair
BSA	bovine serum albumin
CAP	cleaved amplified polymorphism
cDNA	complementary deoxyribonucleic acid
CRISPR	clustered randomly interspersed short palindromic repeats
DAVID	Database for Annotation, Visualization and Integrated Discovery
DEAB	diethylaminobenzaldehyde
DEPC	diethylpyrocarbonate
DIG	digoxigenin
DMSO	dimethyl sulfoxide
DNA	deoxyribonucleic acid
DNase	deoxyribonuclease
dNTP	deoxyribonucleotide triphosphate
dpf	days post-fertilization
DTT	dithiothreitol
E	embryonic stage
EDTA	ethylenediaminetetraacetic acid
EM	embryo media
FRET	fluorescence resonance energy transfer
GCL	ganglion cell layer
GEPRA	genetically encoded probes of RA
gfp	green fluorescent protein
HEPES	4-(2-hydroxyethyl) piperazine-1-ethanesulfonic acid
hpf	hours post-fertilization
HRM	high resolution melt curve
hyb	hybridization solution

INL	inner nuclear layer
IPL	inner plexiform layer
IPTG	isopropyl β -D-1-thiogalactopyranoside
LB	Luria broth
LCA	Leber's Congenital Amaurosis
MAC	Microphthalmia, Anophthalmia, Coloboma
mL	milliliter
mM	millimolar
MO	morpholino oligonucleotide
mRNA	messenger ribonucleic acid
MS222	tricaine methanesulfonate
NBT	4-nitro blue tetrazolium chloride
ng	nanogram
NHEJ	non-homologous end-joining
ONL	outer nuclear layer
OPL	outer plexiform layer
PBS	phosphate buffered saline
PBST	phosphate buffered saline with tween20
PCR	polymerase chain reaction
PFA	paraformaldehyde
pg	picogram
POM	periocular mesenchyme
PTU	1-phenyl-2-thiourea
RA	retinoic acid
RGC	retinal ganglion cells
RNA	ribonucleic acid
RNA-seq	ribonucleic acid sequencing
RNAi	ribonucleic acid interference
RPC	retinal progenitor cell
RPE	retinal pigmented epithelium

RT-PCR	reverse transcription – polymerase chain reaction
RVD	repeat variable diresidue
SOC	super optimal broth
SSC	saline sodium citrate buffer
TALEN	transcription activator-like effector nucleases
UV	ultraviolet
VAD	vitamin A deficiency
X-gal	5-bromo-4-chloro-3-indolyl- β -D-galactopyranoside
ZFN	zinc finger nucleases
μg	microgram
μL	microliter
μM	micromolar

List of Common Gene and Protein Abbreviations

ADH	alcohol dehydrogenases
<i>aldh1a</i>	aldehyde dehydrogenase 1 family, member A
<i>bcmo1</i>	beta-carotene 15'15' monooxygenase
<i>bco2a</i>	beta-carotene 9'10' dioxygenase 2a
BMP	bone morphogenetic protein
CRABP	cellular retinoic acid binding protein
CRBP	cellular retinol binding protein
<i>crx</i>	cone-rod homeobox
<i>cyp1b1</i>	cytochrome p450 family 1, subfamily b, member1
<i>dkk2</i>	Dickkopf-related protein 2
<i>ef1a</i>	Eukaryotic translation elongation factor alpha 1a
Eph	Eph receptors – receptor tyrosine kinases
<i>eya2</i>	eyes absent 2
FGF	fibroblast growth factor
<i>foxn4</i>	forkhead box n4
GDF	growth and differentiation factor
<i>hoxb1b</i>	homeobox B1b
<i>meis1</i>	myeloid ecotropic integration site 1
<i>nr2e3</i>	nuclear receptor subfamily 2 Group E, Member 3 E
<i>nrl</i>	neural retinal leucine zipper
<i>opn1mw1</i>	opsin 1 medium-wave-sensitive 1
<i>opn1sw1</i>	opsin 1 short-wave-sensitive 1
<i>opn1sw2</i>	opsin 1 short-wave-sensitive 2
<i>p53</i>	tumor protein p53
<i>pitx2</i>	paired-like homeodomain 2
<i>prp2</i>	prion protein 2
RALDH	retinaldehyde dehydrogenase
RAR	retinoic acid receptor
RARE	retinoic acid response element

RBP4	retinol binding protein 4
RDH	retinol dehydrogenase
<i>rho</i>	rhodopsin
RXR	retinoid X receptor
SHH	sonic hedgehog
STRA6	stimulated by retinoic acid 6
<i>tbx</i>	T-box transcription factor
<i>vax2</i>	ventral homeobox2
WNT	wingless-type MMTV integration site family
<i>wwtr1/taz</i>	WW domain containing transcription regulator 1

1 Introduction

1.1 Congenital Eye Disorders

Embryonic eye development is composed of a series of complex processes that require tissue induction, cell proliferation and cell differentiation to form mature tissue. Embryonic eye development is highly conserved among most classes of vertebrates. Vertebrate eye formation begins with bilateral evagination of optic vesicles from diencephalon neuroectoderm (Adler and Canto-Soler, 2007; Chow and Lang, 2001). Each optic vesicle undergoes a series of morphogenetic movements that results in the formation of a bilayered optic cup, containing the respective neural retina and retinal pigmented epithelium (RPE) (Figure 1.1) (Chang et al., 2006a). As the optic cup forms, a transient opening forms on the ventral retina called the choroid, or optic, fissure. This fissure allows for the entrance and exit of ocular vasculature and the exit of retinal axons from the eye to the brain (Fitzpatrick and van Heyningen, 2005). Proper fissure closure requires a series of precisely coordinated events to occur. First, the tissue within the optic cup and cells within the POM must proliferate. When the lobes of the choroid fissure are in apposition, the basement membrane of the retina, composed of a variety of adhesive extracellular matrix glycoproteins, including laminin must dissolve to allow for the tissue to fuse (Lee and Gross, 2007). After optic cup morphogenesis, the pool of multi-potent progenitor cells within the retina must differentiate to form a highly organized, laminar structure consisting of seven cell types. Precise coordination of morphological movements and spatial and temporal gene expression is required to properly shape the eye. Aberrant morphological movements or misexpression of these genes often result in a spectrum of disorders. These conditions are highly debilitating, often leading to partial or complete vision loss. An understanding of the biological processes underlying genetic causes of eye defects is essential to understand and these conditions.

1.1.1 Morphogenetic disorders – Microphthalmia, Anophthalmia and Coloboma

During the commencement of eye development, ocular tissue is being specified and major structures of the eye are formed. Disruptions of cellular movements or gene expression associated with these developmental stages result in severe structural defects that often involve multiple ocular tissues, including the lens, retina and the iris. A spectrum of often co-occurring conditions, Microphthalmia, Anophthalmia, Coloboma (MAC) account for a 11 to 20% of childhood blindness (Bermejo and Martinez-Frias, 1998). The overall incidence of MAC has been estimated as 6 – 13 per 100,000 live births (Skalicky et al., 2013; Williamson and FitzPatrick, 2014). Anophthalmia is estimated to occur in 0.6-4.2 per 100,000 live births and microphthalmia and coloboma are reported to occur in 2 – 17 and 2 – 14 per 100,000 live births, respectively.

Coloboma (pl. colobomata) is an eye abnormality that occurs bilaterally or unilaterally and accounts for 3.2 – 11.2% of blindness in children (Onwochei et al., 2000). Coloboma may occur independently or as a phenotypic manifestation of more than 50 human genetic disorders (Online Mendelian Inheritance in Man, 2015). This defect results in a cleft or gap in one or several parts of the eye (Chang et al., 2006b; Fitzpatrick and van Heyningen, 2005; Gregory-Evans et al., 2004). These clefts or gaps represent absent tissue in structures of the eye including the iris, the retina, eye vasculature, and/or the optic nerves. There is a transient opening called the choroid fissure within the ventral retina that relies on morphological movements to close. The closure of the choroid fissure requires precise interactions of growth, morphogenesis and regulated gene expression. Failure of fusion of the choroid fissure is among the most common causes of coloboma and results in the loss of ventral retina. The severity of colobomata can vary from cosmetic defects to vision loss. This vision loss as a result of coloboma ranges from partial loss in portions of the visual field to low vision or total blindness. Choroid fissure closure requires a

complex interplay of developmental events. Several signalling pathways have been implicated in the incidence of coloboma including bone morphogenetic protein (BMP), fibroblast growth factor (FGF) and Wingless-type MMTV integration site family (WNT) (Cai et al., 2013; Morcillo et al., 2006; Verma and Fitzpatrick, 2007; Zhou et al., 2008). Fully understanding the interaction of morphological movements and signalling pathways within the retina can further elucidate the underlying causative mechanisms for coloboma.

Microphthalmia is characterized by small eye whereas anophthalmia is characterized as a lack of ocular tissue resulting in the absence of eyes (Gerth-Kahlert et al., 2013). Microphthalmia and anophthalmia result from aberrations in multiple steps of embryonic eye morphogenesis, for example, eye field specification or optic cup evagination. Defects in these stages often result in the most severe phenotypes, and typically results in anophthalmia. When aberrations occur in later stages of eye development when the optic vesicles have been specified, less severe eye defects of remaining eye tissue are observed. Aberrant steps of later eye development can range from altered dorsoventral patterning, reduction of retinal progenitor cells, increased apoptosis and decreased proliferation (Asai-Coakwell et al., 2013; French et al., 2009). MAC phenotypes have a large genetic component and thus, knowledge of the gene expression and morphological movements will provide insight into the underlying developmental aetiology.

1.1.2 Photoreceptor Diseases – Leber congenital amaurosis

Photoreceptors are specialized cells within the retina that are required to detect light and convey visual signal to the brain. Photoreceptors have high metabolic demands, complex polarized morphology and they rely on support cells for normal function and survival. Therefore, their health is especially sensitive to genetic and environmental perturbations (Brzezinski and Reh, 2015). Several human diseases affect photoreceptors either directly or by altering support cells. Leber congenital amaurosis (LCA) is the most severe

form of inherited retinal diseases that cause childhood blindness (Perrault et al., 1999). LCA is the earliest occurring dystrophy, representing 20% of children with visual impairment and almost 5% of all retinal dystrophies (Koenekoop et al., 2007). LCA is commonly inherited in an autosomal recessive manner and presents around 6 weeks of age. This retinal dystrophy manifests as severe visual impairment in infancy and can be accompanied by other vision problems including photophobia (increased sensitivity to light), and nystagmus (involuntary eye movement) (Chung and Traboulsi, 2009; den Hollander et al., 2008). There are three possible mechanisms that are thought to cause LCA: degeneration of photoreceptor layer, inner retinal layer and the retinal pigmented epithelium (RPE), as characterized by extensive atrophy, dropout and gliosis; aplasia of the retina, based on the absence of the photoreceptor layer; and biochemical dysfunction, as structures of entire retina are intact despite blindness of individual (Koenekoop et al., 2007). Up to 70% of LCA cases result from mutations in a cohort of 14 genes, all of which are necessary for normal vision. The functions of these genes include roles in embryonic retinal development, protein trafficking, outer segment phagocytosis, and ciliary function. Notably, mutations in genes that encode for enzymes required for vitamin A metabolism are implicated in causing LCA, suggesting that signalling pathway involving Vitamin A's biologically active derivative, retinoic acid, plays a role in photoreceptor development function (Asai-Coakwell et al., 2013; Cremers et al., 2002; den Hollander et al., 2008).

1.2 Zebrafish as a model to study embryonic eye development

Eye development and retinal structure are highly conserved among all vertebrates. These processes have been studied in multiple animal models including mice, rats, chick, *Xenopus*, and zebrafish. Mammalian models, such as mouse, are considered preeminent in modeling human diseases, primarily due to the homology among mammalian genomes and similarities in anatomy, cell biology, and physiology. However, zebrafish has emerged as a mainstream

model organism in which to study embryonic eye development. High fecundity rates and short generation times allows zebrafish to be a genetically tractable vertebrate model. Forward genetic screens have enabled the isolation of thousands of mutations affecting hundreds of loci essential to development of the vertebrate embryo, including the eye and visual system. Novel genes and novel gene functions can be uncovered through these genetic screens. Molecular pathways of many developmental genes are conserved among vertebrates and clear orthologs exist between zebrafish and humans. External development and optical transparency during zebrafish embryogenesis allows for the visual analysis of morphogenetic movements and organogenesis. In addition, the zebrafish genome has been sequenced and is well annotated. These characteristics facilitate the use of many gene expression analysis techniques. These techniques include *in situ* hybridization to analyse gene expression in whole embryos. Use of transgenic strains allow for the visualization of ocular development *in vivo* and in real-time. Zebrafish allows for the functional examination of genes in the formation of the eye and the differentiation of retinal progenitor cells.

Zebrafish eye development begins within the first 24 hours post-fertilization (hpf) and differentiation of the neural retinal occurs by 3 days post-fertilization (dpf). Murine models have been commonly used to study embryonic eye development. However these studies may not model human ocular conditions as mice are nocturnal and have limited photoreceptor diversity. Unlike rodent models, zebrafish are diurnal and its retina contains diverse cone subtypes in addition to rods (Schmitt and Dowling, 1996). Taken together, zebrafish serve as an excellent model organism for studying human eye conditions.

1.3 Biology of zebrafish eye development

1.3.1 Embryonic Eye Morphogenesis

Development of the zebrafish eye begins in the diencephalon shortly after gastrulation at approximately 10 hpf with the specification of the eye field (Figure 1.1, Figure 1.2) (Varga et al., 1999; Woo and Fraser, 1995). After the specification of this field, the tissue forms as a flat structure and extends laterally to form an optic lobe at 11.5 hpf. (Schmitt and Dowling, 1994, 1999). At 13 hpf, the posterior part of the optic lobe separates from the brain. The anterior portion remains attached to the brain and will eventually become the optic stalk. Rotation and invagination of the optic vesicle eventually form a bilayered optic cup, a process that begins at 15 hpf and continues to 36 hpf (Schmitt and Dowling, 1994). The outer and inner layers of the optic cup are fated to become the RPE and the neural retina, respectively, and these layers become morphologically distinct at 18 hpf (Li et al., 2000). The choroid fissure forms in the rim of the optic cup next to the optic stalk. This transient fissure allows the entry of retinal vasculature into and axonal exit from the retina (Barishak, 1992; Harada et al., 2007; Li et al., 2000).

Following morphogenetic transformations that shape and orient the optic cup, the immature retina is a relatively homogeneous, single-layered sheet of neuroepithelial cells. It must then develop into a complex layered structure of neurons with multiple different cell types. The highly conserved vertebrate retina contains six neuronal and one glial cell types (Figure 1.3). These cells are organized into three nuclear layers (the ganglion cell layer [GCL]; the inner nuclear layer [INL] composed of amacrine, horizontal, bipolar and Muller glia cells; and the outer nuclear layer [ONL] composed of photoreceptors) and two synaptic layers (the outer plexiform layer [OPL] and the inner plexiform layer [IPL]). Retinal neurogenesis follows a common pattern in vertebrates with the cell classes of the vertebrate retina generated sequentially (Hu and Easter, 1999). In zebrafish, this sequence generates cells

layer by layer with ganglion cells as the first neurons to be generated, followed by cells of the inner nuclear layer and lastly, photoreceptors (Hu and Easter, 1999).

1.3.2 Vertebrate Dorsal-Ventral Retinal Patterning and Retinotectal Mapping

Vision is reliant not only on precise morphogenesis and growth of ocular tissue, but on the proper synthesis of visual stimuli into a single coherent image. The precise spatial organization of the retinal ganglion cells (RGCs) in the retina must be maintained as their axons innervate the visual processing center within the brain, known in zebrafish as the optic tectum. The topographical organization of RGCs from the retina to the tectum is termed retinotectal mapping. The retina is subdivided into four regions (dorsal, ventral, nasal and temporal), each of which expresses retinal patterning genes demarcating its boundaries. The optic tectum is similarly partitioned into anterior, posterior, lateral and medial quadrants. Retinal ganglion cells within a specific quadrant in the eye must project their axons to the corresponding target within the tectum. For example, axons from RGCs within the dorsal retina project to the lateral tectum, while axons from the ventral retina map to the medial tectum (Lemke and Reber, 2005). The projection of RGC axons in an organized topographic manner requires patterning of the axes of the retina as well as spatial restriction of Eph receptors – receptor tyrosine kinases (Eph) and Ephrin guidance molecules in the retina and the tectum (Lemke and Reber, 2005). Taken together, proper vision requires proper dorsoventral patterning of the retina as well as the proper expression of Eph and Ephrins within the retina and the optic tectum.

To ensure the precise projection from RGCs to their positional target in the tectum, the retina must be precisely patterned along this axis. In zebrafish, dorsoventral axis specification occurs between 12 and 15 hpf (Figure 1.1). *Bone morphogenetic proteins 2 and 4 (BMP2 and 4)*, and *growth and differentiation factor 6a (Gdf6a)* are required to initiate dorsal eye patterning.

The ventral retina requires sonic hedgehog for cellular identity and retinoic acid (RA) for tissue morphogenesis (Ekker et al., 1995; Marsh-Armstrong et al., 1994). The expression and spatial restriction of *tbx5a* and *vax2* in the dorsal and ventral retina are necessary for retinotectal mapping, such that misexpression of *tbx5a* and *vax2* result in misprojection of RGC axons (Barbieri et al., 2002; Koshiba-Takeuchi et al., 2000). The dorsal and ventral expression patterns that restrict respective domain identity are antagonistic to each other through regulation of genes upstream of *Tbx5a* and *Vax2*. Overexpression of dorsally restricted BMP ligands results in a dorsalized eye as visualized by an expansion of dorsal eye identity via *tbx5a* expression, and a corresponding reduction of ventrally expressed *vax2* (Koshiba-Takeuchi et al., 2000). Expansion of the dorsal retinal identity has been similarly observed through overexpression of ventral-specific *gdf6a*. The correct restriction of dorsal and ventral domains of the retina is essential for proper retinotectal mapping.

In addition to patterning of the dorsoventral axes, positional identity and directed axon migration of RGCs occur through gradients of Eph and Ephrin guidance molecules. These molecules promote either attractive or repulsive cues between migrating RGC axons and the surrounding tissue (Lemke and Reber, 2005). EphrinB ligands and EphB receptors are expressed in opposing gradients in the tectum and the retina: EphB receptors are highest in the lateral tectum and ventral retina whereas expression of *ephrinB* is highest in the medial tectum and the dorsal retina. Ligand-receptor interactions from the dorsal or ventral retina to their corresponding regions in the tectum are attractive. Therefore *eph*-expressing RGC axons originating from the ventral retina are attracted to the *ephrin*-expressing medial tectum and *ephrinB*-expressing RGC axons from the dorsal retina are attracted to the *ephB*-expressing lateral tectum (Lemke and Reber, 2005). The same genes that are involved in early eye development and eye patterning have a role in eye

morphogenesis. However, it is not entirely understood if or how alterations in eye patterning can lead to ocular defects.

1.3.3 Neural Crest Cells in Ocular Development

In addition to ocular tissues, extraocular cells play essential roles in eye development. One such population of cells is derived from lateral plate mesoderm and neural crest. These cells, termed periocular mesenchyme (POM) give rise to multiple cell lineages required for normal ocular development. POM-derived ocular structures include the ciliary muscle, the sclera, choroidal pericytes, the stroma of the cornea and the iris and ocular blood vessels (Gage et al., 2005). Regulation of POM cell migration is essential to ensure the proper number of cells form ocular structures. The retina plays an essential role in directing migration of the POM. Signals from the retina, including retinoic acid (RA), regulate expression of POM genes (Langenberg et al., 2008; Matt et al., 2008; Molotkov et al., 2006). Not much is known about POM in zebrafish, but studies from other species suggest that that POM also plays roles in early morphogenesis of the optic cup and differentiation of the retina (Fuhrmann et al., 2000; Lupo et al., 2005; Matt et al., 2005; Matt et al., 2008; McMahan et al., 2009; Molotkov et al., 2006). Disruption of mouse RA signalling in POM is sufficient to alter eye morphogenesis and gives rise to coloboma (Matt et al., 2008; McMahan et al., 2009; Molotkov et al., 2006). These studies suggest that complex actions between POM cells and retina are required for normal morphogenesis.

1.3.4 Retinal Neurogenesis and Organization

Prior to neurogenesis, the immature retina consists of a pool of multipotent proliferating retinal progenitor cells that form the neuroepithelium lining of the ventricular zone of the optic vesicles. During neurogenesis, RPCs exit mitosis and are gradually specified into lineage-restricted precursor cells that mature into differentiated neurons or Muller glia. Postmitotic cells then migrate towards one of the three cells layers within the retina. In all

vertebrates analyzed, the generation of retinal cell types follows a stereotypical birth order (Cepko et al., 1996; Livesey and Cepko, 2001). In zebrafish, RGCs are first to exit the cell cycle between 24 – 36 hpf. Interneurons that compose the INL exit the cell cycle between 36 – 48 hpf, followed by the cone photoreceptors exiting from 48 – 72 hpf (Figure 1.2). Each layer of the developing zebrafish retina neurogenesis takes place asynchronously. Fan-shaped waves of neurogenesis begin in a ventral patch near the choroid fissure and spread sequentially to the nasal, dorsal and finally the temporal retina (Raymond and Jackson, 1995; Schmitt and Dowling, 1996; Stenkamp et al., 1996). Rods are slower to mature and their neurogenesis follows a similar pattern of differentiation. Early-forming rods differentiate in a ventronasal patch but the developmental gradient is a more generalized from ventral to dorsal instead of the fan-shaped pattern observed with the other cell types (Fadool, 2003; Stenkamp, 2007).

The organized neuronal architecture of the retina is highly conserved among vertebrates. The neural and glial cell types have migrated into three nuclear layers and two synaptic layers which function together to relay visual information to the brain (Figure 1.3). The photoreceptors, subdivided into rods and cones constitute the ONL where they convert incoming photons into an electrical signal. Upon photoactivation, photoreceptor cells transmit this signal to bipolar cells within the INL, which in turn relay the signal to RGCs located in the ganglion cell layer (GCL) (Luo et al., 2008). The axons of the RGC are the only neurons that exit the retina. Their projections are bundled into the optic nerve to carry the visual information from the eye and innervate the visual processing center of the brain, the optic tectum. Both cell types within the INL integrate and refine visual output from the retina. Horizontal and amacrine cells initiate sidewise interaction in the respective plexiform layer that they are facing (Lagnado, 1998). Horizontal cells face the outer plexiform layer, contacting photoreceptor cells and are responsible for enhancing contrast. Amacrine cells face the inner plexiform layer and contact the GCL

(Centanin and Wittbrodt, 2014). In addition to detecting change in illumination, amacrine cells process movement and direction of light on the retina (Lagnado, 1998). The proper differentiation and lamination of the retina during neurogenesis is crucial for the detection of visual stimuli by the eye and transmission of these signals to the brain.

1.3.5 Cone and Rod Photoreceptor Development

Within the neural retina, photoreceptors carry out phototransduction, a series of signal amplifications that enable photons of light to be detected by the brain. Vertebrates have two classes of photoreceptors: rods and cones. Rod photoreceptors are highly light sensitive and do not discern spectral information. These characteristics allow the rod photoreceptors to be excellent for dim light vision (Luo et al., 2008). Cone photoreceptors function optimally in bright light and are responsible for colour vision. Each class of photoreceptor contains a distinct photopigment called opsin that has sensitivity to different regions of the visible light spectrum. Rods have one photopigment, rhodopsin. Humans and diurnal primates typically possess trichromatic colour vision, mediated by three opsins with different spectral sensitivities. S-opsin is short-wave sensitive and absorbs blue light; M-opsin is medium-wave sensitive and absorbs green light; and L-opsin is long-wave sensitive and absorbs red light (Nathans, 1999). Most mammalian species only have dichromatic vision, resolved by S- and M- opsins (Swaroop et al., 2010). Zebrafish are tetrachromads due to the presence of a fourth opsin with peak sensitivity to ultraviolet (UV) wavelengths (Robinson et al., 1993).

A derivative of vitamin A also has critical roles in phototransduction. Opsins bind to the chromophore 11-*cis*-retinaldehyde in rods where 11-*cis*-retinaldehyde isomerizes to its all-*trans*-isomer following interaction with a light photon. The conformational change of retinaldehyde initiates the visual phototransduction cascade by which light is converted to electrical impulses (Baehr et al., 2003). Following photon absorption, all-*trans*-retinaldehyde is

transported to the RPE to be re-isomerized to 11-*cis*-retinaldehyde. Within the RPE cell, all-*trans*-retinaldehyde is isomerized and oxidated into 11-*cis*-retinaldehyde. The newly converted 11-*cis*-retinaldehyde is transported to the photoreceptors where it can serve its function to initiate the phototransduction cascade (Strauss, 2005). As retinal plays an essential role in phototransduction within dim-light responsive rods, vitamin A deficiency often manifests as night blindness (Cai et al., 2009; Dowling and Wald, 1958).

The development of retinal cells, including photoreceptors, is controlled by a variety of secreted signalling factors. Intrinsic and extrinsic factors can influence photoreceptor fate decisions as they differentiate from photoreceptor progenitors. Several extrinsic factors have important functions in regulating retinal neurogenesis. These include fibroblast growth factors (FGFs), hedgehog signalling proteins (Hh), Wnts, RA, and thyroid hormone (Guillemot and Cepko, 1992; Kelley et al., 1994; Zhang and Yang, 2001). Current studies endeavour to identify additional signals and reveal the molecular mechanisms of cone mosaic formation. Although rods and cones arise from different cell lineages, their precursor cells express photoreceptor-specific transcription factors. Several photoreceptor-specific transcription factors, including *t-box transcription factor 2b (tbx2b)*, *neural retina leucine zipper (nrl)*, and *nuclear receptor subfamily 2, group E, member 3 (nr2e3)*, dictate key roles of photoreceptor differentiation (Nelson et al., 2009). Mutation in zebrafish *tbx2b*, a gene that encodes transcription factor expressed in early retinal progenitors, results in a loss of UV cones with rods occupying their positions (Alvarez-Delfin et al., 2009). This finding suggests that progenitor cell populations that generate rods or cones also have plasticity in fate.

1.4 Vitamin A Metabolism and Retinoic Acid Signalling

1.4.1 Importance of Vitamin A in the human eye

Proper nutrition is essential for normal growth and embryonic development. Vitamin A is a nutrient that is fundamental for the life of all

chordates and regulates major embryonic growth and patterning through its biologically active derivative RA. In humans, the necessity of vitamin A extends from embryonic development into adulthood as derivatives of this nutrient are required during embryonic eye morphogenesis, as well as initiating the phototransduction cascade in the mature eye. Its roles in adult humans include regulating fertility, maintaining normal vision and preventing neurodegenerative diseases. Normal vertebrate eye development requires a complex series of morphological movements and precise patterning. Aberrant eye development can result in birth defects and retinal dystrophies. As these disorders can result in partial or complete loss of vision, it is essential to understand how Vitamin A and the synthesis and signalling of its derivatives regulate the proper development of the eye.

Micronutrient deficiencies are most prevalent in developing countries where the diet lacks variety. Vitamin A deficiency (VAD) is a public health problem affecting more than half of all countries, particularly in Africa and South-East Asia. Deficiency of sufficient duration or severity can cause childhood blindness, anemia and weakened resistance to infection. VAD is a significant cause of preventable blindness in humans (UNICEF, 2011; WHO, 2009). VAD manifestations in the visual system range from night blindness and xerophthalmia (failure to produce tears) to permanent blindness as a result of keratomalacia (irreversible damage to the cornea) (WHO, 1996). Pregnant women and young children are considered to be the most at-risk populations for VAD due to higher required dietary intake and the increased health consequences associated with deficiency during these life stages. One-third of the world's preschool-aged children are vitamin A deficient, with 44 – 50% of these children originating from developing countries in Africa and Southeast Asia (WHO, 2009). It is estimated that 5.2 million and 4.4 million preschool-aged children are affected by night blindness and xerophthalmia, respectively (West, 2002; WHO, 2009). Delivery of high potency supplements in at-risk communities has been shown to reduce risks of xerophthalmia by

approximately 90% and mortality by 23-30% in young children (Imdad et al., 2011; Mayo-Wilson et al., 2011; WHO, 2009). Vitamin A can also be supplemented to these countries through the introduction of carotenoid rich foods, such as the orange-fleshed sweet potato (Gurmu et al., 2014). Another widely practiced approach to increasing the dietary intake of vitamin A is through supplementation of staple food with vitamin A. The most notable example of this supplementation is the development of golden rice, a grain that has been genetically altered to biosynthesize beta-carotene.

1.4.2 Animal models in Vitamin A Deficiency

As Vitamin A is indispensable for ocular development and vision in humans, it is essential to understand the function of this vitamin in ocular development. Pioneering studies of embryos from pregnant rats and pigs that were fed a vitamin A-deficient diet revealed a complex syndrome affecting multiple organ systems, including kidney, eyes, brain and heart (Wilson et al., 1953). Progeny from mothers that were deficient in vitamin A possessed congenital eye abnormalities including anophthalmia, coloboma, folding of the retina and other ocular defects (Hale, 1933, 1935; Hale, 1937; Warkany, 1944; Warkany and Schraffenberger, 1946). Although these studies were among the first to provide insight into the importance of vitamin A, the observations were limited to early stages of eye development, such as ocular morphogenesis and patterning, because foetal survival was low. When nutritional models of late embryonic vitamin A deficiency were later developed, new roles of vitamin A in ocular development were uncovered. Maternal vitamin A supplementation before embryonic stage 11.5 (E11.5) markedly reduced the incidence of eye abnormalities in developing mouse embryos. After E11.5, distinct and essential events in eye development occur, including ventral fissure closure, and development of the anterior chamber and iris. Delayed vitamin A supplementation results in ocular phenotypes including retinas with poor neuronal organization, reduced cellular proliferation, thinning of the ventral

retina and late neuronal differentiation (See and Clagett-Dame, 2009; See et al., 2008). These data emphasize the importance of retinoic acid during the specification and development of ocular tissues.

Previous studies have considered retinoic acid as a largely posteriorizing factor whereby excess RA induces posterior embryonic cell fates. However, studies in quail have challenged the role of RA in anterior patterning. VAD quail embryos have normal cranial neural crest production but at later stages, extensive apoptosis occurs in head mesenchyme and ventral neuroectoderm. Resultantly, aberrant formation of the anterior forebrain, including an abnormal patterning of the diencephalon, is observed in VAD embryos (Halilagic et al., 2003). VAD quail revealed a more severe ocular phenotype than the defects observed in porcine or rodent models (Maden et al., 2007). Unlike microphthalmia and coloboma observed in pig and rat models, the entire ventral retina and the ventral optic stalk fail to form in the absence of RA. Additionally, VAD avian embryos had defects in choroid fissure closure and proliferation as well as growth of the retina and the lens (Maden et al., 2007; Tini et al., 1993). Though phenotypes observed are more severe, research in quail, mouse, and pigs all indicate that RA signalling is essential for the development of the ventral region of the eye.

1.4.3 Retinoic Acid Synthesis

Vitamin A is a generic term that encompasses a group of unsaturated organic compounds that are required for normal embryonic development and vision. As animals cannot synthesize vitamin A *de novo*, it is a necessary dietary nutrient. Retinyl esters (present in animal oils) and carotenoids (present in plants) are stored in liver hepatocytes and stellate cells as retinyl esters (D'Ambrosio et al., 2011). Vitamin A is not the main bioactive mediator of its function. All-trans retinoic acid is the biologically active derivative of Vitamin A and it has been found that retinyl esters and retinoids can be synthesized into retinoic acid. There is one main pathway and other non-

canonical pathways that synthesize retinoic acid. The metabolism of vitamin A into retinoic acid is highly conserved among vertebrates. Mouse retinoic acid synthesis will be described below, unless otherwise indicated.

1.4.3.1 Canonical RA synthesis

The canonical pathway for RA synthesis is used by placental embryos, where maternally supplied retinol is the major source of retinoids, and by oviparous species for which retinol is stored in the egg yolk. Through placental transfer or via the yolk sac, retinol is taken up by embryonic retinol binding protein 4 (RBP4) (Figure 1.4) (Kawaguchi et al., 2007). This retinol/RBP4 complex targets cells through its interaction with nine-transmembrane receptor Stimulated by Retinoic Acid 6 (STRA6).

In the cytoplasm, retinol associates with cellular retinol-binding protein (CRBP). Retinol is oxidized to retinaldehyde by the action of two classes of enzymes: microsomal retinol dehydrogenase (RDHs) and cytosolic alcohol dehydrogenases (ADHs). RDH enzymes are considered to be the first level of RA synthesis regulation as studies in murine models have shown that mutation of RDH10 cause lethal developmental abnormalities that are characteristic of an RA-deficiency phenotype. This suggests that tissues are primed for RA synthesis through the tissue-specific presence of RDH10 and accumulation of retinaldehyde (Cammass et al., 2007; Sandell et al., 2007).

The final step in the pathway involves the oxidation of retinaldehyde to RA. Retinaldehyde dehydrogenase enzymes, (RALDH1-3 or *Aldh1a2* and *3* in zebrafish) catalyze the conversion of RA. RALDH enzymes display distinct expression patterns that are closely correlated with the dynamics of RA signalling (Haskell and LaMantia, 2005). In zebrafish, *aldh1a2* is expressed in the somites, paraxial mesoderm and the dorsal retina (Begemann et al., 2001; Grandel et al., 2002) and *aldh1a3* expression is regionalized to the ventral retina (Pittlik et al., 2008). Homozygous *Raldh1* mouse mutants show only minor defects in the dorsal retina (Matt et al., 2005; Molotkov et al., 2006).

Raldh1 and *Raldh3* null mice reveal no clearly defined ocular defects, possibly due to the paracrine action of RA generated by the remaining enzymes (Dupe et al., 2003; Fan et al., 2003; Mic et al., 2004; Niederreither et al., 1999). *Raldh1/3* null mice embryos display multiple and severe malformations affecting several ocular tissues including the eyelids, cornea, lens and retina (Matt et al., 2005). Disruption of *Raldh2* in mouse leads to developmental abnormalities that are characteristic of Vitamin A deficiency, suggesting that *Raldh2* is the main RA synthesis enzyme in the vertebrate embryo (Niederreither et al., 1999; Niederreither et al., 2000). Taken together, these results suggest a combinatorial role of Raldhs in eye development.

1.4.3.2 Non-canonical signalling

Enzymes involved in alternative RA synthesis pathways have been elucidated and they begin to shed light on ancestral synthesis pathways used in early chordates. In addition to retinol, retinoids are stored in the eggs of marine fishes in alternative forms, namely retinaldehyde/vitellogenin complexes and beta-carotene. Vertebrate genomes encode two types of carotenoid-cleaving enzymes that facilitate carotenoid metabolism: beta-carotene-15, 15'-monooxygenase (BCMO1) and beta-carotene-9', 10'-dioxygenase (BCO2a). Central cleavage of beta-carotene by BCMO1 generates two molecules of retinaldehyde (von Lintig and Vogt, 2000). BCO2a cleaves beta-carotene eccentrically which results one molecule of retinaldehyde and one molecule of one short-chain beta-apo-carotenoid (Kiefer et al., 2001). Retinaldehyde is then oxidized to RA by RALDHs. While implicated in RA synthesis, the contributions of these alternate forms to vertebrate RA signalling are not well established. *Bcmo1* homologues are found in all vertebrates and in some invertebrates, including *Drosophila*. The primary function of BCMO1 across these species is to generate retinaldehyde and in some species appears to regulate aspects of eye development and function. A *Drosophila BCMO1* mutant exhibits significantly reduced rhodopsin content

and reduced visual sensitivity (von Lintig and Vogt, 2000). Zebrafish *bcmo1* is expressed in the head, pectoral fin buds, ventral optic primordia and along the anterior posterior axis close to the yolk boundary (Lampert et al., 2003). Knockdown of *bcmo1* in zebrafish has also been associated with irregular photoreceptor development and aberrant eye morphology (Biehlmaier et al., 2005; Lampert et al., 2003).

Another candidate for RA synthesis was identified in chicken (Chambers et al., 2007). Cytochrome p450 family 1, subfamily b, group 1 (Cyp1b1) is expressed in many embryonic tissues that correspond to sites of RA production. Additionally, *in vitro* studies have found that Cyp1b1 is sufficient to catalyze the conversion of retinol to retinaldehyde and retinaldehyde to RA in a RALDH-independent manner (Chambers et al., 2007). However, this role has yet to be shown *in vivo*. There is much left to be elucidated regarding Cyp1b1 and its role in RA synthesis. However, in zebrafish, *cyp1b1* is expressed in specific spatial and temporal pattern in the dorsal and ventral retina that overlaps with the RA synthesis enzymes *aldh1a2* and *1a3* (Williams and Bohnsack, 2015). The presence of overlapping enzymes that play a role in canonical and non-canonical RA synthesis suggests complex interplay between Cyp1b1 and Aldh enzymes to regulate RA levels.

1.4.4 RA Metabolism

Although RA is indispensable in embryonic development, excess RA can affect embryonic developing and result in teratogenesis. Excess RA in human foetal development often results in malformations of limbs, eyes and central nervous system. The complex effects of excess RA observed in several species emphasizes the importance of tightly controlling its regional specificity and endogenous expression during embryogenesis. *In vivo* cellular concentration of all-trans RA is regulated by b RA degrading enzymes from the cytochrome p450, family 26, CYP26A1, CYP26B1 and CYP26C1, localized in the cytoplasm. These enzymes catalyze reactions that convert RA into polar

metabolites, namely 4-hydroxy-RA and 4-oxo-RA (White et al., 1996). Although 4-oxo-RA is able to bind to retinoic acid receptors, *in vivo* data indicate the role of CYP26-mediated RA metabolism is to remove bioactive RA from specific tissues (Niederreither et al., 2002a; Pennimpede et al., 2010). All three CYP26 genes display distinct expression patterns that often complement the RALDH expression domains during embryogenesis. In zebrafish, *cyp26a1* is expressed within the neural retina, anterior neuroectoderm and tail bud (Kudoh et al., 2002) whereas *cyp26b1* and *cyp26c1* are expressed within the developing telencephalon, diencephalon, and hindbrain (Gu et al., 2005; Hernandez et al., 2007; White and Schilling, 2008). In the neural retina, *cyp26a1* expression forms narrow boundary between the dorsal and ventral Aldh enzymes. This creates a trough of low RA levels between high ventral and moderately high dorsal RA levels (McCaffery et al., 1999). Mouse *Cyp26a1* and *Cyp26b1* mutants strongly recapitulate phenotypes associated with exposure to excess RA (Sakai et al., 2001; Yashiro et al., 2004). To tightly regulate RA levels in specific tissues, RA can control the expression of its own metabolizing enzymes. Studies *in vivo* and in cultured cells have shown that exogenous RA treatments lead to up-regulation of the *Cyp26a1* gene (Loudig et al., 2005).

1.4.5 RA gene regulation

The newly synthesized RA binds to cellular RA-binding proteins (CRABP) (Figure 1.4). When bound to ligand, CRABP undergoes a conformational change that exposes its nuclear localization motif and the apo-protein is transported into the nucleus. Alternatively, RA can be released by the cytoplasm and acquired by other cells. For example, RA synthesized within the somatic mesoderm signals in neighbouring target tissues to contribute to anteroposterior patterning, motor neuron formation and forelimb induction (Niederreither et al., 2002b; Novitch et al., 2003). However the mechanisms through which RA travels to neighbouring tissues and what genes it regulates is yet to be fully understood. Thus RA can signal either in an

autocrine or a paracrine fashion. When the RA/CRABP2 complex enters the nucleus, free RA ligand binds with retinoic acid receptors (RARs) (Rochette-Egly and Germain, 2009). The retinoid receptor family includes RARs as well as retinoid X receptors (RXRs). RARs recognize all-trans RA and 9-*cis* RA, whereas RXRs only recognize the stereoisomer 9-*cis* retinoic acid. RAR forms a heterodimer with RXRs at the retinoic acid-response elements (RAREs) in regulator regions of RA target genes. In the presence of ligand, the RAR ligand-binding domain undergoes a conformational change, thus releasing the co-repressor complex and recruiting of co-activator complexes (Niederreither and Dolle, 2008). When unbound to ligand, RAR/RXR heterodimers recruit co-repressors. Co-repressors maintain target gene repression through the recruitment of histone deacetylase and methyl-transferase complexes.

In general, vertebrate genomes encode three RAR and three RXR genes, referred to as α , β , and γ subtypes. The teleost genome underwent an extra duplication that resulted in the presence of additional paralogs (Meyer and Van de Peer, 2005). During evolution, zebrafish lost the RAR β subtype, thus its resultant genome encodes four RAR genes (*raraa*, *rarab*, *rarya*, and *raryb*) and six RXR genes (*rxraa*, *rxrab*, *rxr β a*, *rxr β b*, *rxrya*, *rxryb*) (Philip et al., 2012; Waxman and Yelon, 2007). The roles of each subtype and isoform during zebrafish embryogenesis are unclear, but their expression levels change during development and from one tissue to another (Hale et al., 2006; Ross et al., 2000; Waxman and Yelon, 2007). Mice carrying null mutation in one RAR exhibited minor defects during embryogenesis and survive postnatally. When two RARs are knocked out together, severe ocular defects, including microphthalmia, coloboma, and abnormalities of the cornea and conjunctiva were observed. These studies of targeted disruption of the murine RAR genes reveal mainly redundant roles among the receptor subtypes (Lohnes et al., 1994). All six murine subtypes are expressed in the eye, three of which specifically expressed within the retina (Cammass et al., 2010). The abundance

of RA receptors within the retina emphasizes the importance of RA signalling in embryonic eye development.

1.4.6 Human genetics of retinoic acid and congenital ocular defects

Ocular defects, like MAC and congenital glaucoma, have a large genetic component. As levels of RA are among the highest within portions of the eye, it is unsurprising that mutations in key components of RA synthesis and signalling pathway have been associated with human ocular defects. Namely, mutations in *ALDH1A3*, *STRA6* and *RAR β* have been associated with MAC, and mutations in *CYP1B1* results in congenital glaucoma.

STRA6 has emerged as a gene mutated in non-syndromic MAC. Homozygous mutations of human *STRA6* have been found to cause both isolated and syndromic cases of microphthalmia (White et al., 2008). Isolated, non-syndromic microphthalmia may also be accompanied by coloboma. Homozygous mutations in *STRA6* can also lead to syndromic cases of microphthalmia or anophthalmia. For example, Matthew-Wood syndrome is associated with multi-system defects including heart defects, lung hypoplasia, microphthalmia, anophthalmia, and mental retardation (Chassaing et al., 2009; Williamson and FitzPatrick, 2014). Recessive and dominant alleles of *RAR β* manifest as microphthalmia and anophthalmia with extraocular developmental anomalies including diaphragmatic hernia, and abnormal cognitive development (Williamson and FitzPatrick, 2014). As the syndromic phenotypes that accompany *STRA6* and *RAR β* result in reduced viability, these mutations are rarely observed in surviving cases. In contrast to *STRA6* and *RAR β* cases, the majority of MAC cases with *ALDH1A3* mutations are viable. Lesions in *ALDH1A3* have been identified as an autosomal recessive cause of MAC. The phenotypes observed in these cases range from mild microphthalmia to microphthalmia accompanied by coloboma or anophthalmia. Further, *ALDH1A3* loss of function has also been found to cause aberrant development of the optic nerve and chiasm (Abouzeid et al.,

2014; Fares-Taie et al., 2013; Mory et al., 2014; Yahyavi et al., 2013). Mutations in several genes that encode for proteins essential in RA synthesis and signalling suggest a strong link between RA regulation and MAC.

In addition to MAC, mutations in *CYP1B1* have been identified in patients with primary congenital glaucoma. Glaucoma, the second leading cause of blindness worldwide, is an ocular condition that leads to progressive damage of the optic nerve and defects in the visual field. If left untreated, glaucoma can result in a loss of central vision (Quigley and Broman, 2006). Primary congenital glaucoma is the most common form of glaucoma in infants (Tanwar et al., 2010; Vasiliou and Gonzalez, 2008). *CYP1B1* was first linked to primary congenital glaucoma in the recessive Romani pedigrees (Stoilov et al., 1997), where 100% of primary congenital glaucoma were accounted for by *CYP1B1* mutations (Plasilova et al., 1999). Worldwide, mutations in *CYP1B1* account for 87% of familial and 27% of sporadic cases of primary congenital glaucoma (Vasiliou and Gonzalez, 2008). Common variants of *CYP1B1* linked to glaucoma can act by either reducing enzymatic activity, by reducing the abundance of the enzyme, or both (Chavarria-Soley et al., 2008). This decrease in activity or abundance may cause lower levels of RA within the tissue. Mutations in *CYP1B1* have also been linked to other structural defects in the eye: juvenile open-angle glaucoma, primary open angle glaucoma, Rieger's anomaly, and Peter's anomaly. These findings strongly support a role for *CYP1B1* in the morphogenesis of the eye. Further investigations are required to provide a more complete understanding of the cellular role that *CYP1B1* plays, as well as its role in specific portions of the eye and its influences on RA levels. *CYP1B1* in the retina may be responsible for replenishing the chromophore 11-*cis*-retinal necessary during phototransduction and the visual cycle. However, as *CYP450* are known to function as xenobiotic-metabolizing enzymes, an alternative, or possibly additional, *CYP1B1* may protect against potentially toxic lipophilic compounds in the retina.

1.5 Purpose of Study

Normal vertebrate eye development requires a complex series of morphological movements and precise patterning. Eye development can be subdivided into early and late stages. In early eye development, tissues must be specified as having ocular identity and undergo morphological movements to transform from an evaginated optic vesicle to a bilayered optic cup. During this phase of ocular development, the eye must be properly patterned across the dorsoventral axis, POM cells must properly migrate to the retina, and the transient choroid fissure must open and later close. Following optic cup formation, retinal neurogenesis must occur where a pool of retinal progenitor cells differentiate into seven cell types and organize into five distinct layers. A major challenge in embryonic ocular development is to determine the signalling pathways that regulate each component of eye development. Aberrant eye development can result in birth defects and retinal dystrophies.

As these disorders can result in partial or complete loss of vision, it is essential to understand how signalling pathways regulate the proper development of the eye. Several signalling pathways are indispensable in the proper formation and patterning of the eyes. The retinoic acid signalling pathway is fundamental to vertebrate eye development. Multiple RA synthesis enzymes are expressed in the dorsal and ventral domains of the developing zebrafish retina, suggesting a complex interplay of *Cyp11b1* and *Aldh* enzymes in the regulation of RA levels. Although much is known about the effects of VAD and excess RA in ocular development, little information exists about the single and combinatorial roles of RA-synthesizing enzymes within the developing zebrafish retina. Consequently, the goal of this work is to contribute to our understanding of RA synthesis and signalling in the embryonic eye.

Previous studies have implicated the RA signalling pathway in vertebrate ocular development. The presence of multiple genes that encode RA synthesis enzymes expressed in dorsal and ventral domains in the eye

suggests interplay among the enzymes to maintain RA levels within the retina. Studies in mouse have revealed that disruption of *Raldh1* or *Raldh3* results in embryos with mild eye defects, suggesting that RA generated by remaining enzymes are sufficient to facilitate ocular development (Dupe et al., 2003; Fan et al., 2003; Mic et al., 2004; Niederreither et al., 1999). Pharmacological inhibition of RA in zebrafish embryos reveals ocular abnormalities including the loss of the ventral retina and the incomplete closure of the choroid fissure (Marsh-Armstrong et al., 1994). However, this approach does not address the spatial requirements for RA or the single and combinatorial roles of RA synthesis enzymes within the retina. The recent availability of *aldh1a3* and *cyp1b1* mutants has allowed for a more targeted approach to investigate the role of retinoic acid in the eye and the contributions of RA synthesis enzymes in retinal development. We hypothesized that the restricted dorsal and ventral domains of *aldh1a2* and *aldh1a3*, respectively synthesize RA that act within their respective retinal domains. We demonstrate that the RA synthesized in the ventral domain of the eye is able to signal within the dorsal retina.

RA synthesis genes *aldh1a2*, *aldh1a3*, and *cyp1b1* are spatially restricted in the dorsal and ventral regions of the eye (French et al., 2009). The dorsal and ventral restriction of these genes within the retina indicates that high levels of RA are required within these domains. However, the function of RA during eye development is not fully understood. Exogenous RA treatment of zebrafish and *Xenopus* reveal the ventralization of the eye and consequentially, the expansion of the ventral patterning marker, *vax2*, suggesting that RA can regulate ventral retinal patterning (Lupo et al., 2005; Schmitt and Dowling, 1996). We hypothesize that high levels of RA are required for the establishment of dorsoventral retinal patterning. Our results suggest that, unlike exogenous RA treatment, loss of *aldh1a3* does not regulate dorsoventral retinal patterning.

Previous studies in mouse and zebrafish have established a function

for RA signalling in POM. *Raldh1* expressed in the dorsal mouse model, synthesizes sufficient levels of RA to direct POM migration in the eye. Loss of both *Raldh1* and *Raldh3* results in the overgrowth of POM resulting from reduced POM apoptosis (Matt et al., 2005; Molotkov et al., 2006). In zebrafish, RA is necessary for normal POM dynamics as pharmaceutical inhibition of RA signalling results in fewer POM cells migrating to the choroid fissure (Lupo et al., 2011; Matt et al., 2008; Molotkov et al., 2006). We hypothesize that *aldh1a3* synthesizes RA within the retina that acts on POM in a paracrine fashion to regulate POM migration. We observed that RA synthesized solely by *aldh1a3* is not sufficient to direct POM migration in the eye.

Human studies have clearly demonstrated a strong correlation between MAC and mutations involved in RA synthesis. Mutations in *ALDH1A3* have been estimated to account for up to 10% of MAC cases, making mutations in this gene one of the most common causes of inherited MAC (Abouzeid et al., 2014; Gerth-Kahlert et al., 2013; Williamson and FitzPatrick, 2014). Pharmaceutical inhibition of RA synthesis in zebrafish results in microphthalmia (Le et al., 2012). Similarly, RA deprivation in chick embryos results in small eyes in comparison to control and the failure of choroid fissure closure (Sen et al., 2005). While RA has been established as essential in choroid fissure closure and maintenance of eye size, the contribution of RA levels by each RA synthesis enzyme within the retina is currently unknown. We hypothesize that ventrally expressed *aldh1a3* contributes to choroid fissure closure whereas dorsal and ventral RA synthesis enzymes are essential in maintenance of eye size. We observed that loss of *Aldh1a2* and *aldh1a3* results in a reduction of total eye area. Additionally we demonstrate that loss of *Aldh1a2* increases the incidence of coloboma in zebrafish retina.

Retinoic acid in the retinal microenvironment is thought to facilitate the differentiation of photoreceptors from retinal progenitor cells. Exogenous retinoic acid has been observed to increase the number of photoreceptors *in*

vitro (Kelley *et al.* 1994). Exogenous treatment of RA in zebrafish promotes the differentiation of rods and red-sensitive cones at the expense of other cone photoreceptor subtypes. (Hyatt *et al.*, 1996a; Kelley *et al.*, 1999; Stevens *et al.*, 2011). While existing studies have revealed that RA influences cell fate decision, these studies do not provide insight as to the contribution of RA synthesis enzymes within the retina during retinal neurogenesis. We hypothesize that retinoic acid that is synthesized by *aldh1a2*, *aldh1a3* and *cyp1b1* aids in the differentiation of photoreceptors. Preliminary data suggests that depletion of RA results in the reduction of rods, UV cones and blue cones with negligible changes in green cone photoreceptors.

Amacrine and horizontal cells are two neuronal cell types that compose the INL in the neural retina. Retinal progenitor cells that are fated to become either amacrine or horizontal cells will exit cell cycle prior to the differentiation of photoreceptors. It has been observed that *forkhead box n4* (*foxn4*) controls the formation of amacrine and horizontal cells (Li *et al.*, 2004). We hypothesize that the reduction of photoreceptors in *Aldh1a2*; *aldh1a3*; *cyp1b1* morphomutants could be attributed to an increase in amacrine and horizontal cells. We obtained preliminary data that suggests that a loss of *Aldh1a2*, *aldh1a3* and *cyp1b1* causes an increase of *foxn4* expression within the retina. The increase of *foxn4* expression provides a possible mechanism of photoreceptor fate determination by which an upregulation of *foxn4* biases cell fate determination to amacrine and horizontal cells at the expense of photoreceptors.

Retinaldehyde and carotenoids are the main retinoids stored in the egg in teleosts, suggesting that retinoic acid may be synthesized by both retinol and betacarotene processing pathways. *Bcmo1* knockdown in zebrafish has been previously shown to cause defects in patterning and differentiation during distinct RA-dependent developmental processes, including craniofacial development, pectoral fins and eyes (Lampert *et al.*, 2003). Studies using morpholino-mediated *Bco2a* targeted knockdown indicate that *Bco2a* is

required for cellular protection against carotenoid-induced oxidative stress and apoptosis. The requirement of Bco2a in retinoic acid production remains to be investigated (Lobo et al., 2012). We endeavored to create *bcmo1*- and *bco2a*-mutant embryos using transcription activator-like effector nucleases (TALENs). Synthetic targeted endonucleases, such as ZFN and TALENs have emerged as powerful tools for targeted mutagenesis. Both ZFNs and TALENs consist of DNA-binding arrays fused to the non-specific FokI nuclease domain. These technologies, while innovative in genome editing, yield variable somatic mutation rate (0 – 100%). We attempted to improve the efficiency of ZFN and TALEN in zebrafish mutagenesis through the use of a FokI nuclease variant termed *Sharkey*. We demonstrated that *Sharkey* ZFNs yield greater *in vitro* cleave of target-site DNA than controls. Further, *Sharkey* ZFNs are capable of producing a higher frequency of insertion/deletion mutations in zebrafish. Conversely, all *Sharkey* TALENs examined fail to produce any insertion/deletion mutations, displaying absent or significantly reduced *in vivo* mutagenic activity in comparison to control TALENs.

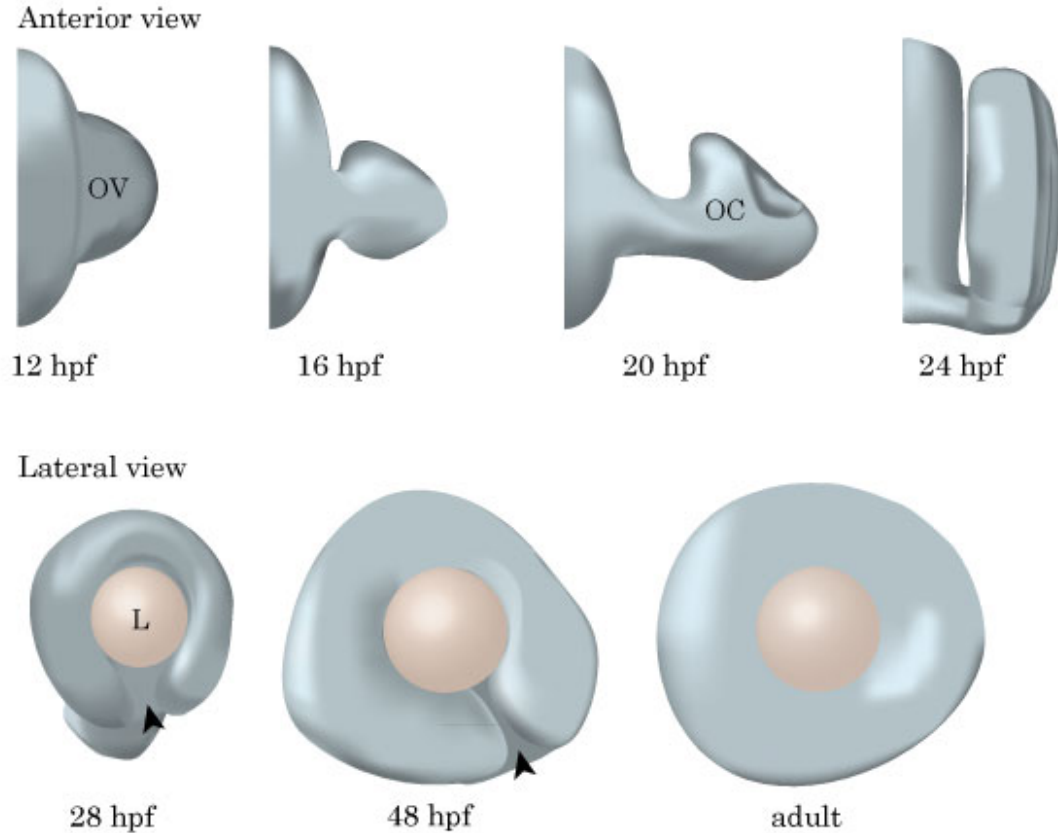


Figure 1.1: Vertebrate eye morphogenesis. Diagrams showing anterior and lateral views of zebrafish eye morphogenesis at indicated time points. At 12 hpf, the optic vesicle (OV) evaginates from the diencephalon towards the overlying ectoderm. Contact of the optic vesicle with the overlying ectoderm induces formation of lens at 16 hpf and the formation of the bilayered optic cup (OC) at 20 hpf. At 28 hpf, the lens (L) is fully formed with the open choroid fissure (arrowhead) at the ventral portion of the eye from 24 to 48 hpf. This transient opening is essential for RGC axon exit from the eye and vascularization of the eye (Based on (Li et al., 2000)).

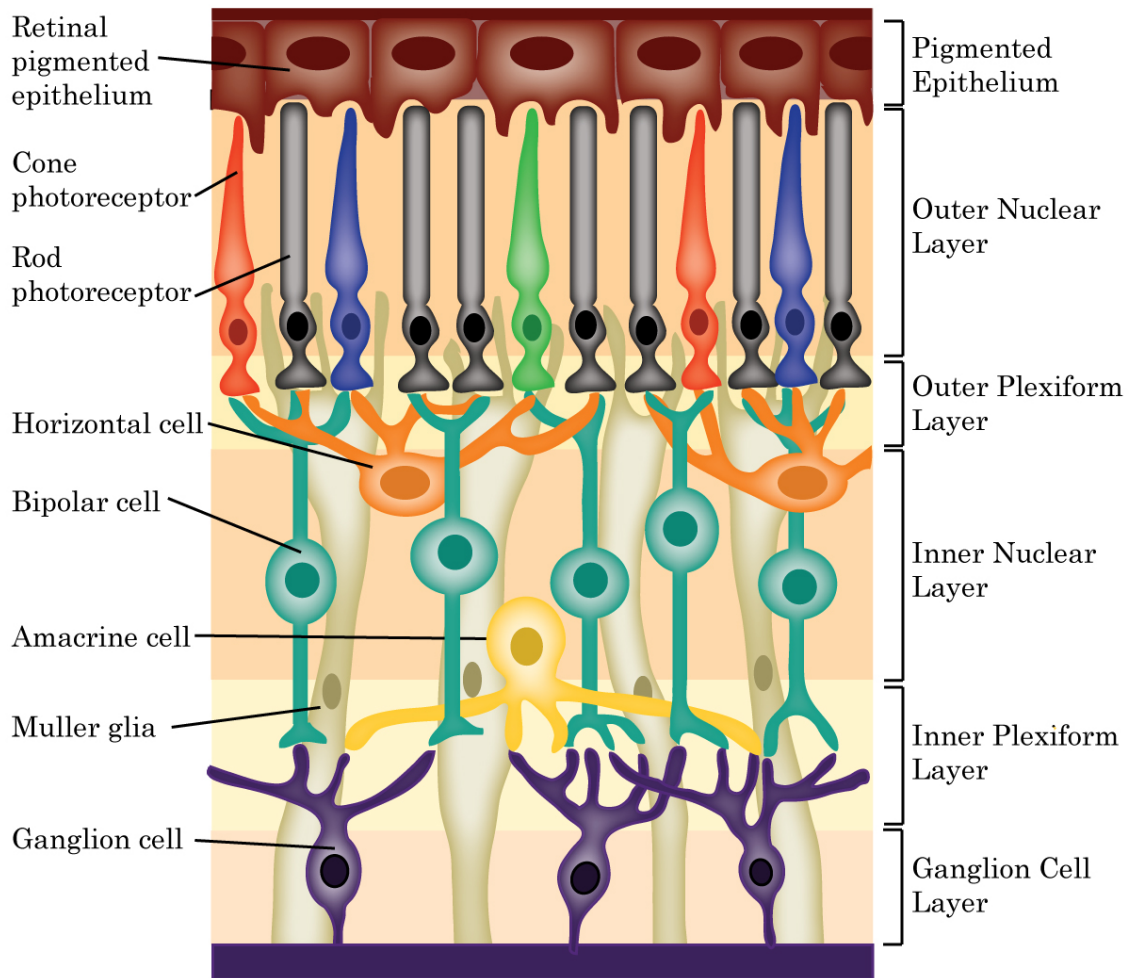
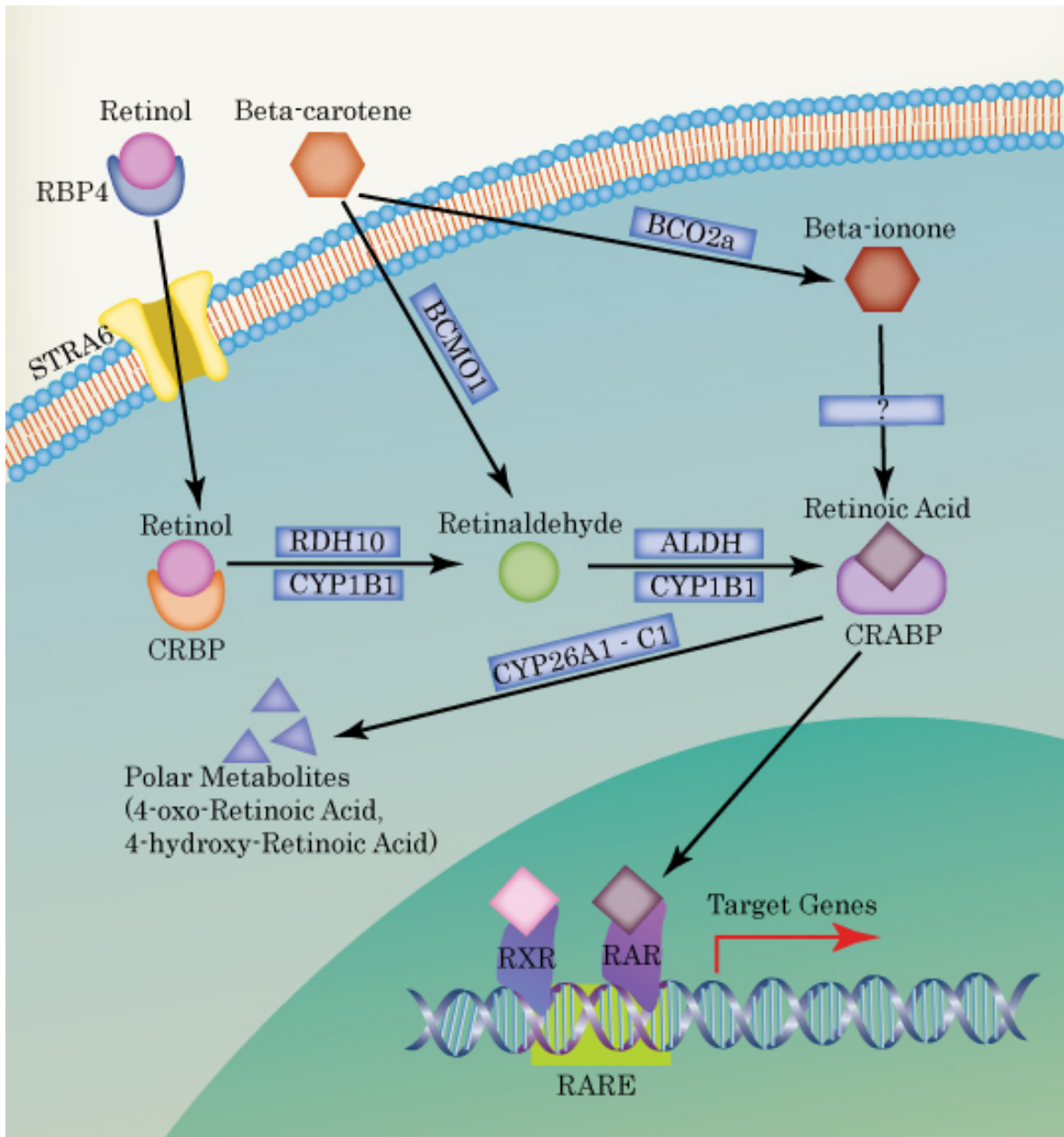


Figure 1.3: The organized laminar structure of the vertebrate retina. Diagram of cross-section of the retina showing the six neuronal and one glial cell types of the retina and the retinal pigmented epithelium. The outer nuclear layer contains rod and photoreceptors. Photoreceptors synapse with bipolar and horizontal interneurons. The cell bodies of the amacrine interneurons, along with bipolar and horizontal cells, compose the inner nuclear layer. Muller glia cell bodies span the thickness of the retina. Signals from the bipolar cells are relayed to retinal ganglion cells, located in the ganglion cell layer. Ganglion cells send their axonal projections to the visual processing center in the brain (Based on (Koeppen, 2008)).

Figure 1.4: Retinoic acid synthesis and signalling pathway. Retinol is taken up by embryonic retinol binding protein 4 and is transported into the cell through Stimulated by Retinoic Acid 6 receptor (STRA6) protein. Intracellular retinol is bound to cellular retinol binding proteins (CRBP) and is transformed intracellularly by retinol dehydrogenase 10 (RDH10). Symmetric cleavage of beta-carotene by beta-carotene 15' 15' monooxygenase (BCMO1) directly generates retinaldehyde. Aldehyde dehydrogenases (ALDH) convert retinaldehyde into retinoic acid (RA). Cytochrome p450 1B1 (CYP1B1) can catalyze both reaction from retinol to retinaldehyde and retinaldehyde to RA. Eccentric cleavage of beta-carotene by beta-carotene 9' 10' dioxygenase (BCO2a) yields one molecule of beta-ionone. Beta-ionone may be converted to RA by a currently unknown enzyme. RA can be bound to cellular retinoic acid binding protein (CRABP) and is transported into the nucleus where it interacts with retinoic acid receptors (RARs). RARs form heterodimers with retinoid X receptors (RXR) bound to retinoic acid response elements (RAREs). RA can also be targeted for degradation through conversion into more polar compounds (4-hydroxy-RA and 4-oxo-RA) by cytochrome p450 26 (CYP26) enzymes (Based on (Niederreither and Dolle, 2008)).



2 Materials and Methods

2.1 General Zebrafish Care

2.1.1 Zebrafish lines and maintenance

Embryonic and adult zebrafish were cared for as outlined in Westerfield (Westerfield, 2007), in accordance with the Canadian Council for Animal Care guidelines and approved by the University of Alberta Animal Care and Use Committee for Biosciences.

Embryos injected with morpholino oligonucleotides, mRNA or are otherwise used for experiments were raised in embryo media (EM) (EM: 15mM NaCl, 500 nM KCl, 1mM CaCl₂, 150 nM KH₂PO₄, 1 mM MgSO₄ 715 nM NaHCO₃) with penicillin-streptomycin solution (10 000 units penicillin, 10 mg/mL streptomycin; Sigma-Aldrich, St. Louis, MO, USA) diluted 1:100 in EM. Embryos were grown at 28.5°C and allowed to develop to the desired stage. Embryos may also be grown at 25.5°C or 33°C to slow or accelerate development, respectively. Stages of development were identified using standardized morphological characteristics described by Kimmel *et al.* (Kimmel et al., 1995). If embryos were grown for more than 24 hpf, the EM was supplemented with 0.006% *N*-phenylthiourea (PTU) (Sigma-Aldrich, St. Louis MO, USA) to inhibit melanin pigmentation development.

Unless otherwise noted, all experiments were performed on the AB line of wild-type fish. The transgenic line Tg(12x RARE – ef1α:eGFP) was used as a retinoic acid signalling reporter (Waxman and Yelon, 2011). Mutant fish lines used in experiments include *aldh1a3*^{sa0118} (Kettleborough et al., 2013) and *cyp1b1*^{ua1014}.

The transgenic line Tg(12x RARE – ef1α:eGFP) provides a readout for retinoic acid signalling. This reporter featured the concatenation of 12 direct repeat5 of the retinoic acid response element upstream of an elongation factor-1 alpha (*efl1a*) promoter driving *egfp* (Waxman and Yelon, 2011) (Figure 2.1A). This line was bred into the *aldh1a3* and *cyp1b1* mutants to generate single or

double mutant embryos that have green fluorescent protein (GFP) expressed in cells that have retinoic acid signalling.

The *aldh1a3*^{sa0118} was obtained through an ENU mutagenesis screen carried out at the Sanger Centre. The mutant has a G to A transition in nucleotide position 264 of the *aldh1a3* open reading frame with nucleotide position 1 corresponding to the A in the initiation methionine codon. This results in a premature stop codon at codon 88 resulting in a truncated protein [NP_000684.2: p.Trp88X] (Figure 2.1B). Genotyping of *aldh1a3* mutant embryos was conducted by cleaved amplified polymorphism (CAP) PCR (Table 2.1), restriction enzyme digest with NmuCI/Tsp451 (ThermoFisher, Waltham MA, USA) and gel electrophoresis to resolve the digested PCR products. The wild-type allele produces a 253 bp band while the mutant allele produces 96 and 154 bp bands.

The *cyp1b1* mutant allele was generated at the University of Alberta through Transcription Activator-Like Effector Nucleases (TALEN) technology. The ua1014 allele contains a 13 base pair (bp) deletion at aa317 that produces a premature stop codon at codon 340 [NP_001038721.1: Cys317Serfs*33] (Figure 2.1C). Embryos containing the *cyp1b1* mutant allele were identified using CAP PCR (Table 2.1), restriction enzyme digest with DraIII/AdeI (ThermoFisher, Waltham MA, USA). Digested PCR products were resolved on a 2% agarose gel. The wild-type allele produces a 503 bp fragment and the mutant allele produces 200bp and 303 bp bands.

Aldehyde dehydrogenase I family, member A2 (Aldh1a2)-depleted embryos were generated by injecting one-cell embryos with approximately 4ng of previously described translation-blocking *aldh1a2* morpholino (ZDB-MRPHLNO-050316-3) (Alexa et al., 2009). *aldh1a2* morpholino was co-injected with 2 ng of *p53* morpholino (ZDB-MRPHLNO-070126-7) to control for p53-mediated apoptosis activated by non-specific morpholino injection.

2.1.2 Fin clipping

To identify adult fish that were carriers for mutant alleles, caudal fin clippings were performed. Individual adult zebrafish were anesthetised in 0.642 mM tricaine methanesulfonate (MS222). The anesthetised fish was removed with a plastic spoon and briefly washed with clean water. The fish was then placed on paper towel and a small portion of the caudal tail was amputated with a scalpel. The fish was returned to fresh water for recovery. The amputated fin was transferred into a 0.2 mL PCR tube. The genomic DNA was extracted from the collected tissue.

2.2 Embryo manipulation and care

2.2.1 Morpholino preparation and injection

Translation-blocking morpholino antisense oligonucleotides (MO) were designed by and ordered from Gene Tools LLC (Philomath OR, USA) (Table 2.2). Lyophilized MO stocks were diluted to a concentration of 10 mg/mL in sterile water and were stored at 4°C. Stock morpholinos were diluted to 2-4mg/mL using Danieau buffer (58mM NaCl, 0.7 mM KCl, 0.4 mM MgSO₄, 0.6 mM Ca(NO₃)₂, 5 mM HEPES [4-(2-hydroxyethyl)piperazine-1-ethanesulfonic acid] pH 7.6). Prior to injection, working morpholino stocks were heated to 65°C for 5 -10 minutes and cooled to room temperature. All morpholinos were injected into the yolk or cell of single-cell zebrafish embryos. Dose was estimated based on known concentration and bolus size delivered by an ASI MPPI-2 Pressure Injector (Applied Scientific Instrumentation, Eugene OR, USA).

2.2.2 mRNA injection

Prior to injection, mRNA was stored at -80°. Before injection, mRNA was thawed on ice and diluted to appropriate working concentration using diethylpyrocarbonate (DEPC)-treated water. mRNA was injected into the cell of one-cell stage embryo using an ASI MPPI-2 Pressure Injector.

2.2.3 Embryo Fixation

Prior to mRNA *in situ* hybridization, embryos were dechorionated either manually or enzymatically. Manual dechoriation was performed using Dumont #5 fine-pointed forceps (Fine Science Tools, North Vancouver BC, CA). Enzymatic dechoriation was performed by immersion of embryos in 1mg/mL pronase E solution with gentle agitation for 3-5 minutes. When the first few chorions began to deflate and crumple, embryos were washed in 100mL of embryo media in a glass beaker to remove trace amounts of enzyme.

Embryos were fixed in 4% paraformaldehyde (PFA) in phosphate-buffered saline (PBS: 137 mM NaCl, 2.7 mM KCl, 10 mM Na₂HPO₄, 1.8 mM KH₂PO₄ pH 7.4) overnight at 4°C or for 4-5 hours at room temperature on a horizontal orbital shaker.

2.3 PCR and cloning

2.3.1 Isolation of genomic DNA

Genomic DNA was extracted using previously described protocols (Meeker et al., 2007). Single embryos, pools of embryos or caudal fin tissue (amputated as described in 2.1.1) were transferred to 0.2 mL PCR tubes and excess growth media was removed. For fin clips, 50 µL of 50 mM sodium hydroxide was added to each PCR tube while 10 µL and 200 µL were used when extracting DNA from single embryos and groups of 20 or more embryos, respectively. Samples were heated to 95°C for 20 minutes and then subsequently cooled to 4°C. Samples were vortexed until material was homogenized. Sodium hydroxide was neutralized by adding 1/10 volume of Tris-HCl pH 8. Genomic DNA was stored at -20°C.

2.3.2 RNA Extraction

RNA was extracted from embryos at varying stages between 24 hours post-fertilization (hpf) to 4 days post-fertilization (dpf) using the RNeasy-4PCR Total RNA Isolation Kit (Life Technologies, Burlington ON, Canada).

Elution Solution is preheated to 70°C prior to RNA extraction. Twenty to fifty dechorionated embryos were added to 350 µL of lysis/binding solution and vortexed to homogenize the tissue. Following homogenization, 350 µL of 64% ethanol was added to the lysate, briefly mixed by pipetting and transferred to a filter cartridge. The filter cartridge was placed in a collection tube and was centrifuged for 1 minute at 14 800 rpm. Flow-through was discarded and filter cartridge was washed. Filter cartridges were rinsed with 700 µL of Wash Solution 1 followed by two consecutive rinses with 500 µL of Wash Solution 2/3. After the addition of each wash solution, filter cartridges were centrifuged for 1 minute at 14 800 rpm and the flow-through was discarded. The filter cartridges were transferred to clean RNase-free tubes. RNA was eluted from filter cartridges in two steps: 40 µL of preheated Elution Solution was added to filter cartridges were centrifuged for 30 seconds at 14 800 rpm followed by the addition of 30 µL of Elution solution to the filter cartridges and centrifuged for another 30 seconds. To remove DNA from isolated RNA sample, 1 µL of DNase I, 10 µL of 10x DNase I Buffer, and 19 µL of DEPC-treated water to each tube. Isolated RNA was incubated at 37°C for 30 minutes and subsequently stored at -80°C.

2.3.3 One Step Reverse Transcription-PCR (RT-PCR)

PCR products were amplified direction from total RNA using the SuperScript III One-Step RT-PCR kit with Platinum Taq Polymerase (Life Technologies, Burlington ON, CA). Each reaction was composed of 12.5 µL 2x Reaction mix, 1 µL of SuperScript III RT/Platinum Taq mix, 1 µL each of 5 µM forward and reverse primers, 1 µL of total RNA and 9.5 µl of DEPC-treated water. The PCR cycle conditions were 30 minutes at 54°C, 2 minutes at 94°C followed by 40 cycles of denaturation at 94°C for 15 seconds, annealing for 30 seconds at 2-5°C below the melting temperature of the primers, and extension at 68°C for 1 minute/kilobase pair. A final extension was done at 68°C for 5 minutes.

PCR products were analyzed by gel electrophoresis and the appropriate-sized band was excised from the gel and purified using QIAquick gel extraction kit (Qiagen, Hilden, DE). The excised DNA-containing gel slice was transferred into a 1.5 mL microcentrifuge tube. 500 μ L Buffer QG was added to the gel slice. This mixture was incubated in a 55°C water bath and was vortexed every 15 minutes until the gel dissolved. Once dissolved, the solution was transferred into a filter cartridge placed in a collection tube and was centrifuged at 13 000 rpm for 1 minute. The flow-through was discarded and 750 μ L of Buffer PB was added to the column, which was centrifuged at 13 000 rpm for 1 minute. The flow-through was discarded and the column was centrifuged for 1 minute at 13 000 rpm. The flow-through was discarded and the column was placed in a new collection tube. DNA was eluted from the column by adding 50 μ L of Buffer EB. Column was left to stand for 1 min and then centrifuged at 13 000 rpm for 1 minute. Gel-purified DNA was stored at -20°C.

2.3.4 Polymerase Chain Reaction (PCR)

PCR reactions were performed on isolated genomic DNA or cDNA synthesized from total RNA. PCR reactions are composed of 2 - 5 μ L of template DNA, 2 μ L of 5 μ M forward and reverse primer, 2 μ L 10mM dNTPs, 2 μ L 10x buffer, 0.25 μ L Ex Taq DNA polymerase (Clontech, Mountain View CA, USA), and sterile water to a final volume of 20 μ L. The PCR cycle conditions were 94°C for 3 minutes followed by 40 cycles of denaturation at 94°C for 15 seconds, annealing at 2-5°C below melting temperature of primers and extension at 72°C for 1 minute/kilobase pair. A final extension was performed at 72°C for 3 minutes. PCR products were stored at either 4°C or -20°C.

2.3.5 TOPO Cloning and transformation

Ligation of blunt ended PCR products was performed using the TOPO-TA cloning kit (Life Technologies, Burlington ON, CA). For inserts used as a template for riboprobe synthesis, pCR4-TOPO TA vector was used. pCR 2.1-

TOPO vector was used for all other purposes. For PCR products amplified using a proofreading polymerase, 3' adenine overhangs were added after gel purification using Ex Taq (Clontech, Mountain View CA, USA). In a 0.2 mL PCR tube, 2 μ L of 10x Ex Taq buffer, 1 μ L 10 mM dNTPs, and 1 μ L of Ex Taq were combined with 16 μ L of gel-purified PCR product. The reaction was incubated for 10 minutes at 72°C. For PCR products amplified with non-proofreading Taq, undiluted PCR product was used for the TOPO-TA ligation. Each ligation consisted of 2 μ L of purified PCR product, 0.5 μ L salt solution and 0.5 μ L of appropriate pCR TOPO vector. Reactions were incubated for 5 minutes at room temperature.

The entire ligation was added to 25 μ L of One-Shot TOP10 chemically competent *E. coli* (Life Technologies, Burlington ON, CA). The transformation mixture was incubated on ice for 20 minutes followed by a 45 second heat shock at 42°C and a 5-minute incubation on ice. 250 μ L of super optimal broth with catabolite repression (SOC: 2% bacto tryptone, 0.5% bacto yeast extract, 10 mM NaCl, 2.5 mM KCl, 10 mM MgCl₂, 10 mM MgSO₄, and 20 mM glucose) was added to the cells. This mixture was incubated for one hour at 37°C. Cells were plated on Luria broth agar plates (LB: 1% bacto tryptone, 0.5% bacto yeast extract, 0.17 M NaCl, and 1.5% bacto agar, pH 7) containing the required antibiotic. Plates were incubated inverted at 37°C overnight. Single colonies were used to inoculate 3 mL of liquid LB containing the appropriate antibiotic and incubated for 16 hours at 37°C. Plasmid DNA was isolated from the liquid culture using the QIAprep Spin Miniprep Kit (Qiagen, Hilden, DE). Plasmids were sequenced to verify that the correct fragment was cloned.

2.3.6 Isolating and purifying linear DNA

Isolated plasmid DNA was linearized with NotI. Following linearization, DEPC-treated water was added to the reaction to a total volume of 50 μ L. Ribonuclease denaturation was performed by adding 2.5 μ L of 10% sodium dodecyl sulphate (SDS) and 2 μ L of 10 mg/mL proteinase K and

incubating for one hour at 50°C. Following incubation, 50 µL of DEPC-treated water and 10 µL of 3M sodium acetate pH 5.3. DEPC-treated water was added to the reaction to bring the final volume to 200 µL.

Plasmid DNA was purified by phenol-chloroform-isoamyl alcohol extraction and ethanol precipitation. Equal volume of phenol-chloroform-isoamyl alcohol (FisherScientific, Pittsburgh PA, USA) was added to the reaction. All centrifugation steps were performed at 4°C. The solution was vortex for 20 seconds and then centrifuged for 5 minutes at maximum speed. The upper layer was transferred to a new tube and 200 µL of chloroform was added. The solution was vortexed for 20 seconds and centrifuged for 5 minutes at maximum speed. After centrifugation, the upper layer was transferred to a new tube. To precipitate DNA, 600µL of 100% ethanol was added to the tube and incubated at -20°C for 15 minutes. The solution was centrifuged for 20 minutes at maximum speed. The supernatant was removed and the pellet was washed with 100 µL of 70% RNase free ethanol and air-dried. The DNA pellet was resuspended in 10 uL of DEPC-treated water.

2.3.7 Sequencing

Sequencing reactions were performed using the BigDye Terminator v3.1 Cycle Sequencing Kit (ThermoFisher, Waltham MA, US). Reactions were composed of 2 µL 10x BigDye premix, 3 µL 5x buffer, 50 – 500 ng template DNA, 1 µL 5µM sequencing primer and sterile water to a final volume of 20µL. Reactions were placed in a thermocycler and the following cycle conditions were performed: 96 °C for 2 minutes; 25 cycles of 96°C for 30 seconds, 50°C for 15 seconds, 60°C for 1.5 minutes; and 5 minutes at 60°C. Samples were purified with 2 µL 1.5 NaOAc/250mM EDTA followed by the addition of 80 µL of 95% ethanol. The reaction was vortexed and incubated at -20°C for 30 minutes. After incubation, the mixture was centrifuged at 16 000 xg for 10 minutes at 4°C. Supernatant was removed and pellet was washed with 500 µL 70% ethanol and centrifuged at 16 000 xg at 4°C for 10 minutes. The

supernatant was carefully aspirated and the pellet was dried. Dried sequencing reactions were submitted to the Molecular Biology Service Unit at the University of Alberta for sequencing. Samples are run on an ABI 3730 Genetic Analyzer (ThermoFisher, Waltham MA, USA).

2.3.8 In vitro mRNA Synthesis

Capped mRNA was transcribed from linearized, purified plasmid DNA using the SP6 mMessage mMachine kit (Life Technologies, Burlington ON, CA). Each reaction consisted of 2 µg of template DNA, 10µL 2x NTP/CAP, 2µL 10x reaction buffer, 2 µL enzyme mix, and nuclease-free water to a total volume of 20 µL. Reactions were incubated for 2 hours at 37°C. DNA template was degraded with the addition of 1µL TURBO DNase (Life Technologies Burlington ON, CA) and incubation at 37°C for 15 minutes.

Synthesized mRNA was purified using Amicon Ultra 0.5 mL centrifugal filters (Millipore, Billerica MA, USA). 400 µL of DEPC-treated water was added to reaction to raise reaction volumes to 500 µL. The solution was transferred into a column placed in a collection tube. The reaction was centrifuged for 4 minutes at 14 000 rpm and the flow-through was discarded. The column was inverted into a clean tube and centrifuged for 2 minutes at 1 000 rpm. 480 µL of DEPC-treated water was added to centrifuged mixture and transferred into a new column. Columns were centrifuged for 3 minutes at 14 000 rpm and the flow-through was discarded. The column was inverted into a clean tube and centrifuged for 2 minutes at 1 000 rpm. mRNA concentration was determined using a NanoDrop spectrophotometer (ThermoFisher, Waltham MA, USA). mRNA was stored at -80°C.

2.4 Whole Mount In Situ Hybridization

2.4.1 Digoxigenin-labeled anti-sense RNA riboprobe synthesis

Anti-sense digoxigenin (DIG)- labeled riboprobes were synthesized from either a gene-specific PCR product (Table 2.3) with an integrated T3 or T7 RNA polymerase site (Thisse and Thisse, 2008) or from purified, linearized plasmid DNA containing the insert (as described in section 2.4.3) (Table 2.4). For each riboprobe synthesis reaction, 200 – 400 ng of linearized, purified DNA plasmid or PCR product was incubated with 2 μ L 10x transcription buffer, 2 μ L DIG-labeling mix, 1 μ L RNA polymerase (T7 or T4) (Roche Applied Science, Penzberg, Germany), and 0.5 μ L of RNase-OUT Recombinant Ribonuclease Inhibitor (Life Technologies, Burlington ON, CA). DEPC-treated water was added to a total volume of 20 μ L. Reactions were incubated at 37°C for 2 hours. After the first hour of incubation, an additional 1 μ L of RNA polymerase was added to the reaction. Following incubation, 1 μ L of TURBO DNase (Life Technologies, Burlington ON, CA) was added to the reaction and incubated for 10 minutes at 37°C. To stop transcription, 2 μ L 0.2 M ethylenediaminetetraacetic acid (EDTA) pH 8.0 was added to each reaction.

Probes were purified using SigmaSpin Post-Reaction Clean-up Columns (Sigma-Aldrich, St. Louis MO, USA). Column was placed in a collection tube and centrifuged for 2 minutes at 2 500 rpm. The base of the column was removed and the column was centrifuged for 2 minutes at 2 500 rpm. Flow-through was discarded and the column was placed in a new collection tube. Synthesized riboprobe was transferred into the column and was centrifuged for four minutes at 2 500 rpm. Following centrifugation, 0.5 μ L RNaseOUT was added to probe to inhibit degradation by RNases. Probe was stored at -80 °C

2.4.2 Whole Mount mRNA in situ Hybridization Protocol (ISH)

In situ hybridization protocol was modified from protocol published by Thisse and Thisse (Thisse and Thisse, 2008). All washes were performed at

room temperature on a horizontal orbital shaker unless otherwise stated. Fixed, dechorionated embryos were rehydrated out of methanol through successive 5-minute incubations in solutions of decreasing methanol concentration (70% methanol in PBST, 50% methanol in PBST, and 25% methanol in PBST). Rehydration was followed by four 5-minute washes in PBST. Embryos were then transferred into 1.5 mL microcentrifuge tubes (between 20 and 30 embryos per tube). Embryos were permeabilized with 10 µg/mL of proteinase K. Length of permeabilization depended on developmental stage of embryo: 28 hpf embryos were incubated for 3 minutes, 48hpf embryos were incubated for 40 minutes, embryos between 4 and 5 dpf were incubated for 90 minutes. Permeabilization was stopped by incubation in 4% paraformaldehyde for 20 minutes, followed by five 5-minute washes in PBST. Prehybridization was performed for a minimum of 2 hours incubation in hybridization solution (hyb) in a 65°C water bath (hyb: 50% formamide, 5X saline sodium citrate buffer [SSC], 50 µg/mL heparin, 0.1% Tween-20, 0.002M citric acid in sterile water) with 500 µg/mL tRNA (hyb+tRNA). Working stocks of antisense DIG labeled RNA probe were made by diluting probe in hyb+tRNA from 1:200 to 1:500 and stored in -20°C. RNA probe was warmed in 65°C water bath for 20 minutes. Embryos were hybridized in 250µL of pre-warmed probe in a 65°C water bath overnight.

Embryos were washed for 5 minutes each at 65°C in [1] 66% hyb/33% 2xSSC, [2] 33% hyb/66% 2xSSC and [3] 2x SSC. Embryos were washed for 20 minutes in 0.2xSSC/0.1% Tween-20 followed by two consecutive 20-minute washes in 0.1x SSC/0.1% Tween-20. Next, embryos were washed for 5 minutes each in [1] 66% 0.2x SSC/33%PBST, [2] 33% 0.2xSSC/66% PBST and [3] PBST at room temperature. Embryos were then blocked for 2 hours at room temperature in blocking buffer made in PBST containing 2% sheep serum and 2mg/mL bovine serum albumen (BSA). After blocking, embryos were incubated in 1 mL of anti-digoxigenin-AP, Fab fragments (Roche Applied Science, Penzberg, Germany) diluted 1:5000 in blocking solution. Embryos

were incubated in antibody solution overnight at 4°C under slow agitation on a horizontal orbital shaker.

Antibody was rinsed from the embryos with five 15-minute washes in PBST. Embryos were prepared for staining reaction by being washed four times for 5 minutes each in colouration buffer (100 mM Tris- HCl pH 9.5, 50 mM MgCl₂, 100 mM NaCl and 0.1% Tween-20 in sterile water). Embryos were incubated in the dark at room temperature in staining solution (0.45 mg/mL 4-nitro blue tetrazolium chloride [NBT], 0.175 mg/mL 5-bromo-4-chloro-3-indolyl-phosphate [BCIP] in colouration buffer). Staining reaction was monitored regularly under a dissecting microscope to ensure the embryos are sufficiently stained. Colour solution was rinsed from embryos with five 5-minute washes in stop solution (PBST, pH 5.5) and stored at 4°C. Embryos were rinsed with 100% methanol/0.1% Tween-20 for 10 minutes.

2.4.3 Mounting and photography

Embryos were prepared for mounting through successive washes in 30%, 50% and 70% glycerol in phosphate buffered saline (PBS). Tissues were dissected manually and mounted on glass slides in 70% glycerol. Mounted embryos stained by *in situ* hybridization were photographed using a Zeiss AxioImager Z1 compound microscope using an AxioCam HRm camera and Axiovision SE64 Rel.4.8 software (Zeiss, Oberkochen, DE). An Olympus SZX12 stereomicroscope (Olympus, Richmond Hill ON, CA) with a Micropublisher 5.0 RTC camera and QCapture Suite PLUS Software v3.3.1.10 (QImaging, Surrey BC, CA) was used to photograph whole embryos. Figures were assembled in Photoshop (Adobe Systems, San Jose CA, USA).

2.5 Eye Area Measurements

Prior to photography, 48 hpf, 72 hpf, or 4 dpf live embryos were anaesthetised in 0.642 mM MS222 for five minutes. Embryos were placed in a ceramic plate with 3% methyl cellulose (Sigma-Aldrich, St. Louis MO, US) for positioning purposes. Embryos were positioned laterally and imaged on an

Olympus SZX12 stereomicroscope (Olympus, Richmond Hill ON, CA) with a Micropublisher 5.0 RTC camera and QCapture Suite PLUS Software v3.3.1.10 (QImaging, Surrey BC, CA). All images were taken at the same magnification. Eye area was measured using ImageJ software (National Institutes of Health, Bethesda MD, USA) and an Intuos Pro tablet (Wacom, Saitama, JP). Total eye area was outlined manually and measured using ImageJ software (National Institutes of Health, Bethesda MD, USA). The use of a stage micrometer allowed for absolute quantification of eye size. Images of laterally mounted 4 dpf zebrafish embryos were considered to have a coloboma phenotype either if the lobes of the ventral eye were unapposed or if the lobes were in apposition but the fissure was not fully closed. All embryos presented coloboma or small eye phenotypes bilaterally. Following measurement, the embryos were placed in individual PCR tubes to be genotyped (described in 2.1.1). Genotypes of embryos are identified after measurement and coloboma analysis.

To quantify gaps in photoreceptor layer, 4 dpf dissected retinas with removed lens were imaged using a Zeiss AxioImager Z1 compound microscope using an AxioCam HRm camera and Axiovision SE64 Rel.4.8 software (Zeiss, Oberkochen, DE). Photoreceptor-less patches and total eye area were outlined manually and measured using ImageJ software (National Institutes of Health, Bethesda MD, USA).

2.6 Zinc Finger Nuclease Construction

Algorithm-based (<http://pgfe.umassmed.edu/ZFPsearch.html>) detection of suitable zinc finger nuclease (ZFN) target sequences was performed as previously described (Meng et al., 2008), with preference given to purine-rich sequences, guanine-rich sequences, and sequences containing a six-nucleotide spacer region between ZFN recognition sites (Table 2.5).

All selected zinc finger arrays were cloned into the previously described pCS2-HA-GAAZFP-FokI-RR (5' arrays) or pCS2-Flag-TTGZFP-FokI-DD (3' arrays) ZFN expression vectors (Addgene)(Meng et al., 2008). The DD and RR

cleavage domain mutations favour heterodimeric cleavage activity, and therefore reduce ZFN toxicity (Miller et al., 2007; Szczepek et al., 2007). ZFNs containing the *Sharkey* FokI cleavage domain have previously been shown to exhibit greater *in vitro* activity than those containing the wild type FokI cleavage domain (Guo et al.). *Sharkey* variants of the aforementioned heterodimeric ZFN expression vectors (pCS2-Flag-TTGZFP-*Sharkey*FokI-DD; pCS2-HA-GAAZFP-*Sharkey*FokI-RR) were synthesized through site-directed mutagenesis of the original expression vectors using primers listed in Table 2.6.

2.7 Transcription Activator-Like Effector Nuclease (TALEN) construction

Transcription activator-like effector arrays were designed using the TALEN Targeter 2.0 (<https://tale-nt.cac.cornell.edu>). Arrays were each designed as previously described (Cermak et al., 2011) and were designed to consist of 15 to 20 Repeat Variable Diresidues (RVDs) and for each pair of arrays to be 15 to 24 bp apart (Table 2.7). Target sequences were selected if they were positioned either on or near the translation start site of the gene of interest; or within a conserved functional domain.

TALENs were assembled using the Golden Gate TALEN and TAL Effector Kit 2.0 (Cermak et al., 2011). All plasmids that were used were provided in this kit with the exception to the GoldyTALEN modified scaffold, which was designed by Stephen Ekker's group (Bedell et al., 2012; Ma et al., 2013). Both sets of plasmids were acquired from AddGene (Cambridge MA, USA). TALEN assembly was performed in two stages Golden Gate reaction 1 and reaction 2. RVDs were first assembled into intermediate arrays of 1 to 10 repeats (Golden Gate reaction 1). These intermediate arrays are subsequently ligated together to form the final construct within the GoldyTALEN backbone (Golden Gate reaction 2).

2.7.1 Golden Gate Reaction 1

Two intermediate arrays, each containing a portion of the TALEN array were assembled. The first array contains the first 10 RVD modules in the array and will be cloned into the array plasmid pFUS_A. The remaining 1-10 RVD modules were concurrently assembled into a pFUS_B array plasmid. pFUS_B plasmids are numbered 1 to 10 and should be selected according to the number of modules being assembled in that array. For example, if an array of 15 modules were to be assembled, the first 10 modules would be cloned in pFUS_A and the last five modules would be cloned in pFUS_B5.

For both intermediate arrays, module and array plasmids were digested and ligated in a single 20 μ L reaction. Each reaction contains 150 ng of each RVD module plasmid, 150 ng pFUS plasmid, 1.5 μ L bovine serum albumin (BSA, 100x), 1.5 BsaI (New England Biolabs, Ipswich MA, USA), 1.5 μ L T4 DNA ligase (New England Biolabs, Ipswich MA, USA), 1 μ L dATP (25 mM), 2 μ L 10x T4 DNA ligase buffer and sterile water to a total volume of 20 μ L. Reactions were incubated in a thermocycler under the following cycle conditions: 10 cycles of [1] 37°C for 5 minutes, [2] 16 °C for 10 minutes, then subsequently 50 °C for 5 minutes and 80°C for 5 minutes. Then, 1 μ L ATP (25 mM) and 1 μ L Plasmid-Safe DNase (ThermoFisher, Waltham MA, USA) were added to the reaction and incubated at 37°C for 1 hour. The mixture was used to transform 50 μ L One Shot TOP10 chemically competent *Escherichia coli* cells as previously described. These cells were plated on LB agar plates containing 50 μ g/mL spectinomycin with 5-bromo-4-chloro-3-indolyl- β -D-galactopyranoside (X-gal) and isopropyl β -D-1-thiogalactopyranoside (IPTG) for blue/white screening of recombinants.

After the plates were incubated overnight, 6 white colonies from each transformation were picked, re-streaked on a new agar plate and used in a colony PCR reaction. Each reaction consisted of forward and reverse primers, pCR8_F1 and pCR8_R1, respectively. The thermocycler program had 30 to 35 cycles and used an annealing temperature of 55 °C and an extension time of 1

minute 35 seconds. PCR reactions were resolved using gel electrophoresis. Correct clones had a 1200 bp fragment and laddering every 100 bp between 200 and 500 bp. Overnight cultures of correct clones were prepared and bacterial cultures were miniprepped the following morning. These minipreps were validated by restriction digest with Esp3I. Restriction digest reactions also contained 5 mM dithiothreitol (DTT). Correct clones were visualized as a fragment that was 100 bp per RVD repeat in the array.

2.7.2 Golden Gate Reaction 2

Before the TALEN arrays were ligated together, 5 μ g of GoldyTALEN backbone plasmid was linearized by digesting with Esp3I with 5 mM DTT. This reaction was run on a 1% agarose gel and the 2000 bp fragment was gel extracted. To assemble the two intermediate TALEN arrays into the GoldyTALEN plasmid, the digestion and ligation reaction consisted of 150 ng of each pFUS plasmid containing the intermediate TALEN arrays, 150 ng GoldyTALEN plasmid, 150 ng of the last repeat RVD module plasmid, 1 μ L Esp3I (New England Biolabs, Ipswich MA, USA), 1 μ L T4 DNA ligase, 2 μ L 10x Tango buffer (ThermoFisher, Waltham MA, USA), 1 μ L dATP (25 mM) and sterile water to a total volume of 20 μ L. The reaction was incubated in a thermocycler using the following conditions: 10 cycles of [1] 37°C for 5 minutes and [2] 16 °C for 10 minutes, next heated to 37 °C for 15 minutes and 80°C for 5 minutes. 5 μ L of this reaction was transformed into 50 μ L of One Shot TOP10 cells (ThermoFisher, Waltham MA, USA) and cells were plated on LB agar plates containing 50 μ g/mL carbenicillin, with X-gal and IPTG for blue/white screening of recombinants.

Correct clones were identified using colony PCR as previously described for the Golden Gate 1 reaction. Each reaction used TAL_F1 (forward) and TAL_R2 (reverse) primers and PCR reactions were run with an extension time of 3 minutes. Correct clones were visualized using gel electrophoresis and appeared as a large smear with the brightest fragment between 3000 and 5000

bp, a fragment at 1600 bp and laddering from 1000 bp and smaller. The positive clones were prepared as overnight cultures and miniprepmed the following morning. To validate these clones, miniprepmed DNA was digested with BamHI and SphI and run on a 0.6% agarose gel. Correct plasmids from digestion results in two bands at 3000 bp. Fully assembled GoldyTALEN arrays were linearized with SallI prior to TALEN mRNA synthesis. mRNA was synthesized using T3 RNA polymerase as previously described in section 2.4.4.

2.8 Targeted endonuclease protein synthesis and *in vitro* DNA cleavage assay

The *in vitro* DNA cleavage assay was adapted from the *in vitro* transcription-translation assay for rapid screening of ZFNs for sequence-specific cleavage activity (Mani et al., 2005). ZFN or TALEN constructs were transcribed and translated using the TNT SP6 Coupled Rabbit Reticulocyte Lysate System (Promega, Madison WI, USA). Each reaction was composed of 6.25 μ L Rabbit reticulocyte lysate, 0.5 μ L TNT reaction buffer, 0.25 μ L SP6 RNA polymerase, 0.25 μ L amino acid mixture minus leucine, 0.25 μ L amino acid mixture minus methionine, 0.25 μ L RNase inhibitor, 100-500 ng of circular plasmid and DEPC-treated water to a total volume of 12.5 μ L. This reaction was incubated at 30 °C for 90 minutes. Following this incubation, 1 μ L of RNase H was added to each reaction and incubated for 15 minutes at 37 °C.

Following synthesis, 0.1-2 μ L of 5' ZFN or TALEN (RR; control or Sharkey) and 3' ZFN or TALEN (DD; control or Sharkey) protein lysates were combined with 500 ng of target-site-containing plasmid DNA, 2 μ L 10X Restriction Buffer 4 (NEB) or 10X FastDigest Buffer (Fermentas), and 0.5 μ L of NcoI (20 μ L total volume). This reaction was incubated at 37°C for 2 hours. Digested plasmid DNA was purified using a gel extraction kit (QIAquick Gel Extraction Kit, QIAGEN; GeneJET Gel Extraction Kit, Fermentas), and digested DNA fragments were analyzed by agarose gel electrophoresis.

Anecdotal evidence suggests that the plasmid purification step improves the resolution and separation of DNA fragments.

2.9 Zebrafish Mutagenesis

The following amounts of 5' and 3' control or *Sharkey* ZFN mRNAs were injected into single-cell zebrafish embryos: *prion protein 2 (prp2)* ZFN mRNA, 20 pg; and *cone-rod homeobox (crx)* ZFN mRNA, 100 pg. The dosage of each injected ZFN mRNA was titrated and chosen to minimize embryonic toxicity and lethality (producing 65%-75% 'normal' embryos for control ZFN mRNAs). For each category of injected embryos, genomic DNA was isolated from pooled 24 hours post-fertilization embryos, essentially as previously described (Meeker et al., 2007). PCR fragments containing the ZFN recognition site were amplified and cloned into pCR4-TOPO (*crx*), or pCR2.1-TOPO (*prp2*). The cloned product was used to transform OneShot TOP10 cells (Life Technologies, Burlington ON, CA). Following transformation, 96 independent colonies from each sample were picked, and from these the cloned PCR product was amplified using *Taq* DNA polymerase. The amplified clones were sequenced using M13R primer to determine the frequency and type of mutations present at the ZFN target-site.

One-cell stage embryos were injected with 200 pg of TALEN mRNA. After 24 hours of development, pools of 24 hpf embryos were dechorionated and their genomic DNA was isolated. The remaining embryos were raised to adulthood to analyse for germline mutation transmission. Region of interest was PCR-amplified from isolated genomic DNA and this fragment was gel purified, and cloned into pCR2.1-TOPO. The cloned product was used to transform OneShot TOP10 cells (Life Technologies, Burlington ON, CA). Individual colonies were picked and suspended in 10 μ L of HRM mastermix (described in section 2.7). Amplified clones were sequenced using M13R or M13F primer to determine the frequency and nature of mutations present at the TALEN target site.

2.10 High resolution melt curve analysis

High-resolution melt curve analysis was used to identify polymorphisms and mutations in genomic DNA. Primers were optimized for HRM and designed to have a length of ~22 nucleotides long, a %GC content of 55%, a melting temperature of ~62 °C, and to amplify a ~90 bp amplicon (Table 2.8).

When analysis was performed using the ABI 7500 HT Fast RT PCR machine (ThermoFisher, Waltham MA, USA), the following was combined for each reaction: 5 µL 2x MeltDoctor HRM Master Mix (ThermoFisher, Waltham MA, USA), 0.6 µL each of 5 µM forward and reverse primers, 2 µL DNA template and 1.8 µL sterile water.

When reactions were prepared using the Type-it HRM PCR Kit (Qiagen, Hilden, DE), each reaction is composed of 5 µL 2x HRM PCR Master Mix, 7 µL each of 10µM forward and reverse primers, 2 µL template DNA and 1.6 µL sterile water. PCR reactions were performed on a Rotor Gene Q qPCR machine (Qiagen, Hilden, DE)

Both types of reactions were run under the following reaction conditions: [1] initial denaturation 95 °C for 5 minutes; 40 cycles of denaturation at 95 °C for 10 seconds, annealing and extension at 60 °C for 30 seconds; and an HRM ramp where the temperature was increased by 0.1 °C every second until the temperature rose from 65 °C to 95°C. Melting profiles were analysed using either the HRM 2.0 Software (ThermoFisher, Waltham MA, USA) or the Rotor Gene Software 2.0 (Qiagen, Hilden, DE). Variants were confirmed by Sanger sequencing as previously described in section 2.3.6.

2.11 Analyses of targeted endonuclease toxicity

The following amounts of 5' and 3' control or *Sharkey* ZFN mRNAs were injected into single-cell zebrafish embryos: *prp2* ZFN mRNA, 20 pg; and *crx* ZFN mRNA, 100 pg. 200 pg each of 5' and 3' control or *Sharkey WW domain containing transcription regulator 1 (wwtr1)* TALEN mRNAs were injected into single-cell zebrafish embryos. At ~24 hpf, embryos were categorized

according to morphological phenotype (normal, ‘monster’, which indicates any morphological phenotype that differs from wild type, or dead) and counted. The morphological phenotypes of control, uninjected embryos were likewise assessed. Each set of injections/assessment was conducted in triplicate.

2.12 RNA sequencing

RNA sequencing was performed on *aldh1a3*^{-/-}; *cyp1b1*^{-/-} and wild type sibling embryos. Dissected heads from 48 hpf zebrafish embryos were collected for RNA sequencing. Tissue from 40 to 60 embryos was combined to obtain an adequate amount of RNA for sequencing. To stabilize cellular RNA, individual dissected heads were stored in 10 µL RNAlater at 4°C (Life Technologies, Burlington ON, CA). Genomic DNA was extracted from the dissected tails using the sodium hydroxide extraction method as previously described. Collected genomic DNA was used to identify homozygous mutants. Dissected heads were pooled and sent to Otagenetics Co (Norcross GA, USA) for analysis. Gene ontology analysis was performed using the online tool, Database for Annotation, Visualization and Integrated Discovery (DAVID).

2.13 Statistical Analysis

All bar graphs and box and whisker plots were constructed in Microsoft Excel. Categorical data was analysed with a Fisher’s Exact test. Bonferroni adjustments were performed to account for multiple comparisons. Quantitative data was analysed using Analyses of Variance (ANOVA) followed by a post-hoc Tukey’s Honest Significant Difference test. All statistical analyses were performed in R (<http://r-project.org>).

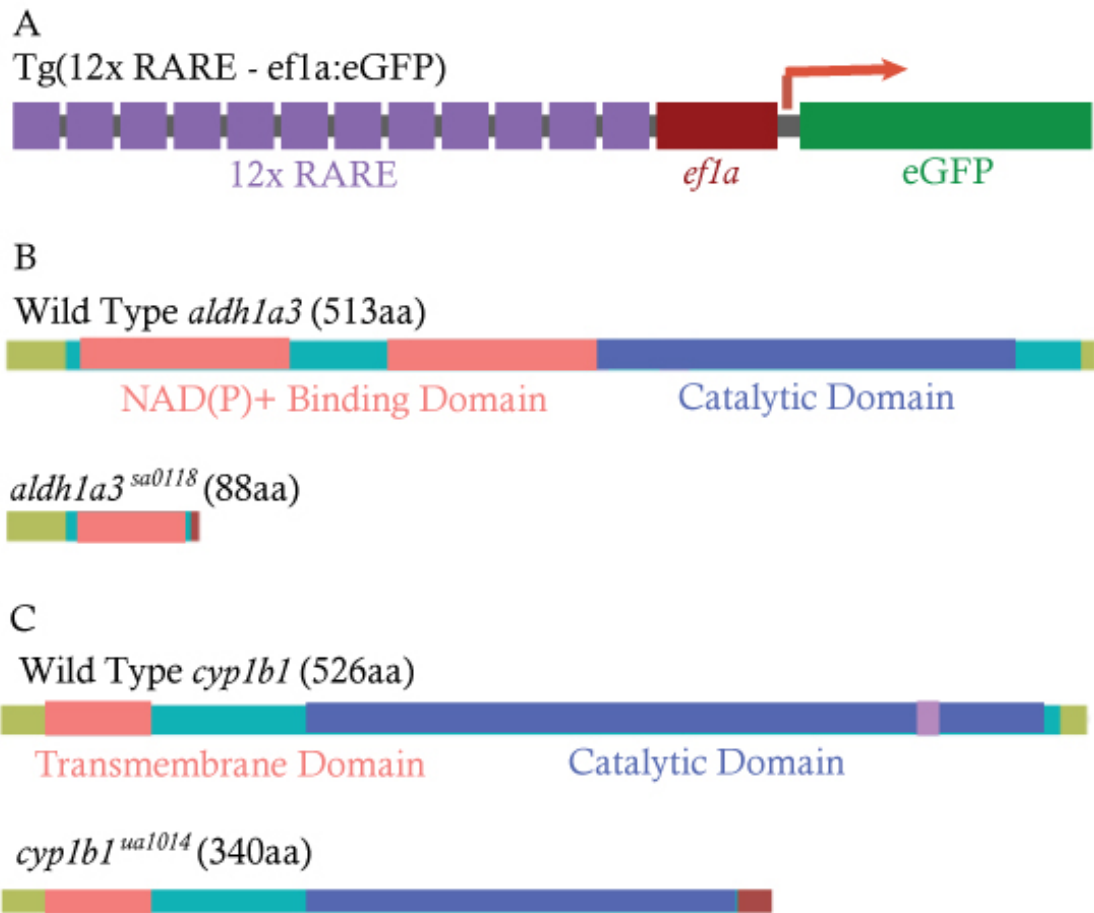


Figure 2.1: Diagrams of transgenes and mutations in zebrafish lines used. A) Tg(12xRARE-*ef1a*:eGFP) is composed of 12 repeats of Retinoic Acid Response Element sites upstream of an *ef1a* promoter driving the transcription of eGFP. B) Diagram of *aldh1a3* protein with known conserved and functional domains indicated. The sa0118 allele contains a G to A transition at nucleotide position 264 of the coding sequence. This results in a premature stop codon at codon 88. C) Diagram of *cyp1b1* protein with known conserved and function domains indicated. The ua1014 allele contains a 13 bp deletion at nucleotide position 951. This results in 33 additional amino acids and a premature stop codon at amino acid position 340.

Table 2.1: Primers used for genotyping carriers of mutant alleles

Gene	Forward Primer (5' – 3')	Reverse Primer (5' – 3')	Size (bp)	T(m) (°C)
<i>aldh1a3</i>	GTCACTGTAGTCTAA CATGCTGCTG	TGAGCTCGCTAATGA AACGTCAAAAT	253	63
<i>cyp1b1</i>	GAACCCTCTTTGACC AGTTTAAAG	CGTTGGGTCAAATG GGCACACCCGTTG	503	63

Table 2.2: Translation-blocking morpholino sequences and injected dosage.

Gene	Sequence (5' – 3')	Dosage (ng)
<i>aldh1a2</i>	GCAGTTCAACTTCACTGGAGGTCAT	4
<i>p53</i>	GCGCCATTGCTTTGCAAGAATTG	2

Table 2.3: Primer sequences used for PCR-based RNA riboprobe synthesis

Gene	Forward (5' – 3')	Primer	Reverse Primer (5' – 3')	Promoter	Size (bp)	T(m) (°C)
<i>eya2</i>	ATGCGAGCTTA CGGACAG		TTCTTGTATGTG TTGTAGATCTCT TTA	T7	1000	51.5
<i>foxn4</i>	GAGAAGGTAGA GAATAAGATGA GCGG		TGCTCCCTCTC GCTAAATACTT CAC	T3	1041	58
<i>opn1lw1</i>	TTCTGCTGGGG TCCTTACAC		TGTACATGGGC AGGCATCTA	T3	718	60.1
<i>opn1mw1</i>	CCGTCACCACA ATTTTCTT		TTCCATTGCCTC CACCTAAC	T3	632	59.8
<i>opn1sw1</i>	ATTCCGATGAG CCAAACAAG		TTGGACAGGAG CAGACAGTG	T3	753	60
<i>opn1sw2</i>	TGCTCTTGTGG ACCTGACTG		ATGTTCAGCAA GCCAAGACC	T3	646	60
<i>rho</i>	TGCACTTCTTCA TCCCCTG		CTGCTGCGTTT TAGGAGGAG	T3	712	59.8
<i>tbx5a</i>	GTCACGTCTTA CCAAAACCACA		ACATGTGTGAT GTGTCCAGTG	T7	899	60
<i>vax2</i>	ACAGGAACGAA CTTCGCTAGAC		ATTACAGGAGC GCTTTTAGGA	T7	1030	60

T3 promoter sequence (5'-AATTAACCCTCACTAAAGGGA-3') added to the 5' end of indicated reverse primer.

T7 (5'- TAATACGACTCACTATAG-3') promoter sequence added to the 5' end of indicated reverse primer.

Table 2.4: Plasmids used for RNA riboprobe synthesis

Gene	Vector	Linearize)	Promoter
<i>aldh1a3</i>	pSPORT	EcoRI	T3
<i>eGFP</i>		NotI	SP6

Table 2.5: ZFN target sequence

Gene	Target Sequence (5' – 3')
<i>crx</i>	<u>AG</u> CCCCATATGCTGTGAACGGGTTA
<i>prp2</i>	CCACCTCCCTACCTGGTGCTGGAGG

ZFN recognition sites are underlined.

Table 2.6: Site-directed mutagenesis primers

Gene	Mutation	Forward Primer (5' – 3')	Reverse Primer (5' – 3')
<i>SharkeyFokI-DD</i>	S418P	ATTGAATTAATTG AAATTGCCAGAAA <u>TCCCACTCAGGAT</u> AGAATTCTTG	CAAGAATTCTATC CTGAGTGGGATTT CTGGCAATTTCAA TTAATTCAAT
<i>SharkeyFokI-RR</i>	K441E	GAAAGTTTATGGA TATAGAGGT <u>G</u> AAC ATTTGGGTGGATC AAGGAA	TTCCTTGATCCAC CCAAATGTT <u>C</u> ACC TCTATATCCATAA ACTTTC

Altered nucleotide sequences are underlined.

Table 2.7: TALEN target sequence.

Gene	Target Sequence (5' – 3')
<i>bcmo1</i>	<u>ACAACCAT</u> TGGTTTGATGGAATGGCACTTTTGC <u>CACAGT</u> TTTGCAATTAAT
<i>bco2a</i>	<u>ACGACCACTATTACAGGTAACGTCCCTAGCTGGATCAAGGGCAATTT</u> CCTCAGG
<i>hoxb1b</i>	GGTTCTAACACTTATAGTTCGAAAGTTGGGTGTTTTCTGT <u>AGAGCAAGAATACTTGCC</u>
<i>wwtr1</i>	TGAGCGGTAATCCTCTCCAGCCGATACCGGGCCACCAGGTGATCCATGTCGCCA

TALEN recognition sites are underlined.

Table 2.8: Primers for HRM analysis

Name	Sequence (5' – 3')	T _m (°C)	Size (bp)
<i>bcmo1</i> F	TTGGAGAGACGACATACAACCA	55.7	109
<i>bcmo1</i> R	AAACGTAATGGCCAATCAAGGT	55.1	
<i>bco2a</i> F	CAGAGCCCATTACGACCACTATT	56.6	106
<i>bco2a</i> R	ACTCACCTGCTTCTTCCGATCT	57.9	

3 Retinoic acid synthesis enzymes function in early zebrafish eye development

3.1 Introduction

Retinoic acid (RA) is a small lipophilic molecule that is derived from vitamin A. As a morphogen, RA plays an essential role in morphogenesis and patterning of several tissues in the developing embryo including the eye. In avian and murine models, vitamin A deficiency causes a complex spectrum of abnormalities in the embryo. Vitamin A studies in rodents revealed congenital malformations spanning several organ systems, including the kidneys, brain, genito-urinary tract, eyes and the heart (Wilson et al., 1953). Vitamin A is required for vertebrate eye development, as severe ocular defects have been observed as a result of gestational vitamin A deficiency. In mouse, RA is required for the growth of the ventral retina, optic vesicle invagination and anterior segment formation (Duester, 2008, Matt 2005, Molotkov 2006).

Vitamin A is an essential dietary nutrient that must be converted into its bioactive derivative RA to serve as a signalling molecule. Vitamin A is synthesized into RA through two sequential oxidation reactions, which convert retinol to retinaldehyde, and retinaldehyde to RA (Figure 1.4). Aldehyde dehydrogenase (Aldh in zebrafish, RALDH in mouse) enzymes catalyze the second reaction, converting retinaldehyde to RA. Additionally, cytochrome p450 1b1 (Cyp1b1) can catabolize both retinaldehyde and RA synthesis steps in an Aldh-independent manner (Chambers et al., 2007). During early vertebrate development, the genes encoding for Aldhs, Cyp1b1 and RA receptors all have discrete sites of expression, which lends to the specificity of retinoids within the developing embryo (Blentic et al., 2003). Precise spatial restriction of RA synthesis genes and RA signalling within the vertebrate eye suggests that high levels of RA are required in the dorsal and ventral domains of the eye, however the function that RA has in this tissue is yet to be fully understood. There are several hypothesized roles of RA in the early development of the vertebrate eye including mediation of choroid fissure

closure, establishment of dorsoventral patterning and/or regulation of eye size.

One possible role for high levels of RA within dorsal and ventral regions of the eye is the establishment or maintenance of dorsoventral retinal patterning. Exogenous RA results in the ventralization of the eye, manifesting as the expansion of the ventral patterning marker, *vax2* (Hyatt et al., 1996b). At 28 hpf, zebrafish RA signalling has been found to be spatially restricted to the dorsal and ventral domains of the developing retina. RA synthesis enzymes are also restricted to different regions of the zebrafish eye: *aldh1a3* is expressed in the ventral retina; and *aldh1a2* is expressed in the dorsal retina. While an important role for RA in vertebrate eye development is clear, studies in rodents, zebrafish and *Xenopus* have produced conflicting results (Gregory-Evans et al., 2004; Hyatt et al., 1996b; Lupo et al., 2005; Marsh-Armstrong et al., 1994; Sen et al., 2005).

In humans, mutations in *CYP11B1* have been reported in patients with the syndrome Peters Anomaly, a severe disorder affecting vision and manifesting as ocular defects including glaucoma, cataracts, and microphthalmia. Additionally, several variants of *CYP11B1* were identified in patients with non-syndromic microphthalmia (Prokudin et al., 2014). *CYP11B1* is expressed in human embryonic and adult ocular tissues, including the retina and the iris. *CYP11B1* expression is higher in embryos in comparison to adults and is therefore speculated to play an essential metabolic role in the development and maturation of the eye (Kaur et al., 2011). Expression of *Cyp11b1* ortholog in chick is associated with RA activity during early development. Zebrafish *cyp11b1* is expressed in both the dorsal and ventral domains of the eye (French et al., 2009). In zebrafish, *cyp11b1* expression domains overlap with the domains of RA synthesis enzymes *aldh1a2* and *aldh1a3* in the retina. This suggests that there could be compensatory roles in RA synthesis during eye development.

Interestingly, mouse *Raldh* mutants showed that while RA is not necessary for dorsoventral retinal patterning, the action of RA occurs

specifically in neural crest-derived periocular mesenchyme (POM) (Matt et al., 2008). *Raldh1*, an RA synthesis gene localized to the murine dorsal retina, synthesizes sufficient RA to direct POM migration in the eye (Molotkov et al., 2006). Mutations in both *Raldh1* and *Raldh3* cause overgrowth of POM due to reduction of POM apoptosis. The resultant embryos had thickened eyelids and severe ventral eye defects (Matt et al., 2005; Molotkov et al., 2006). Zebrafish studies have also shown a role of RA in POM cell migration. Pharmacological inhibition of RA signalling in zebrafish results in fewer POM cells localizing to the choroid fissure (Matt et al., 2005; Matt et al., 2008). Additionally, decrease in *cyp1b1* levels in zebrafish correlated with the decrease of RA signalling in the POM (Williams and Bohnsack, 2015). As *Cyp1b1* and other RA synthesizing enzymes are expressed within the retina and not the POM, RA synthesized within the retina may be released by these cells and act within neighbouring POM cells. Further, it is unknown which enzyme in the retina synthesizes RA that will eventually signal within the POM cells.

Molecularly, isolated occurrences of microphthalmia and anophthalmia can be due to the mutations in many genes encoding different signalling and structural proteins in the developing eye including Wnt and RA signalling. Mutations in genes that are members of the RA synthesis pathway have been identified as causative in MAC patients (Aldahmesh et al., 2013; Fares-Taie et al., 2013; Mory et al., 2014; Roos et al., 2014; Yahyavi et al., 2013). As high levels of RA are found in the ventral portion of the embryonic eye, when RA levels are depleted, ocular defects often manifest in the ventral domain of the retina (Marsh-Armstrong et al., 1994). Tight control of RA is critical for choroid fissure closure, as both RA deficiency and excess during embryogenesis induces colobomata in mice and zebrafish (Bohnsack and Kahana, 2013; See and Clagett-Dame, 2009). Studies in pigs and rats have shown that maternal vitamin A deficiency results in piglets with anophthalmia and pups with coloboma (Maden, 2002; Wilson et al., 1953). Avian species lack ventral optic stalk and ventral retina in the absence of vitamin A (Maden et al., 2007).

Zebrafish embryos treated with RA synthesis inhibitors develop microphthalmia. The slow rate of eye growth may suggest that proliferation of ocular tissue may be impaired. Similarly, when RA is deprived in chick embryos, eyes were smaller than control embryos and the choroid fissure failed to fuse throughout ocular development (Sen et al., 2005). Pan-inhibition of RA synthesis or exogenous RA treatment alters ventral eye development (Lupo et al., 2005). Treatment of organisms with exogenous RA does not mimic the endogenous dorsoventral gradient of RA within the eye (Marsh-Armstrong et al., 1994; Perz-Edwards et al., 2001). Additionally, these embryos are often exposed to concentrations of RA that far exceed physiologically relevant levels and pharmaceutical pan-inhibition of RA synthesis does not provide insight on the single or combinatorial roles of RA-synthesizing enzymes in ocular development. Furthermore, exact spatial requirements for RA cannot be determined based on this approach alone.

We analyzed the role of *aldh1a3* and *cyp1b1* in ocular development using zebrafish mutants. Despite their unique expression patterns, our studies have found no overt phenotypes in *aldh1a3* mutants or *cyp1b1* mutants. This finding suggests that RA synthesizing enzymes within the retina are functionally redundant and that RA generated by remaining enzymes are acting cell-nonautonomously. To better understand how RA synthesized in the retina is required for vertebrate eye development, we used a combinatorial approach to block RA synthesizing enzymes thereby reducing endogenous levels of RA during embryogenesis. To achieve this, we used *aldh1a3* and *cyp1b1* zebrafish mutants coupled with Aldh1a2 knockdown. We hypothesize that reduction of RA contributes to defects in early eye development including morphology, choroid fissure closure and ocular patterning. Reduction of *aldh1a3* and Aldh1a2 results in an increased incidence of coloboma and decreased eye size. Interestingly, loss of ventral specific *aldh1a3* regulates RA levels within the entire eye. These results suggest multiple sources of RA within the eye involved in eye development. Additionally, RA synthesis

enzymes restricted to the ventral domain of the eye contribute to RA levels in both the dorsal and ventral retina. Given that RA is essential for proper ocular development, we wanted to determine the contributions of RA-synthesizing enzymes to embryonic eye development.

3.2 Results

3.2.1 *Aldh1a3* mutants are strong hypomorphs

The zebrafish *aldh1a3* sa118 allele contains a G to A transition that results in the premature truncation of the protein (Kettleborough et al., 2013). We hypothesized that if the mutant allele was not functional, *aldh1a3* mutants would demonstrate a loss of *aldh1a3* expression. Compared to wild-type embryos, *aldh1a3* expression is reduced within the ventral domain of the retina in heterozygous *aldh1a3* carriers (Figure 3.1A, B). A greater reduction, but not a complete loss, of *aldh1a3* expression is observed in homozygous *aldh1a3*^{sa0118/sa0118} mutants (hereafter referred to as *aldh1a3*^{-/-}) (Figure 3.1C). The reduction of *aldh1a3* expression in heterozygous and homozygous mutants suggests those mutant transcripts are degraded through nonsense-mediated decay. While we cannot conclude that these mutants are null mutants from these findings, it can be inferred by the strong reduction of *aldh1a3* expression that these mutants are strong hypomorphs.

3.2.2 *Aldh1a3* mutants have reduction of RA signalling in both dorsal and ventral retina.

Expression domains of *aldh1a2* and *aldh1a3* are restricted to the dorsal and ventral domains, respectively of the zebrafish retina (French et al., 2009). We hypothesize that the spatial restriction of these genes are correlated with RA synthesis and RA signalling within these regions, such that *aldh1a2* synthesizes RA that initiates RA signalling in the dorsal eye and *aldh1a3* synthesizes RA and initiates signalling in the ventral eye. We assayed for levels of RA signalling using a transgenic RA reporter line, *Tg(12xRARE – efla:egfp)* (Waxman and Yelon, 2011). At 48 hpf, we detect RA signalling in

the dorsal and ventral domains of the eye corresponding to the region of *aldh1a3* and *aldh1a2* expression (Figure 3.2A). Although *aldh1a3* expression is localized only to the ventral eye, *aldh1a3*^{+/-} mutants exhibit a mild reduction of GFP expression in both dorsal and ventral retina (Figure 3.2B). Homozygous mutants exhibit profound reduction of GFP expression in the dorsal and ventral regions of the eye. Depletion of *aldh1a3* results in a loss of *RARE:egfp* expression in ventral eye, as expected (Figure 3.2C). Further, these findings show that *aldh1a3* is also involved in regulating dorsal RA levels in the eye. However the mechanism through which this happens remains to be elucidated. These results provide one possible explanation as to why mouse *Raldh1* mutants are viable with no discernable eye defects, as *Raldh3* may generate enough RA to fulfill RA function in this tissue (Molotkov et al., 2006).

3.2.3 *aldh1a3* mutants have normal dorsoventral retinal patterning

RA synthesis enzymes are spatially restricted to the dorsoventral axis of the developing retina. It was previously observed that zebrafish treated with exogenous RA produced a ventralized eye (Hyatt et al., 1996b). However, previous research has found confounding results of whether RA signalling affects dorsoventral patterning. This led us to hypothesize that RA generated in different domains of the retina control dorsal versus ventral patterning of the retina. Thus, we expect that *aldh1a3* mutants would have a dorsalized eye with the reduction of ventral eye identity. Observation of dorsal and ventral retina markers, *tbx5a* and *vax2* respectively, show no change in domain or expression intensity among wild type, *aldh1a3* heterozygotes and *aldh1a3*^{-/-} mutants (Figure 3.3). Although *aldh1a3* is strongly reduced, dorsoventral patterning is normal. Our findings correspond with the lack of dorsoventral patterning defects observed in *Raldh1; Raldh3* double mutants (Matt et al., 2005; Matt et al., 2008; Molotkov et al., 2006; See and Clagett-Dame, 2009).

3.2.4 aldh1a3 mutants do not show detectable defects in migration of periocular mesenchyme

Previous research suggests a role for RA in the proliferation and migration of POM cells. Pharmacological inhibition of RA signalling in zebrafish reduces POM migration to the choroid fissure (Lupo et al., 2005). Ventral POM in mouse *Raldh1; Raldh3* double mutants had decreased apoptosis that resulted in POM overgrowth (Matt et al., 2005; Molotkov et al., 2006). In order to investigate RA function in the POM, *eyes absent 2 (eya2)* expression was examined in *aldh1a3*^{-/-} mutants. During normal zebrafish development, *eya2* is expressed in the POM between 28 hpf and 48 hpf (Figure 3.4). Overall expression of *eya2* is not altered in *aldh1a3*^{-/-} mutants. RA signalling in zebrafish and mouse embryos has been reported to be necessary for the proper maintenance and migration of POM cells (Lupo et al., 2005; Matt et al., 2005; Matt et al., 2008; Molotkov et al., 2006). Our observed reduction of RA signalling is not sufficient to prevent POM migration to the eye. Since low levels of RA signalling persist in *aldh1a3* mutants, these results suggest that POM migration requires only a low level of RA in the ventral eye.

3.2.5 Loss of RA synthesis enzymes result in decreased eye size

Microphthalmia has been induced in mouse models by reduction of RA levels in the developing retina (Matt et al., 2008; Molotkov et al., 2006). To determine if *aldh1a3* contributes to microphthalmia, total eye area of 4 dpf wild type and *aldh1a3*^{-/-} mutants was measured. There is no significant difference in eye size between wild type and *aldh1a3*^{-/-} mutant embryos. Despite the reduction of RA signalling in the ventral eye, eye size overall is unaffected in *aldh1a3*^{-/-} (Figure 3.5A). This would suggest that other factors, likely other RA synthesis enzymes, have a possible compensatory role in the eye. Studies in mouse have found that knockdown of one *Raldh* within the eye has a subtle effect in eye morphogenesis while knockdown of both *Raldh1* and

Raldh3 reveals more profound eye defects (Matt et al., 2005). To examine the contribution of RA produced by both Aldh present in the retina, *aldh1a3*^{-/-} mutants were injected with previously described *aldh1a2* translation-blocking morpholino (Alexa et al., 2009). Knockdown of Aldh1a2 in an *aldh1a3*^{-/-} mutant leads to significantly reduced mean eye size in morphomutants (Figure 3.5A, Table 3.1) suggesting that, like mouse, RA synthesis enzymes together are critical for eye size.

The use of morpholino for zebrafish gene knockdown may also cause off-target effects within the organism. Namely, morpholinos are able to activate tumour protein p53 (p53) -mediated cell death pathway (Bedell et al., 2011; Gerety and Wilkinson, 2011). It is possible that the microphthalmic phenotype observed is an artefact of non-specific apoptosis caused by the morpholino. To control for these non-specific effects, eye size was measured in wild type and *aldh1a3*^{-/-} mutants co-injected with *aldh1a2* and *p53* morpholino. Co-knockdown of *p53* causes decreased eye size in injected wild type embryos and *aldh1a3*^{-/-} morphomutants (Figure 3.5B, Table 3.2). This finding suggests that RA produced by Aldh1a2 is sufficient to maintain eye size in the developing zebrafish.

3.2.6 Loss of RA synthesis enzymes Aldh1a3 and Aldh1a2 results increased incidence of coloboma

Generation of the choroid fissure is essential for the entry of ocular vasculature during eye development. The closure of the choroid fissure is essential to the formation of a continuous tissue (Harada et al., 2007). Deletion of combinations of RA-synthesis enzymes or RARs in mice results in embryos with severe ocular defects, including coloboma (See and Clagett-Dame, 2009). Human studies have demonstrated a strong correlation between MAC and mutations in genes involved in RA synthesis and signalling. We hypothesize that, if RA plays a role in choroid fissure closure, knockdown of ventrally expressed *aldh1a3* in zebrafish would yield an increased incidence of

coloboma. To assess colobomatous phenotypes, wild type and *aldh1a3*^{-/-} mutant zebrafish were grown to 4 dpf. Neuroepithelial fusion of the zebrafish ocular fissure initiates at 36 hpf and is completed between 48 and 60 hpf. A persistent ocular fissure at 4 dpf (96 hpf) is indicative of fissure closure defects. Incidence of coloboma in *aldh1a3*^{-/-} mutants is unchanged in comparison to wild type siblings (Figure 3.6A, Table 3.3). Due to the combinatorial effect we have shown in the decreased RA levels in the eye and the functional redundancy of mouse RALDH enzymes, we hypothesized that reduction of *Aldh1a2* in *aldh1a3*^{-/-} mutants would reveal a coloboma phenotype. Knockdown of *Aldh1a2* in *aldh1a3*^{-/-} mutants significantly increases the coloboma phenotype relative to uninjected wild type siblings (p-value = <0.0001) and uninjected *aldh1a3*^{-/-} mutants (p-value = <0.0001), however no significant difference of coloboma phenotype is observed between *Aldh1a2*-injected wild type embryos and *Aldh1a2*-injected mutants (p-value = 0.38) (Table 3.3). This suggests that a reduction in *Aldh1a2* has no additive effect on coloboma phenotype in *aldh1a3*^{-/-} mutants. The lack of additive effect between *Aldh1a2* and *Aldh1a3* may be expected, as the genes that encode these enzymes are not expressed in the same domains of the retina.

The failure of the lobes of the choroid fissure to fuse may be attributed to death of POM or retinal cells. To exclude off-target effects of morpholino caused by p53-mediated apoptosis, the analysis was repeated with the co-injection of *p53* morpholino with *aldh1a2* morpholino. Results obtained from *p53* morpholino co-injections recapitulate observations in *Aldh1a2* injection alone: incidence of coloboma increased in comparison to all other treatments (p-value<0.0001) with the exception to uninjected *aldh1a3*^{-/-} mutants (p-value=1) (Figure 3.6B, Table 3.4). Previous studies have suggested that abnormal activation of apoptotic cell death pathways is associated with ocular coloboma (Moosajee et al., 2008; Ozeki et al., 2000). These findings suggest the requirement for RA synthesized by *aldh1a2* in the retina to close the

choroid fissure and this process may be mediated by apoptosis in a p53 independent manner.

3.2.7 Depletion of three RA synthesis enzymes greatly reduces RA signalling in the dorsal and ventral retina

Studies in mouse have found that RALDH1, RALDH2 and RALDH3 functionally compensate for each other despite having non-overlapping expression patterns (Halilagic et al., 2003; Matt et al., 2005; Molotkov et al., 2006). To better understand the single and combinatorial roles of RA synthesis genes in the zebrafish eye, we examined the levels of RA signalling in the absence of Aldh1a2, *aldh1a3* and *cyp1b1* individually and in combination. Homozygous mutations in *cyp1b1^{ua1014/ua1014}* (hereafter referred to as *cyp1b1*^{-/-}) caused a reduction of RA signalling in the dorsal retina, but not the ventral domain (Figure 3.7C). Loss of *aldh1a3*^{-/-}; *cyp1b1*^{-/-} resulted in a reduction of RA signalling in the dorsal and ventral domains of the retina in comparison to wild type (Figure 3.7D). Knockdown of dorsally expressed Aldh1a2 ablates RA signalling levels in the dorsal retina but not in the ventral retina (Figure 3.7E-H). Further reduction of RA signalling is observed in Aldh1a2 knockdown in *aldh1a3*^{-/-} mutants, which results in the ablation of RA signalling levels in the dorsal eye and a great reduction of RA signalling levels in the ventral retina (Figure 3.7F). Analysis of Aldh1a2; *aldh1a3*^{-/-}; *cyp1b1*^{-/-} morphomutants reveals a profound reduction of RA signalling greater than the reduction observed in any of the double knockdowns. This supports combinatorial action of all three RA synthesis enzymes in regulating RA levels in the eye. Interestingly, a small amount of *RARE:egfp* expression persisted in triple knockdown. This suggests that while these genes are important to establish RA levels within the retina, a small amount of RA remains, possibly due to the incomplete knockdown of these RA-synthesis genes. Alternatively, there may still be another yet undiscovered source of RA in the developing eye.

3.3 Discussion

RA synthesis levels are tightly regulated in the dorsal and ventral domains of the developing eye (Lupo et al., 2011; Lupo et al., 2005; Matt et al., 2005; Molotkov et al., 2006). Furthermore, human studies have demonstrated that mutations in ventrally localized ALDH1A3 are associated with MAC phenotypes, namely microphthalmia and coloboma (Aldahmesh et al., 2013; Fares-Taie et al., 2013; Mory et al., 2014; Roos et al., 2014; Yahyavi et al., 2013). Our study reveals that MAC phenotypes are not fully recapitulated in zebrafish *aldh1a3* mutants. However, concomitant with a loss of Aldh1a2, *aldh1a3*^{-/-} mutant embryos revealed a coloboma phenotype (Figure 3.6). We propose that RA synthesis enzymes have partial functional redundancy to maintain RA levels within the retina. Through targeted ablation of Cyp1b1 and Aldh proteins, we demonstrate that RA signalling is not restricted to the domain in which the RA is synthesized. In the absence of Aldh1a3, embryos exhibit no severe defects in eye size or dorsoventral patterning.

3.3.1 *aldh1a3* contributes to RA signalling in the dorsal and ventral retina

Our study shows that loss of *aldh1a3* reduces RA signalling in the dorsal and ventral retina. This finding suggests that RA synthesized in the ventral eye contributes to RA in the dorsal retina through an, as yet, unknown mechanism. RA has been shown to signal in a paracrine fashion, such that RA is released from Aldh-expressing cells and initiates signalling in neighbouring cells (Molotkov et al., 2006). As previously described, loss of either *Raldh1* or *Raldh3* does not result in a loss of RA that impedes POM. In mouse, *Raldh1* and *Raldh3* provide an RA signal that functions to control morphogenetic movements in neighbouring POM cells of the ventral eye (Molotkov et al., 2006). However this functional redundancy has not previously been noted in the dorsal retina. The presence of dorsal RA signalling by RA synthesized in the ventral retina suggests that RA synthesized in one domain of the eye can diffuse throughout the tissue and directly initiate signalling. A second

possibility to explain the ability of RA synthesized in the ventral retina to alter RA signalling in the dorsal retina is that RA produced by *Aldh1a3* could indirectly alter RA signalling levels through the regulation of RA synthesis genes or enzymes in the dorsal eye.

*3.3.2 Loss of *aldh1a3* does not affect dorsoventral patterning*

Localized dorsal and ventral expression of RA-synthesis enzymes led to the hypothesis that RA is involved in retinal patterning. In zebrafish and *Xenopus*, pharmaceutical inhibition of RA signalling causes loss of ventral retina (Durston et al., 1989; Holder and Hill, 1991; Sive et al., 1990). Further, ventralization of the zebrafish eye, as visualized by an expansion of the *vax2* expression domain results from exogenous RA treatment (Hyatt et al., 1996b). Despite the reduction of *RARE:egfp* representing a decrease in RA signalling levels in the ventral eye, *aldh1a3*^{-/-} embryos possess no overt morphological defects. Additionally, our mutants exhibit no molecular abnormalities in dorsoventral patterning genes, as wild type expression of *tbx5a* in the dorsal retina and *vax2* and ventral retina was observed. As *tbx5a* and *vax2* precede the retinal expression of *aldh1a3* and *aldh1a2*, we used these markers to ascertain the size of dorsal and ventral domains in the eye (Chapman et al., 1996; Mui et al., 2002; Sen et al., 2005). Genetic mouse models also show that RA is not required for early dorsoventral patterning (Matt et al., 2005; Molotkov et al., 2006; See and Clagett-Dame, 2009). Our findings suggest that RA signalling occurring within the retina is not required for establishing dorsoventral patterning, similar to that found in mouse may be required for later patterning events, such as retinotectal mapping or other ocular developmental processes, such as controlling morphogenetic movements of optic cup formation.

*3.3.3 *aldh1a3* may not have a role in POM migration*

To examine the role of RA function in the POM, we examined the effect of RA depletion on expression of a POM-specific marker. POM localization was

not obviously different between *aldh1a3*^{-/-} embryos and wild type siblings. This reflects what is observed in mouse where *Raldh1* and *Raldh3* can function alone to supply sufficient levels of RA for the control of POM invasion (Matt et al., 2005; Molotkov et al., 2006). Loss of both *Raldh1* and *Raldh3* is necessary to observe defects in POM. Our findings taken together with the observations made in mouse suggest that *aldh1a2* and/or *cyp1b1* supply sufficient levels of RA in the eye to allow for paracrine signalling within the POM. As the RA synthesis enzymes have compensatory functions within the retina, it would be interesting to observe how RA depletion in *Aldh1a2*; *aldh1a3*^{-/-}; *cyp1b1*^{-/-} morphomutants affects POM migration.

3.3.4 Retinoic acid plays a role in regulating eye size

Mutations in the RA synthesis gene *Aldh1a3* have been observed in human patients that present with MAC (Aldahmesh et al., 2013; Fares-Taie et al., 2013; Mory et al., 2014; Roos et al., 2014; Yahyavi et al., 2013). Zebrafish *aldh1a3*^{-/-} mutants do not have microphthalmia. To account for the functional redundancy of Aldh enzymes within the retina, we knocked down *Aldh1a2* in *aldh1a3*^{-/-} mutants. Concomitant loss of *Aldh1a2* causes a microphthalmic phenotype in *Aldh1a2/aldh1a3*^{-/-} morphomutants. Further, loss of *Aldh1a2* in wild type embryos also results in microphthalmia suggesting that RA synthesized by *Aldh1a2* is sufficient in maintaining eye size in embryonic zebrafish. Microphthalmia can occur as a consequence of a several potential mechanisms, including but not limited to developmental delay, increased cell death, and reduced cell proliferation (Stenkamp et al., 2002). Currently, specific mechanisms in which RA deficiency causes microphthalmia are not clear. As a reduction in eye size can be influenced by many factors, it would be interesting to investigate if microphthalmic phenotypes observed in RA-depleted embryos is attributed to defects in proliferation, or apoptosis.

3.3.5 *RA mediates the closure of the choroid fissure*

We found that *Aldh1a2* acts as a regulator of choroid fissure closure during eye development. Reduction of *Aldh1a2* and *p53* in either a wild type or *aldh1a3*^{-/-} mutants increases incidence of coloboma. Our observations find that RA generated from ventrally localized *aldh1a3* is not sufficient in choroid fissure closure and that *Aldh1a2* synthesizes RA required to complete ventral optic cup formation. Further we found that solely RA synthesized by *aldh1a3* cannot fulfill this function. In mouse, *Raldh1* expression generates RA in the dorsal retina and no profound ocular defects are observed in the absence of this gene (Fan et al., 2003). *Raldh3*^{-/-} embryos begin to form an optic cup, however the ventral retina is shortened (Molotkov et al., 2006). *Raldh2* is localized to the POM cells and RA generated by this enzyme directs morphogenetic movements of optic cup formation but is not required for closure to reach completion (Molotkov et al., 2006). Additionally While RA has been found to be indispensable in the development in the retina in both mouse and zebrafish development, contributions of dorsally and ventrally localized sources of RA play different roles in eye development.

3.3.6 *Redundancy of retinoic acid synthesis in the eye*

To examine the functional compensation of RA synthesis enzymes in the developing eye, we examined RA signalling levels in zebrafish embryos that were depleted of the three known RA synthesis enzymes in the eye: *Aldh1a2*, *Aldh1a3* and *Cyp1b1* (Figure 3.7). RA signalling was markedly reduced, but not entirely ablated, in *Aldh1a2*; *aldh1a3*^{-/-}; *cyp1b1*^{-/-} morphomutants. The transgenic zebrafish line does not effectively resolve very low levels of RA, such as RA signalling within the POM. It is possible that the transgenic line used is not sensitive enough to detect residual RA produced in the retina and that the remnant RA is sufficient to direct eye development. The use of a more sensitive RA reporter would provide better insight into their distribution and their requirement for correct patterning. For example, genetically encoded

probes of RA (GEPRA) to detect free RA concentrations within the embryo using fluorescence resonance energy transfer (FRET) microscopy. These GEPRA transgenics make use of the conformation changes that RARs undergo in response to RA binding into a change in FRET from a cyan-emitting to a yellow-emitting fluorescent protein (Shimozono et al., 2013). This highly sensitive technique allows for the quantitative measurement of physiological RA concentrations and will also allow a greater understanding of the precise molecular mechanisms in patterning the vertebrate eye.

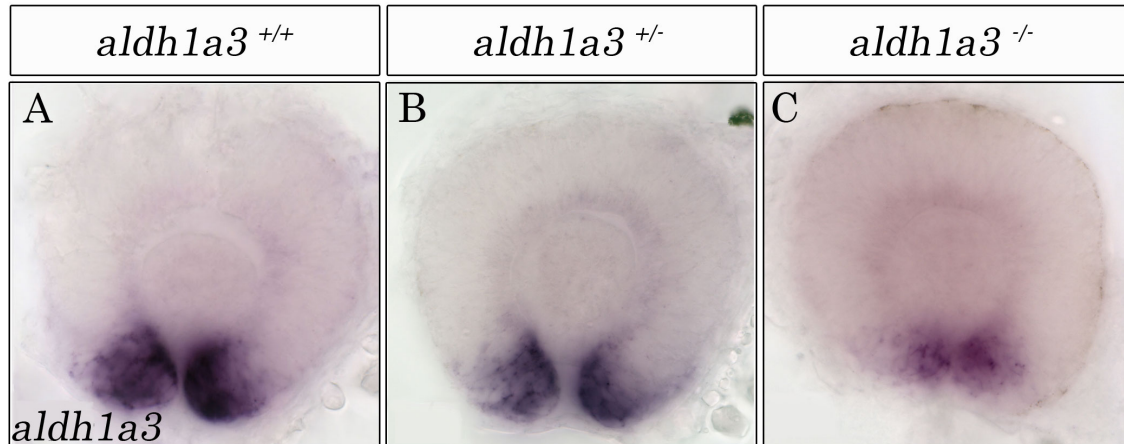


Figure 3.1: Expression of *aldh1a3* is reduced in *aldh1a3* mutants. Shown are representative dissected eyes from embryos following *in situ* hybridization analysis of *aldh1a3* gene expression at 28 hpf. Compared to wild type (*aldh1a3*^{+/+}) embryos (A), *aldh1a3* expression is slightly reduced in *aldh1a3*^{+/-} (B) and is almost completely lost in *aldh1a3*^{-/-} mutants (C).

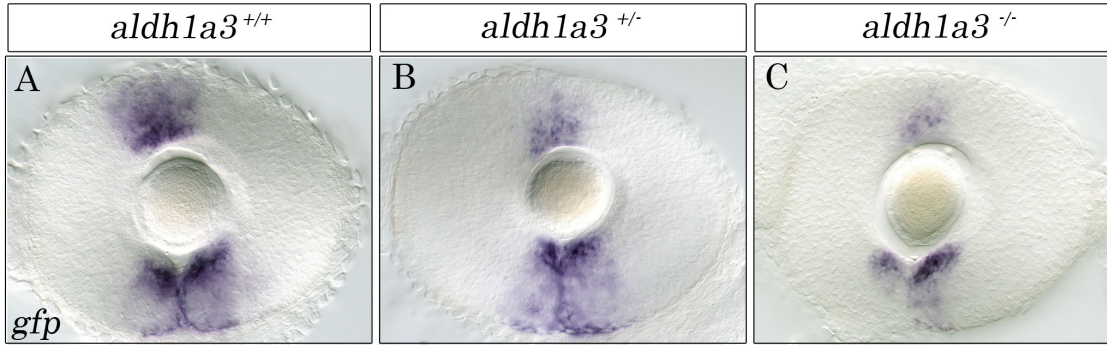


Figure 3.2: *aldh1a3* mutant embryos exhibit reduced RA signalling. Shown are dissected eyes from *RARE:egfp* embryos following *in situ* hybridization analysis of *gfp* gene expression at 48 hpf. In wild type embryos, RA signalling is localized to the dorsal and ventral regions of the eye. In comparison to wild type (A), RA signalling *aldh1a3*^{+/-}embryos is slightly reduced in the dorsal and ventral retina. In *aldh1a3*^{-/-}, RA signalling is strongly reduced in both dorsal and ventral regions of the eye.

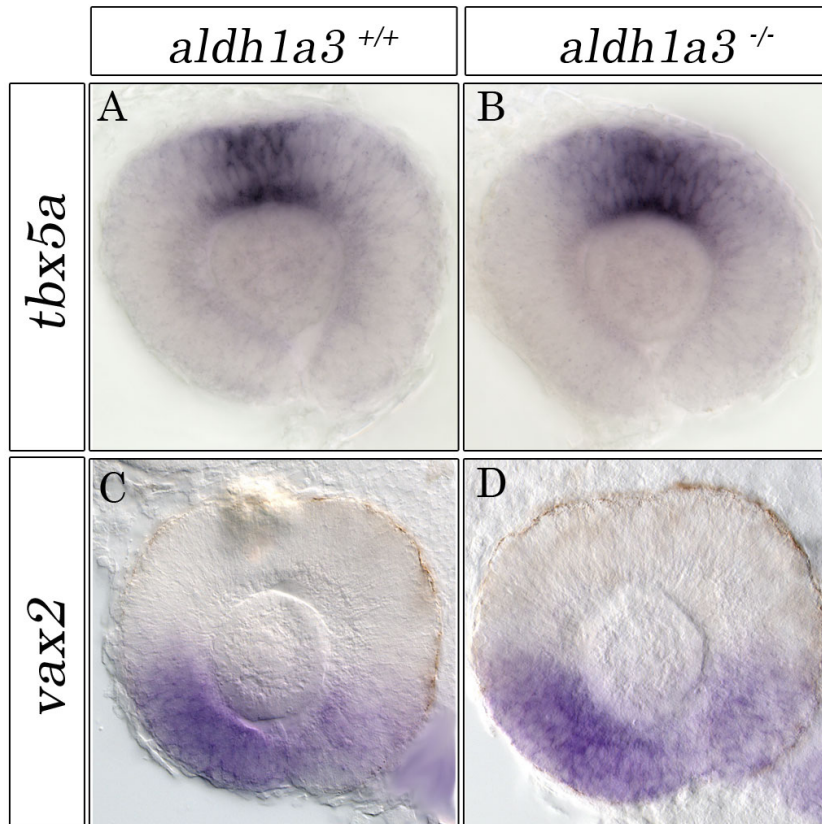


Figure 3.3: *aldh1a3*^{-/-} mutants do not display overt defects in dorsoventral patterning. Dissected eyes from 28 hpf following *in situ* hybridization analysis for dorsal retinal marker, *tbx5a* (A, B) or ventral marker *vax2* (C, D). *aldh1a3*^{+/+} and *aldh1a3*^{-/-} mutants demonstrate no change in *tbx5a* or *vax2*.

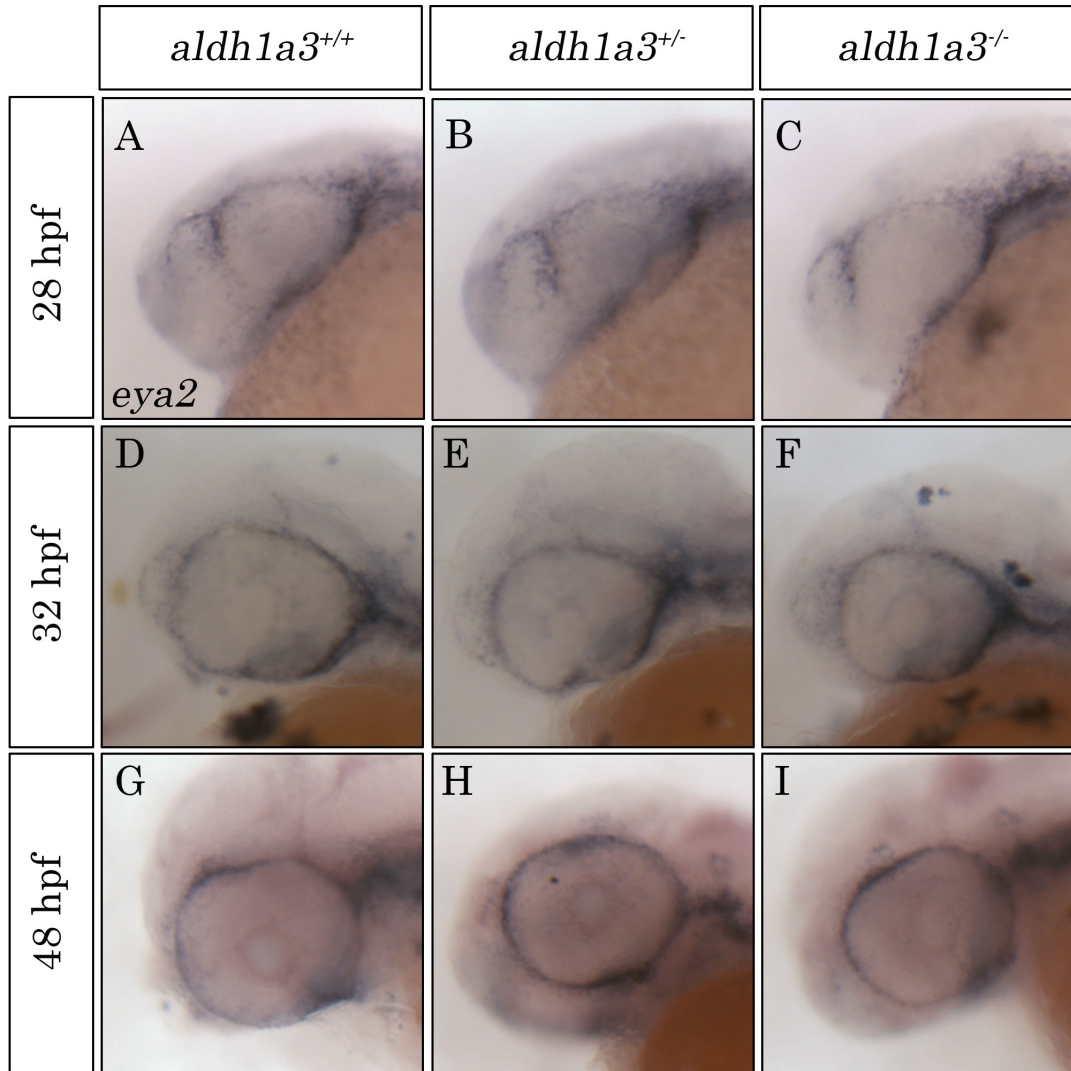


Figure 3.4: POM migration is not obviously affected in *aldh1a3* mutants. Shown are representative embryos following *in situ* hybridization analysis of expression of POM marker *eya2* at 28 hpf (A-C), 32 hpf (D-F), and 48 hpf (G-I). Lateral view of gene expression in the head region is shown; anterior to the left. At all observed time points, *aldh1a3*^{+/+} and *aldh1a3*^{-/-} embryos exhibit similar levels of *eya2* expression in wild type siblings compared to wild type siblings.

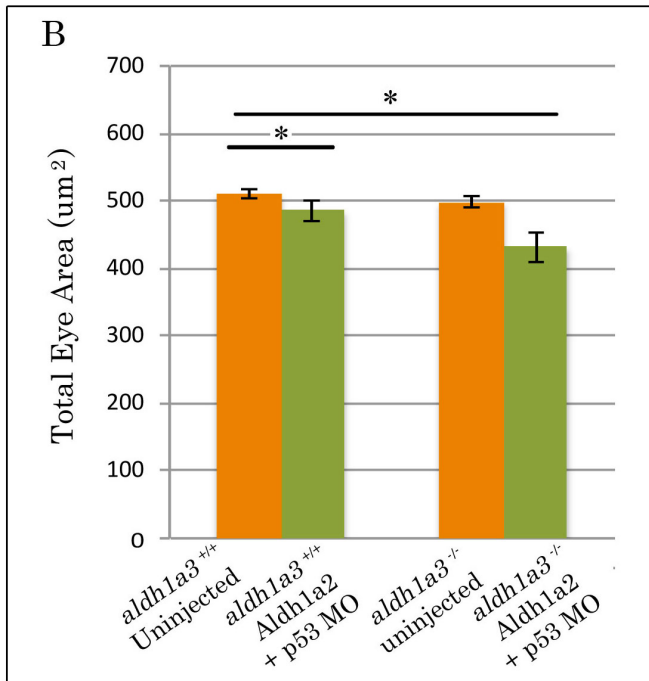
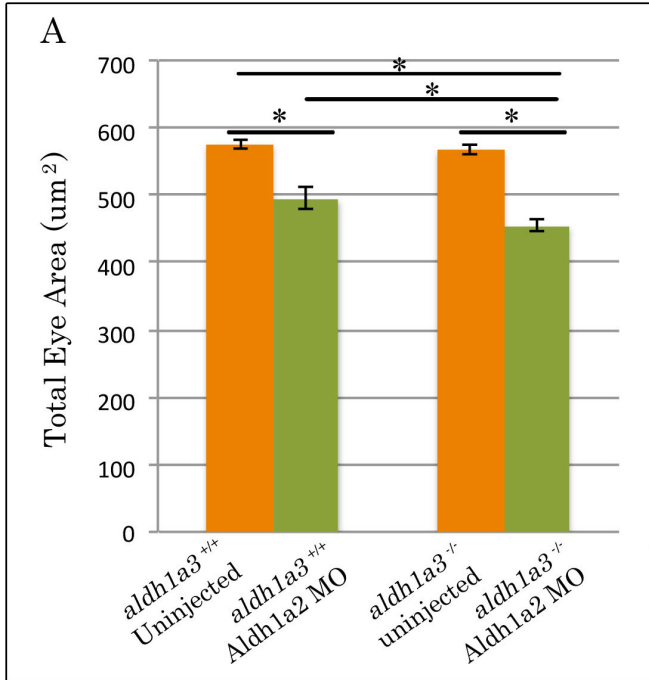


Figure 3.5: Total eye area is reduced in *Aldh1a2*; *aldh1a3*^{-/-} morphomutants. Quantification of total eye area at 4 dpf in wild type embryos, *aldh1a3*^{-/-} mutant embryos and simultaneous knockdown of *Aldh1a2* (A). Experiment was repeated with co-injection of *Aldh1a2* with p53 MO (B) (A: n = 3 experiments = 210 embryos; B: n = 2 experiments = 167 embryos). Error bars indicate standard error of the mean. Asterisk (*) indicates statistical significance as calculated by Analysis of Variance (ANOVA) followed by *post hoc* Tukey's honest significant difference test (*P*-value < 0.05) (Table 3.1 and 3.2).

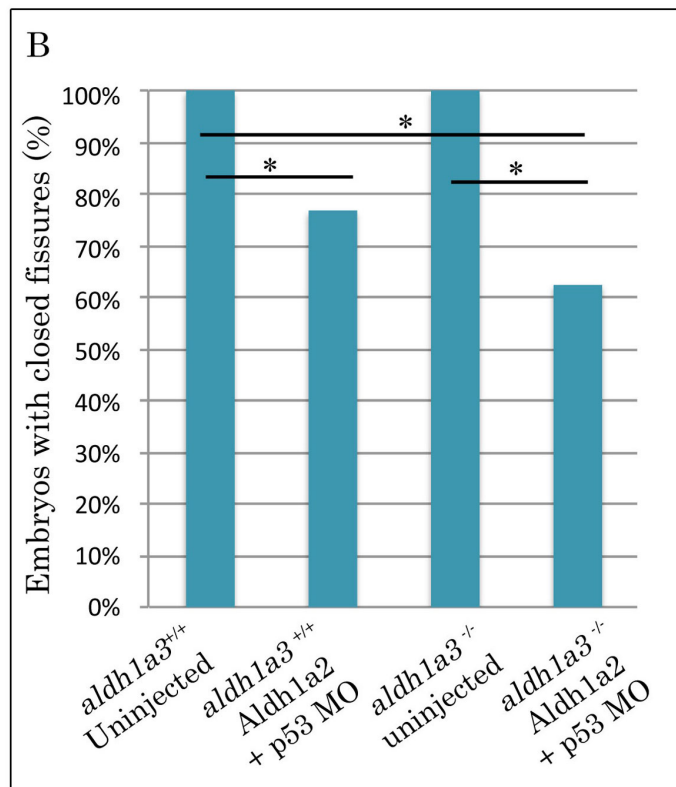
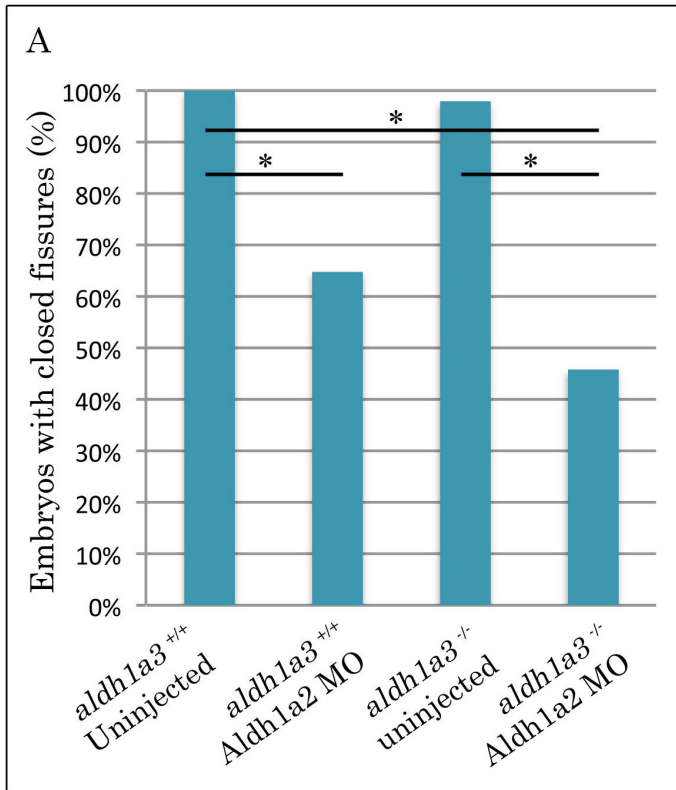


Figure 3.6:

Knockdown of RA synthesis enzymes delays choroid fissure closure.

Quantification of coloboma phenotypes at 4 dpf in wild type embryos, *aldh1a3*^{-/-} mutant embryos and simultaneous knockdown of Aldh1a2. Knockdown of Aldh1a2 (A) or co-knockdown with p53 MO (B) in *aldh1a3*^{-/-} mutants increases the incidence of coloboma. (A: n = 3 experiments = 210 embryos; B: n = 2 experiments = 167 embryos)

Asterisk (*) indicates statistical significance as calculated by Fisher's Exact test with Bonferroni correction on cumulative raw counts (adjusted *P*-values <0.05) (Table 3.3 and 3.4).

**Figure 3.7: RA signalling is greatly reduced in Aldh1a2;
aldh1a3^{-/-}; *cyp1b1*^{-/-} morphomutants.**

Shown are representative dissected eyes from *RARE:egfp* embryos following *in situ* hybridization analysis of *gfp* gene expression at 48 hpf. Panels A and B were previously presented in Figure 3.2. Compared to wild type embryos (A), RA signalling in dorsal and ventral retina was greatly reduced in *aldh1a3*^{-/-} mutants (B) and *aldh1a3*^{-/-}; *cyp1b1*^{-/-} double mutants (D). *cyp1b1*^{-/-} mutants exhibited normal RA signalling in ventral retina but is reduced in the dorsal domain of the eye (C). Embryos injected with Aldh1a2 and p53 MO exhibited abolished *gfp* expression in the dorsal retina (E-H). Aldh1a2; *aldh1a3*^{-/-}; *cyp1b1*^{-/-} morphomutants revealed nearly abolished *gfp* expression (H). Number in each panel represents the proportion of embryos that have overt reduction of *RARE:gfp* expression.

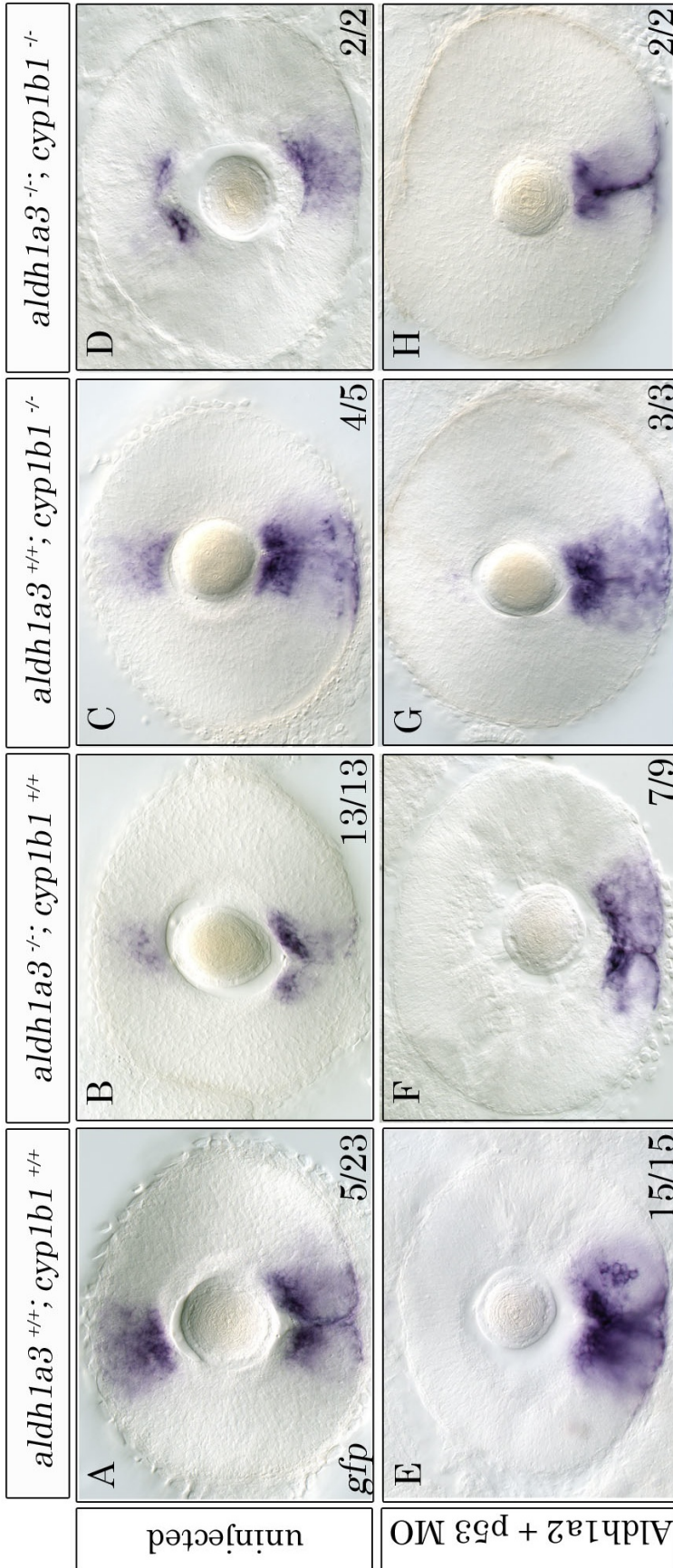


Table 3.1: Quantification of total eye area in 4 dpf *Aldh1a2* MO injected *aldh1a3*^{-/-} mutant embryos.

Treatment	Sample Size	Mean Total Eye Area (μm ²)	SEM (μm ²)	Adjusted P-value*	Adjusted P-value**
<i>aldh1a3</i> ^{+/+} ; uninjected	51	576.1	7.09		
<i>aldh1a3</i> ^{+/+} ; <i>Aldh1a2</i> MO	39	495.2	15.76	0.94334	<0.00001
<i>aldh1a3</i> ^{-/-} ; uninjected	48	568.2	7.49	<0.00001	0.01867
<i>aldh1a3</i> ^{-/-} ; <i>Aldh1a2</i> MO	72	454.8	8.37	<0.00001	

* indicates comparison of treatment to wild type with ANOVA and *post-hoc* Tukey's honest significant difference test on raw total eye area.

** indicates comparison of treatment to *aldh1a3*^{-/-}; *Aldh1a2* MO morphomutants with ANOVA and *post-hoc* Tukey's honest significant difference test on raw total eye area.

Blue shading indicates significant result

Table 3.2 Quantification of total eye area in 4 dpf Aldh1a2 MO and p53 MO injected *aldh1a3*^{-/-} mutant embryos.

Treatment	Sample Size	Mean Total Eye Area (μm ²)	SEM (μm ²)	Adjusted P-value*	Adjusted P-value**
<i>aldh1a3</i> ^{+/+} ; uninjected	43	510.1	7.59		
<i>aldh1a3</i> ^{+/+} ; Aldh1a2 MO; p53 MO	67	485.6	15.71	0.00524	0.99873
<i>aldh1a3</i> ^{-/-} ; uninjected	28	498.3	8.10	0.99808	0.28846
<i>aldh1a3</i> ^{-/-} ; Aldh1a2 MO; p53MO	29	431.7	22.15	0.03872	

* indicates comparison of treatment to wild type with ANOVA and *post-hoc* Tukey's honest significant difference test on raw total eye area.

** indicates comparison of treatment to *aldh1a3*^{-/-}; Aldh1a2 MO; p53 MO morphomutants with ANOVA and *post-hoc* Tukey's honest significant difference test on raw total eye area.

Blue shading indicates significant result

Table 3.3: Quantification of incidence of coloboma in 4 dpf *Aldh1a2* MO injected *aldh1a3*^{-/-} mutant embryos.

Treatment	Sample Size	Closed Fissure	Open Fissure	Two-tailed P-value*	Two-tailed P-value**
<i>aldh1a3</i> ^{+/+} ; uninjected	51	51	0		
<i>aldh1a3</i> ^{+/+} ; <i>Aldh1a2</i> MO	39	25	14	<0.0001	<0.0001
<i>aldh1a3</i> ^{-/-} ; uninjected	48	47	1	1	0.38
<i>aldh1a3</i> ^{-/-} ; <i>Aldh1a2</i> MO	72	33	39	<0.0001	

* indicates comparison of treatment to wild type by Fisher's Exact test with Bonferroni correction on cumulative raw counts.

** indicates comparison of treatment to *aldh1a3*^{-/-}; *Aldh1a2* MO morphomutants by Fisher's Exact test with Bonferroni correction on cumulative raw counts.

Blue shading indicates significant result

Table 3.4: Quantification of coloboma in 4 dpf Aldh1a2 MO and p53 MO injected *aldh1a3*^{-/-} mutant embryos.

Treatment	Sample Size	Closed Fissure	Open Fissure	Two-tailed P-value*	Two-tailed P-value**
<i>aldh1a3</i> ^{+/+} ; uninjected	43	43	0		
<i>aldh1a3</i> ^{+/+} ; Aldh1a2 MO	67	49	18	<0.0001	<0.0001
<i>aldh1a3</i> ^{-/-} ; uninjected	28	28	0	1	0.4985
<i>aldh1a3</i> ^{-/-} ; Aldh1a2 MO	29	16	13	<0.0001	

* indicates comparison of treatment to wild type by Fisher's Exact test with Bonferroni correction on cumulative raw counts.

** indicates comparison of treatment to *aldh1a3*^{-/-}; Aldh1a2 MO; p53 MO morphomutants by Fisher's Exact test with Bonferroni correction on cumulative raw counts.

Blue shading indicates significant result

4 A role for retinoic acid in photoreceptor development

4.1 Introduction

Embryonic retinal neurogenesis begins with a population of common multi-potent retinal progenitor cells (RPCs). Seven major cell classes are generated from this progenitor population. In zebrafish, the cell classes of the retina are generated layer-by-layer, from outside to inside relative to the apical surface of the retina (Hu and Easter, 1999). Ganglion cells that compose the ONL are first to be generated between 24 - 36 hpf. The generation of horizontal, amacrine and bipolar cells of the INL follows from 36 – 48 hpf. Between 48 – 72 hpf, cone photoreceptors are born (Figure 1.2B). Generation of rod photoreceptors is delayed and extended in comparison to the genesis of cone photoreceptors. The precise, non-overlapping production of each retinal layer suggests that each neurogenic period has distinct developmental mechanisms (Raymond and Jackson, 1995). The specification of cell type from a multipotent progenitor depends on intrinsic genetic programs, the expression of specific combinations of transcription factors, as well as extrinsic factors. Forkhead box N4 (Foxn4), a winged helix/forkhead transcription factor, has been found to be essential for commitment to the amacrine cell fate and the genesis of horizontal cells. Targeted disruption of murine *Foxn4* results in the near-ablation of amacrine neurons and horizontal cells, while overexpression of *Foxn4* strongly biases RPC differentiation to amacrine cell fate while suppressing photoreceptor fates (Li et al., 2004). *In vitro* studies have demonstrated that locally diffusible signals in the extracellular environment influence the differentiation of RPCs to photoreceptors (Altshuler and Cepko, 1992; Watanabe and Raff, 1992). A number of extrinsic factors have been found to affect the specification of retinal cell types, including Fibroblast Growth Factors (FGFs), Sonic Hedgehog (Shh), thyroid hormone, and retinoic acid (Guillemot and Cepko, 1992; Kelley et al., 1994; Zhang and Yang, 2001). However, the mechanisms regulating cell fate decisions of RPCs remain poorly understood.

In addition to the proper lamination of the retina, proper vision depends on photon capture by rod and cone photoreceptor cell types. Rods contain the photopigment rhodopsin and while they have little, if any, role in color vision, they are highly sensitive and enable low light vision. Cones have a lower light sensitivity but are suited for bright light and colour vision. Further, different types of cone photoreceptors are distinguished by the expression of distinct opsin genes, which determines their wavelength sensitivity. Each unique opsin is sensitive to different regions of the visible light spectrum, thus facilitating color vision. Humans have trichromatic vision as their retinas are composed of three cone subtypes. Based on the four cone types in zebrafish, their vision is tetrachromatic (Fleisch and Neuhauss, 2006). Similar to mammals, zebrafish have opsins for red (L-opsin), green (M-opsin) and blue (S-opsin) colour vision. Zebrafish have an additional short wave opsin that confers detection of ultraviolet wavelengths (Robinson et al., 1993).

The developing retina not only generates photoreceptor diversity, but also distributes rod and cone types in precise patterns over the retina. The pattern of photoreceptors over the retina differs among species that reflects the adaptation of visual systems to the diversity of lifestyles and habitats (Adler and Raymond, 2008; Szel et al., 2000). For example, the three cone subtypes within the human retina are arranged in a mosaic and are concentrated in and around a region lacking rods called the fovea. In contrast, dichromatic mice retinas have two cone subtypes that are distributed in opposing gradients over the retina around the more numerous rods (Forrest and Swaroop, 2012). In zebrafish, the four cone subtypes are organized in a 12-cone repeating motif with internal and mirror-image symmetry (Allison et al., 2010; Chinen et al., 2003; Larison and Bremiller, 1990; Nawrocki et al., 1985; Salbreux et al., 2012) with rods occupying the spaces between these rows in a rectangular lattice pattern (Allison et al., 2010; Fadool, 2003; Larison and Bremiller, 1990). The precise, organized mosaic of the photoreceptors over the retina suggests that photoreceptors may be sending and receiving signals that

influence the neighbouring cell types. The interactions between neighbouring cells as well as the molecules that mediate the interactions have not been well characterized.

The proper distribution of the photoreceptor subtypes is essential to the correct perception of visual stimuli, especially in zebrafish. The disturbance of non-random organization of photoreceptors, through the formation of gaps in distribution or random clustering, results in the underrepresentation or over-sampling of information within those regions in the visual field. Although photoreceptors originate from common pools of pluripotent progenitor cells, the diversity of rods and cone types is generated in photoreceptor precursors. The signalling factors that regulate the precise spatial distribution of photoreceptors over the retina are yet to be fully elucidated. Current models of cell fate determination in the retina propose that progenitor cells are responsive to environmental cues and results in the appearance of distinct retinal cell types (Cepko, 1999; Cepko et al., 1996). Photoreceptor cell identity is thought to be influenced by multiple extrinsic and intrinsic factors, including hormones, trans-membrane and nuclear receptors, secreted polypeptides, and transcriptional regulators (Doerre and Malicki, 2002). Developmental shifts between cone fates have been observed by perturbations of photoreceptor-specific genes in mouse and zebrafish. Notably, the transcription factor, *T-box 2b* (*tbx2b*), can influence the fate of retinal progenitor cells, in which UV cones in *tbx2b* mutants are absent and replaced with rod photoreceptors (Alvarez-Delfin et al., 2009). This finding suggests plasticity between rod and cone subtype fates during development (Forrest and Swaroop, 2012).

In addition to roles in early eye morphogenesis, RA is speculated to be an extrinsic factor that affects later events in ocular development. RA is one of the multiple diffusible or secreted signalling factors that control photoreceptor development. Studies *in vivo* and *in vitro* have suggested an important role for RA in photoreceptor differentiation and survival (Hyatt et al., 1996a;

Soderpalm et al., 2000; Stenkamp and Adler, 1993). Addition of exogenous RA to cell cultures of embryonic rat retina influences the generation of photoreceptors at the expense of other retinal cell types. RA promotes differentiation of RPCs into photoreceptors and suppresses amacrine cell fate (Kelley et al., 1994). Additionally, studies have revealed a role for RA in promoting the rod photoreceptor fate and the differentiation of cone photoreceptor subtypes. Exogenous treatment of RA in zebrafish promotes the differentiation of rods and red-sensitive cones while inhibiting differentiation of blue- and UV-sensitive cones and having negligible effect on green-sensitive cones (Hyatt et al., 1996a; Kelley et al., 1999; Prabhudesai et al., 2005). Interestingly, another study in zebrafish revealed high levels of RA signalling during retinal neurogenesis alters the rod and cone mosaic by increasing the number of rod photoreceptors at the expense of red-sensitive cones (Stevens et al., 2011). RA signalling also modulates the expression of photoreceptor-specific genes, including the transcription factor NRL and opsins (Kelley et al., 1995; Kelley et al., 1999; Khanna et al., 2006; Prabhudesai et al., 2005). In sum, these data suggest an essential role of RA signalling in the differentiation of rod and cone photoreceptors from RPCs as well as the determination of photoreceptor cell fate decisions.

Although existing studies have revealed that RA influences retinal cell fate decisions, the requirement for RA synthesized in the retina during retinal neurogenesis is unknown. We used zebrafish lines with recessive mutations in *aldh1a3* and *cyp1b1* genes coupled with *aldh1a2* translation-blocking morpholino to reduce endogenous levels of RA and to study the contribution of these RA synthesizing enzymes to retinal neurogenesis. Preliminary data suggest that reduction of endogenous RA causes the loss of UV- and blue-sensitive cone photoreceptors with negligible change in red- and green-sensitive cone photoreceptors. Further, our preliminary data also shows that a reduction of RA levels within the retina causes an upregulation of expression of *foxn4*. This suggests that *foxn4* is downstream of the RA signalling

pathway in zebrafish retinal neurogenesis. These findings suggest that RA within the retina may have a role in RPC differentiation and photoreceptor cell fate decisions.

4.2 Results

4.2.1 RA depletion reduces UV- and blue-sensitive cone photoreceptor differentiation

Sustained high levels of exogenous RA in zebrafish cause photoreceptor pattern abnormalities, where more rods and red sensitive cones develop at the expense of the other cone photoreceptor subtypes (Hyatt et al., 1996a; Kelley et al., 1999; Prabhudesai et al., 2005). We hypothesize that loss of RA levels will result in the loss of photoreceptors. To test this, we examined wild type embryos and embryos with *aldh1a3* mutation, the *cyp1b1* mutation, or both mutations. Subsets of these embryos were also co-injected with *aldh1a2* and *p53* morpholino. Photoreceptor fates were determined by analyzing the expression of cone opsin mRNA at 4 dpf, at which time cone photoreceptors are postmitotic and differentiated. In control embryos, cells expressing cone opsin mRNA is evenly distributed over the retina. Preliminary data reveal that 23% of control embryos exhibit patches of retina lacking UV-sensitive cone opsin mRNA, *opn1sw1*, expression (Figure 4.1A, Figure 4.3A). 66% of *aldh1a3*^{-/-} mutant embryos exhibit patches lacking *opn1sw1* expression, while no *cyp1b1*^{-/-} mutant embryos demonstrate patches lacking *opn1sw1* expression (Figure 4.1B, C; Figure 4.3A). 100% of retinas of *aldh1a3*^{-/-}; *cyp1b1*^{-/-} double mutants contain gaps in *opn1sw1* expression (Figure 4.1D; Figure 4.3A). Knockdown of Aldh1a2 and p53 results in all embryos containing a gap in *opn1sw1* expression over the retina regardless of genotype (Figure 4.1E – H; Figure 4.3A). The patches of retina lacking *opn1sw1* suggest that some UV cones are missing from the normal mosaic.

To further quantify the effects of a loss of RA synthesis genes on photoreceptor development, we measured the area of retinal patches lacking

opn1sw1 expression in relation to the total area of the retina. In flat-mounted retinas, the optic stalk is visible as a small gap lacking photoreceptors in the retina. This space was excluded when gaps lacking opsin expression were measured. As the size of the gaps varied in relative area, a box and whisker plot was used to show the full range of variation within and among the experimental treatments (Figure 4.2). Preliminary data reveals that, on average, 2% of total retinal area lacked *opn1sw1* expression in wild type embryos (Figure 4.1A; Figure 4.3B). The average retinal area lacking *opn1sw1* in *aldh1a3*^{-/-} mutants is 8.5% of total retinal area (Figure 4.1B; Figure 4.3B). The average *opn1sw2*-negative retinal area in *aldh1a3*^{-/-}; *cyp1b1*^{-/-} double mutants is increased in comparison single mutants or controls (10.8%) (Figure 4.1D; Figure 4.3B). Further, preliminary data reveals that the relative area of retina lacking *opn1sw1* is higher with the concomitant loss of RA synthesis genes. Knockdown of Aldh1a2 and p53 in a wild type background results in an average area of 21% of total retina that lacks *opn1sw1* expression (Figure 4.1D; Figure 4.3B). Loss of *aldh1a3* or *cyp1b1* results in average retinal area lacking *opn1sw1* expression of 8.3% and 36% of total retinal area, respectively (Figure 4.1E, F; Figure 4.3B). The retinas of Aldh1a2; *aldh1a3*^{-/-}; *cyp1b1*^{-/-} morphomutant display large gaps in *opn1sw1* expression at an average of 63% of total area lacking *opn1sw1* (Figure 4.1G; Figure 4.3B). Taken together, these preliminary findings suggest that RA loss, most notably through the depletion of Aldh1a2, is associated with a loss of *opn1sw1* expression and thus disrupts the pattern of the UV cone mosaic.

Similar to observations of *opn1sw1*, preliminary studies suggest that a loss of RA synthesis genes affects expression of blue-sensitive opsin mRNA, *opn1sw2*. A proportion of embryos in each genotype and experimental group had patches of retina lacking *opn1sw2*. 50% of wild type embryos contain *opn1sw2*-negative patches and the proportion of *aldh1a3*^{-/-} (Figure 4.4A; Figure 4.5A) and *cyp1b1*^{-/-} single with *opn1sw2*-negative patches is 20% and 33%, respectively (Figure 4.4B, C; Figure 4.5A). 75% of *aldh1a3*^{-/-}; *cyp1b1*^{-/-} double

mutants exhibit retinal patches lacking *opn1sw2* expression. Knockdown of Aldh1a2 and p53 in wild type and *aldh1a3*^{-/-} embryos results in retinal patches lacking *opn1sw2* across all embryos (Figure 4.4E, F; Figure 4.5A). Knockdown of *cyp1b1*^{-/-} mutants and *aldh1a3*^{-/-}; *cyp1b1*^{-/-} mutants causes an appearance of *opn1sw2*-negative patches in 75% of embryos (Figure 4.4G, H; Figure 4.5A). The relative eye area of *opn1sw2*-negative patches in wild type embryos, *aldh1a3*^{-/-}, *cyp1b1*^{-/-}, and *aldh1a3*^{-/-}; *cyp1b1*^{-/-} mutants ranged from 0.8 – 9% (Figure 4.4A-D; Figure 4.5B). Knockdown of Aldh1a2 and p53 in wild type embryos, *aldh1a3*^{-/-}, and *cyp1b1*^{-/-} mutant embryos does not seem to profoundly affect the size of *opn1sw2*-negative patches with relative eye area ranging from 5 – 8% of total eye area (Figure 4.4E-G; Figure 4.5B). The most profound loss of *opn1sw2* expression is observed in double mutant embryos (*aldh1a3*^{-/-}; *cyp1b1*^{-/-}) injected with *aldh1a2* morpholino, where *opn1sw2*-negative patches compose 30% of total eye area (Figure 4.4H; Figure 4.5B). This preliminary data suggests that all three RA synthesis genes within the retina may be required for blue-sensitive cone photoreceptors.

Unlike the expression of *opn1sw1* and *opn1sw2*, preliminary data suggests that the loss of RA synthesis genes does not affect the expression of green-sensitive opsin mRNA, *opn1mw1*. Preliminary data reveals that 58% of wild type embryos and 13.3% of *aldh1a3*^{-/-} mutants displayed retinal patches lacking *opn1mw1* expression (Figure 4.6A, B; Figure 4.7A). The average size of these patches in wild type and *aldh1a3*^{-/-} are 3% and 0.3% of total retinal area, respectively (Figure 4.7B). Retinas from *cyp1b1*^{-/-} mutants and *aldh1a3*^{-/-}; *cyp1b1*^{-/-} double mutant embryos displayed normal expression of *opn1mw1* over the entire retina (Figure 4.6C, D; Figure 4.7A). Knockdown of Aldh1a2 and p53 in wild type, *aldh1a3*^{-/-} and *cyp1b1*^{-/-} results in *opn1mw1*-negative patches in 33%, 44% and 66% of embryos, respectively (Figure 4.6 E – G; Figure 4.7A). The average size of *opn1mw1*-negative patches in Aldh1a2-depleted embryos and Aldh1a2; *aldh1a3*^{-/-} morphomutants were both measured to be 14% of total retinal area (Figure 4.7B). Retinas of Aldh1a2; *cyp1b1*^{-/-}

morphomutants contain patches lacking *opn1mw1* expression that on average compose 4.6% of total retinal area. No *Aldh1a2;aldh1a3^{-/-};cyp1b1^{-/-}* morphomutants were collected in this preliminary experiment. These preliminary findings suggest that reduction of RA synthesis genes within the retina does not affect differentiation of green-sensitive photoreceptors.

4.2.2 RA depletion reduces rod photoreceptor differentiation

Previous studies have revealed that high levels of RA influence photoreceptor cell fate, biasing differentiation of rods over cone photoreceptors (Stevens et al., 2011). To examine how loss of RA synthesis genes affects rod photoreceptor differentiation within the zebrafish retina, we examined the expression of rod-specific photopigment, *rhodopsin* (*rho*), in the absence of *Aldh1a2*, *aldh1a3* and *cyp1b1* individually and in combination. In control embryos, rod photoreceptors appear in the dorsal and ventral parts of the retina with a smaller number of rods found in the central retina. *rho* expression is unchanged among wild type embryos, *aldh1a3^{-/-}* mutants, *cyp1b1^{-/-}* mutants and *aldh1a3^{-/-}; cyp1b1^{-/-}* double mutants (Figure 4.8A-D). Depletion of *Aldh1a2* and p53 results in a reduction in *rho* expression in wild type, *aldh1a3^{-/-} mutants* and *aldh1a3^{-/-}; cyp1b1^{-/-} double mutants* (Figure 4.8E, F, G). However, *Aldh1a2; cyp1b1^{-/-}* morphomutants do not display a reduction in *rho* expression (Figure 4.8H). This preliminary data suggests that *Aldh1a2* synthesizes sufficient levels of RA to regulate rod photoreceptor differentiation.

4.2.3 RA signalling may act upstream of foxn4, a regulator of amacrine cell fate

Studies in murine retinal cell culture have revealed that high levels of RA influence the generation of photoreceptors at the expense of other retinal cell types, notably amacrine cells (Kelley et al., 1994). Our observed loss of photoreceptors within the mosaic as a result of the depletion of RA synthesis genes could be at the expense of supernumerary amacrine cells. Studies in

mouse have identified Foxn4 as a key intrinsic factor in the commitment of amacrine and horizontal cell fate (Li et al., 2004). To determine if RA regulates the expression of *foxn4*, we examined its expression in the absence of *Aldh1a2*, *aldh1a3* and *cyp1b1* individually and in combination at 3 dpf, a time at which amacrine and horizontal cells are differentiating. In control embryos, *foxn4* in the zebrafish retina is restricted to the germinal zone of the retinal margin, surrounding the lens. Depletion of *Aldh1a2*, *aldh1a3* and *cyp1b1* singly results in the upregulation and expansion of *foxn4* throughout the zebrafish eye (Figure 4.9). This preliminary data suggests that RA levels regulate the expression of *foxn4* within the retina.

4.3 Discussion

Previous research has implicated RA as a regulator of zebrafish photoreceptor cell fate. Using a combinatorial approach to block RA synthesizing enzymes during zebrafish embryogenesis, we have obtained preliminary data suggesting that loss of RA synthesis genes results in the loss of rods and, blue- and UV-sensitive cone photoreceptor subtypes. Further our preliminary data suggests that loss of RA synthesis genes results in an upregulation of a gene determining amacrine and horizontal cell fate, *foxn4*.

4.3.1 *RA in the photoreceptor differentiation*

Alterations in RA levels influence photoreceptor development. In zebrafish, exogenous RA treatment results in zebrafish retinas with increased densities of rod- and red cone-specific opsin expression and a corresponding reduction of opsins specific to blue- and UV-sensitive cone photoreceptors (Prabhudesai et al., 2005). Further, exogenous RA alters the mosaic of photoreceptors over the retina resulting in supernumerary rods clustered among normally distributed red cones (Stevens et al., 2011). Our preliminary data suggests that zebrafish embryos with depleted RA synthesis genes, and thus reduced endogenous RA levels, fail to establish normal distribution of UV- and blue- sensitive cone photoreceptors and rod photoreceptors (Figure

4.1; Figure 4.4; Figure 4.8). However, we do not observe changes in expression or distribution of green cone-specific opsin (Figure 4.6). Our preliminary data reveals that reduction of *Aldh1a2* results in an increased proportion of embryos with opsin-negative patches (Figure 4.1; Figure 4.4). Further, these patches are, on average, larger in *Aldh1a2*-depleted embryos than in their uninjected counterparts. These findings suggest that *Aldh1a2* may synthesize higher levels of RA in comparison to other RA synthesis enzymes present in the retina as depletion of *Aldh1a2* increases the incidence and the severity of UV- and blue-sensitive opsin-negative patches (as measured by the proportion of the retina lacking specific opsin expression). Interestingly, loss of *aldh1a3* affects the mosaic of UV cones, but not blue or green cones (Figure 4.1B; Figure 4.4B; Figure 4.6B). The depletion of *aldh1a3*, *cyp1b1*, and *Aldh1a2* reveals the most severe loss of blue- and UV-specific opsins (Figure 4.1H; Figure 4.4H). This preliminary finding suggests that *aldh1a3*, *aldh1a2*, and *cyp1b1* have functionally redundant roles in photoreceptor differentiation and the establishment of the photoreceptor mosaic. Further, this creates a possible model where RPCs are sensitive to levels of RA and relative levels of RA bias cone cell fate, such that high levels of RA influence the UV-cone fate, lower levels of RA influence the blue-sensitive cone fate and green-sensitive cones require little or no RA.

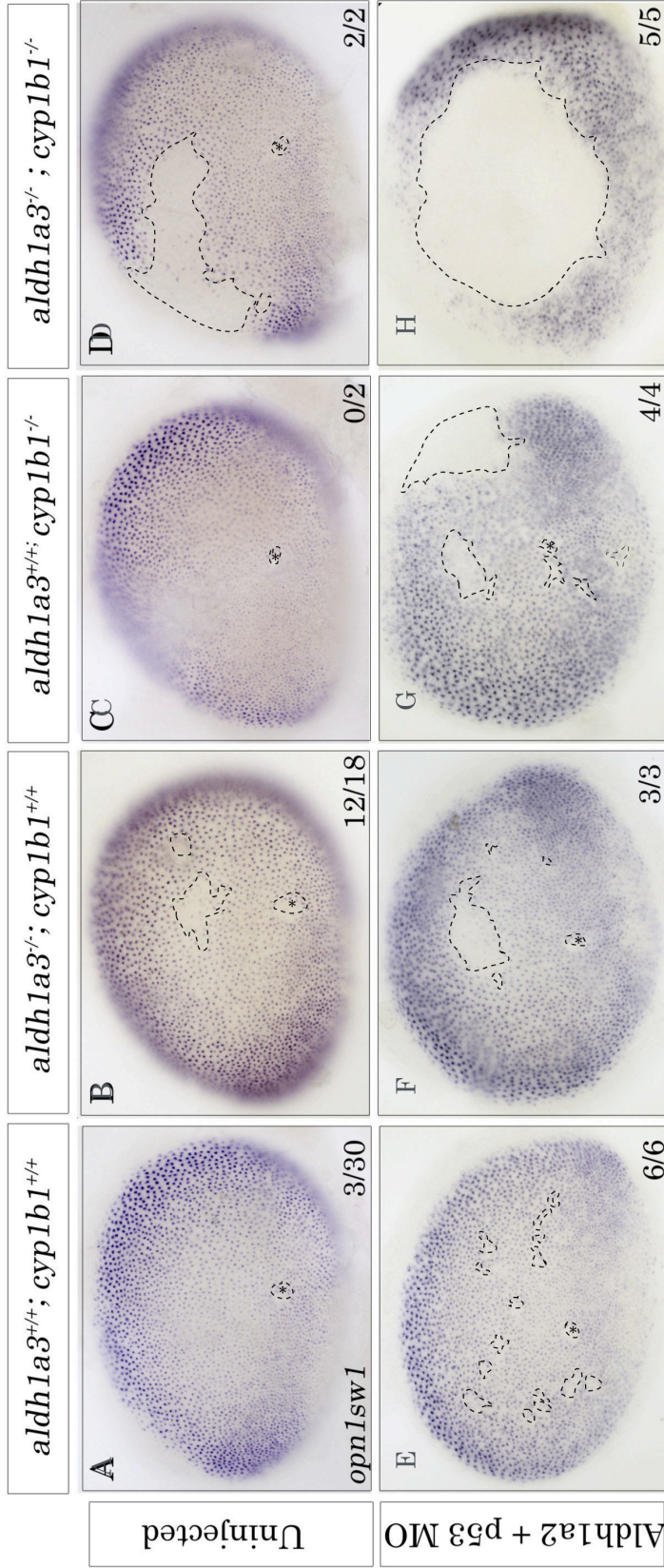
We observe opsin-negative patches over the retina with no correlation to the domains of RA synthesis genes (Figure 4.1; Figure 4.4). It is possible that the level of RA, not the contribution from individual RA synthesis enzymes, influences cone photoreceptor cell fate. Reduction of endogenous RA levels via the knockdown of the RA receptor *RAR α* causes a reduction in the number of rod photoreceptors with no alterations in other retinal cell types (Stevens et al., 2011). In zebrafish, the determination of photoreceptor fate may be a stochastic event that requires extrinsic and intrinsic factors to influence the development of a specific photoreceptor subtype. Retinal progenitors may assume a transient state of plasticity that requires extracellular and

intracellular cues to influence the fate of their progeny. RA may be acting as an extracellular cue where relative levels of this morphogen impel a progenitor towards a specific photoreceptor fate. This model is consistent with the preliminary results of the present study demonstrating that loss of *aldh1a3* causes an increase in UV-sensitive opsin mRNA but does not cause alteration in blue- or green-sensitive opsin mRNA.

4.3.2 *RA and the regulation of foxn4*

Retinal progenitor cells within the retina differentiate sequentially: RGCs exit cell cycle first, followed by the cells of the INL, and lastly cone photoreceptors. Previous studies performed *in vitro* suggest that RA promotes rod photoreceptor fate at the expense of other non-photoreceptor retinal cell fates, notably amacrine and horizontal cells (Kelley et al., 1994; Stenkamp and Adler, 1993). The observed loss of blue- and UV-specific opsin mRNA in embryos lacking RA synthesis genes may be caused by RA promoting amacrine or horizontal cell fate decision and inhibiting photoreceptor cell fates (Figure 4.9). Our preliminary findings reveal that reduction of endogenous RA levels via the loss of RA-synthesis genes causes a domain expansion and upregulation of *foxn4*, a gene that controls the genesis of amacrine and horizontal cells (Li *et al.*, 2004). Analysis of amacrine cell markers will provide insight into whether the loss of photoreceptors in RA-depleted embryos is a result of an increase of amacrine and horizontal cells.

Figure 4.1: Loss of RA synthesis genes results in gaps of UV-sensitive photoreceptors. Shown are representative dissected eyes from zebrafish embryos following *in situ* hybridization analysis of *opn1sw1* gene expression at 4 dpf. In comparison to wild type (A), this preliminary data suggests that *aldh1a3*^{-/-} mutants (B) and *aldh1a3*^{-/-}; *cyp1b1*^{-/-} double mutants (D) exhibit patches lacking *opn1sw1* expression. *cyp1b1*^{-/-} mutants display no overt alterations in *opn1sw1* expression. *opn1sw1* - negative patches increased in severity with the knockdown of Aldh1a2 and p53 (E-G). Dotted line demarcates *opn1sw1*⁻ negative patches in photoreceptor layer. Asterisk (*) denotes presence of optic stalk. Number in each panel represents the proportion of embryos that have overt patches lacking *opn1sw1* expression.



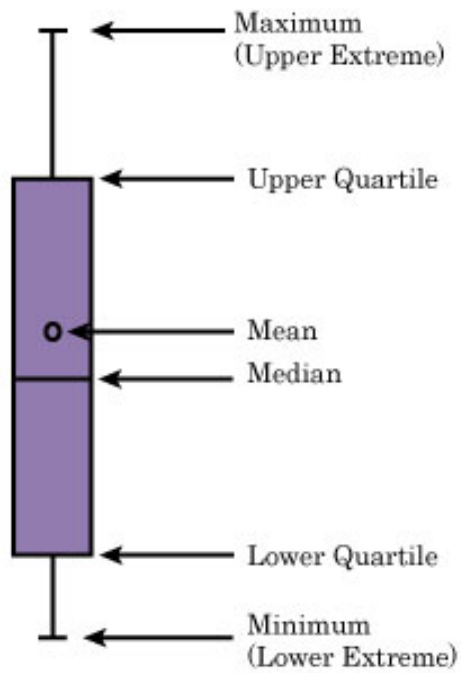


Figure 4.2: Diagram of box and whisker plot. The main features of a box and whisker plot, including minimum, maximum, median and mean. Range includes all data. Box represents interquartile range containing the 25th to 75th percentile.

Figure 4.3: Frequency and severity of gaps in *opn1sw1* expression increases with decrease in RA synthesis genes. (A) Quantification of the phenotypes shown in Figure 4.1. Shown is the proportion of 4 dpf embryos with gaps in the retina that lack expression of *opn1sw1*. (B) Box and whisker plots of the proportion of area that is lacking *opn1sw1* in 4dpf zebrafish retina by genotype and experimental treatment. The horizontal line within the box indicates the median, boundaries of the box indicate the 25th- and 75th -percentile, and the whiskers indicate the highest and lowest values of the results. The open circle indicates the mean.

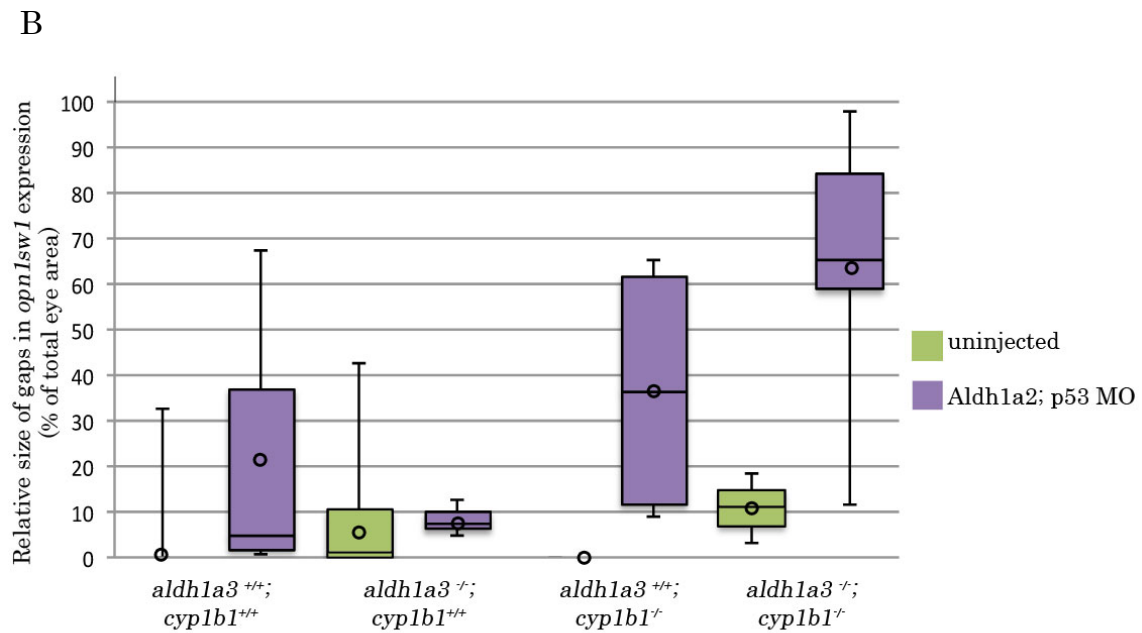
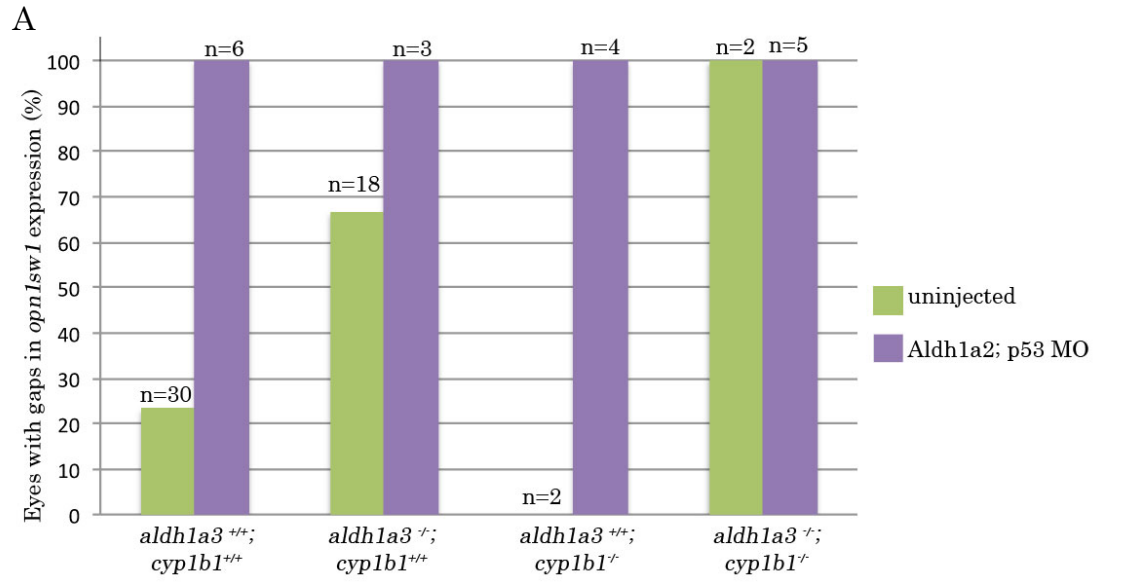


Figure 4.4: Loss of RA synthesis genes results in gaps of blue-sensitive photoreceptors. Shown are representative dissected eyes from zebrafish embryos following *in situ* hybridization analysis of *opn1sw2* gene expression at 4 dpf. In comparison to wild type (A), this preliminary data suggests that *aldh1a3*^{-/-} mutants (B) and *cyp1b1*^{-/-} mutants (C) exhibit no changes in *opn1sw2* distribution. *aldh1a3*^{-/-}; *cyp1b1*^{-/-} double mutants exhibit patches lacking *opn1sw2* expression. *opn1sw2* - negative patches increased in severity with the knockdown of Aldh1a2 and p53 (E-G) with the most profound effects observed in Aldh1a2; *aldh1a3*^{-/-}; *cyp1b1*^{-/-} morphomutants (F). Dotted line demarcates *opn1sw1*⁻ negative patches in photoreceptor layer. Asterisk (*) denotes presence of optic stalk. Number in each panel represents the proportion of embryos that have overt patches lacking *opn1sw2* expression.

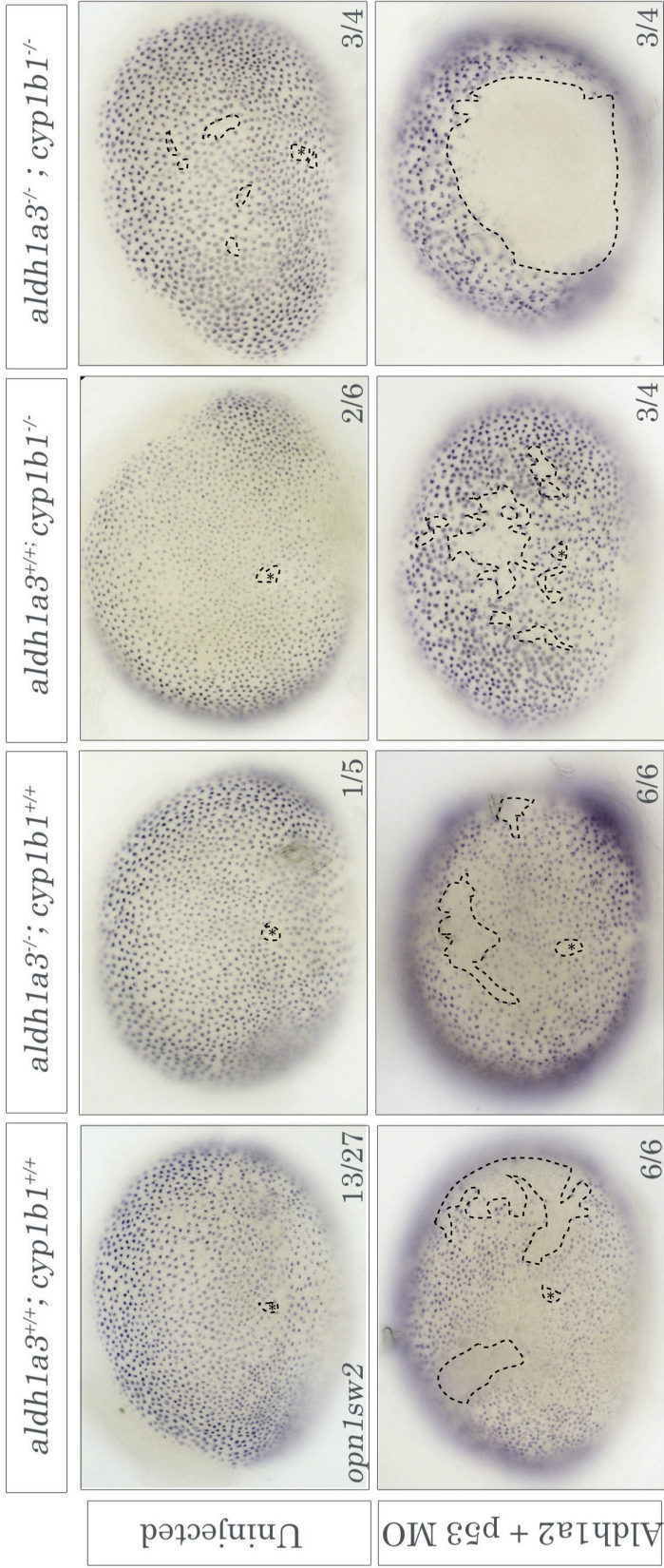
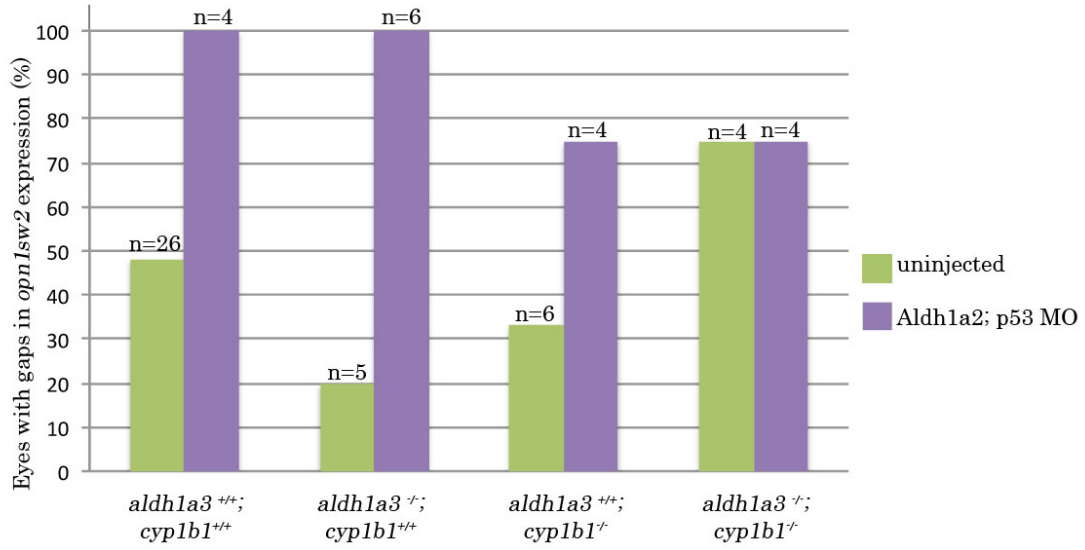


Figure 4.5: Frequency and severity of gaps in *opn1sw2* expression increases with decrease in RA synthesis genes. (A) Quantification of the phenotypes shown in Figure 4.4. Shown is the proportion of 4 dpf embryos with gaps in the retina that lack expression of *opn1sw2*. (B) Box and whisker plots of the proportion of area that is lacking *opn1sw2* in 4dpf zebrafish retina by genotype and experimental treatment. The horizontal line within the box indicates the median, boundaries of the box indicate the 25th- and 75th -percentile, and the whiskers indicate the highest and lowest values of the results. The open circle indicates the mean.

A



B

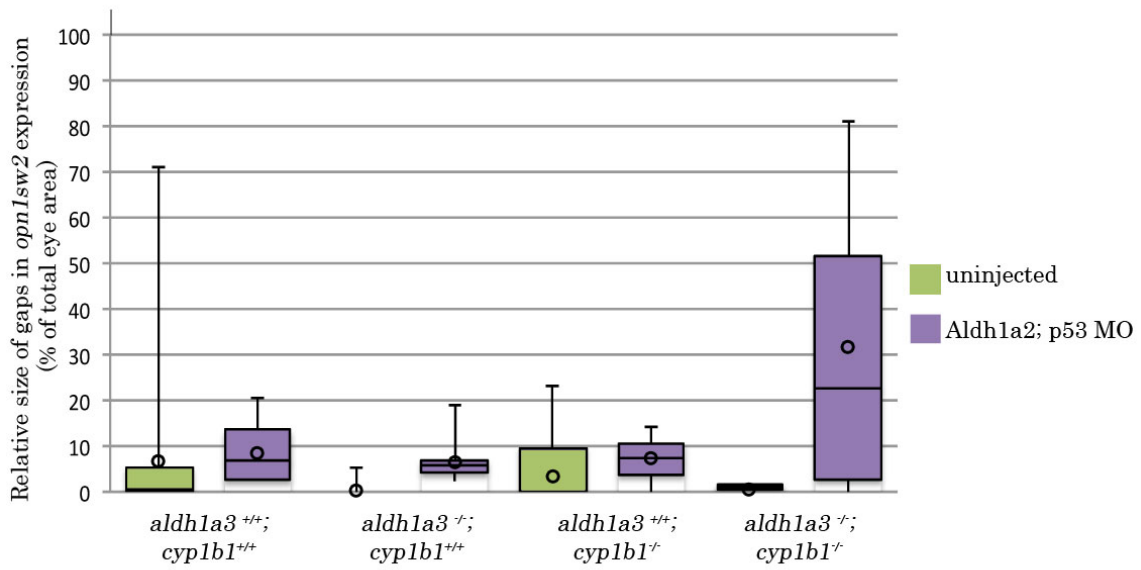


Figure 4.6: Loss of RA synthesis genes does not strongly alter green-sensitive photoreceptor distribution. Shown are representative dissected eyes from zebrafish embryos following *in situ* hybridization analysis of *opn1mw1* gene expression at 4 dpf. Wild type embryos and embryos depleted in *Aldh1a2*, *aldh1a3* and *cyp1b1* singly or in combination exhibit similar levels of *opn1mw1* expression. Dotted line demarcates *opn1mw1*-negative patches in photoreceptor layer. Asterisk (*) denotes presence of optic stalk. Number in each panel represents the proportion of embryos that have overt patches lacking *opn1mw1* expression.

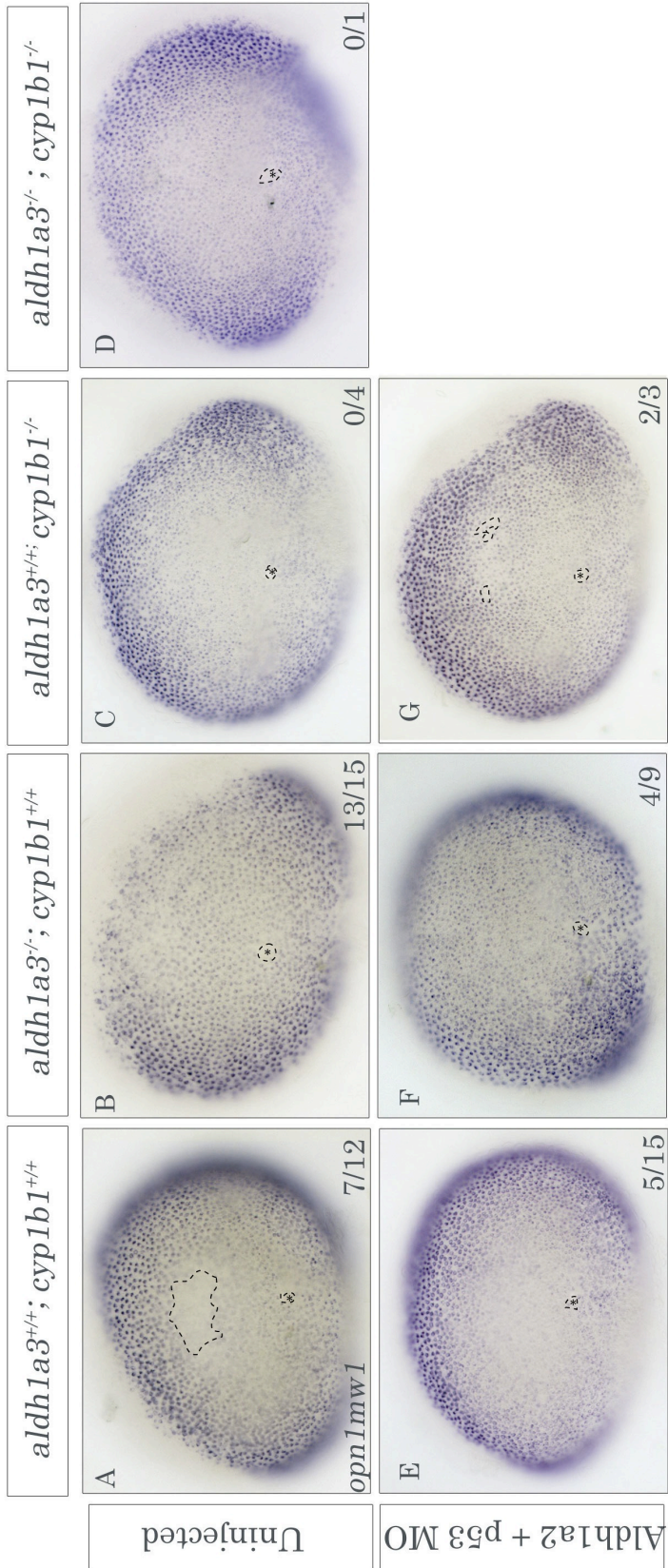


Figure 4.7: Frequency and severity of gaps in *opn1mw1* expression in unchanged with decrease in RA synthesis genes. (A) Quantification of the phenotypes shown in Figure 4.6. Shown is the proportion of 4 dpf embryos with gaps in the retina that lack expression of *opn1mw1*. (B) Box and whisker plots of the proportion of area that is lacking *opn1mw1* in 4dpf zebrafish retina by genotype and experimental treatment. The horizontal line within the box indicates the median, boundaries of the box indicate the 25th- and 75th -percentile, and the whiskers indicate the highest and lowest values of the results. The open circle indicates the mean. n.d. denotes no data collected for specified experimental treatments.

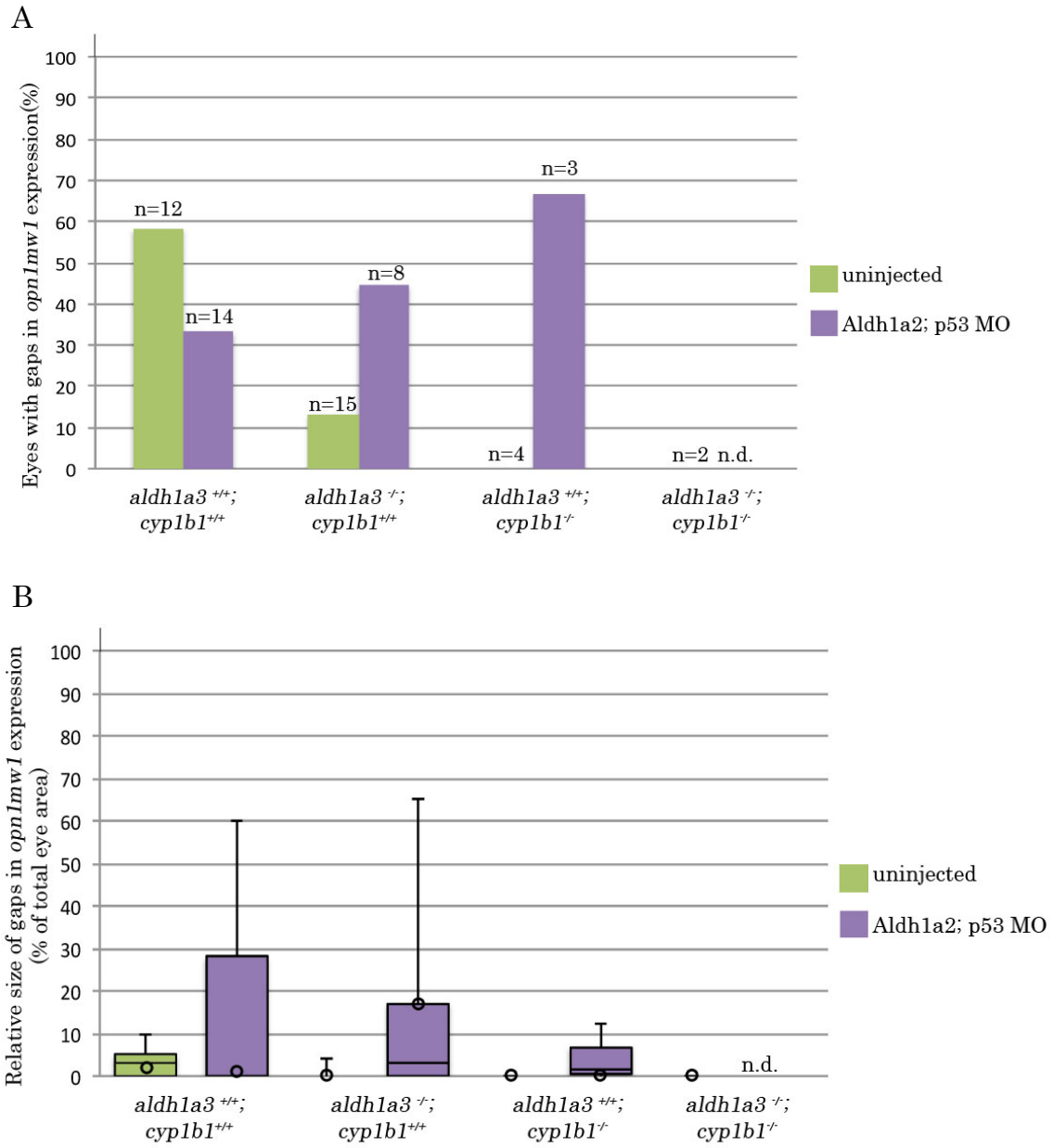


Figure 4.8: Loss of RA synthesis genes reduces rhodopsin expression. Shown are representative dissected eyes from zebrafish embryos following *in situ* hybridization analysis of *rho* gene expression at 4 dpf. Preliminary data shows that wild type embryos and embryos depleted of Aldh1a2, *aldh1a3* and *cyp1b1* singly or in combination exhibit similar expression and distribution of *rho* over the retina (A-D). Knockdown of Aldh1a2 and p53 results in the decrease of expression and aberrant distribution of *rho* (E-G). Number in each panel represents the proportion of embryos that have overtly reduced expression of *rho*.

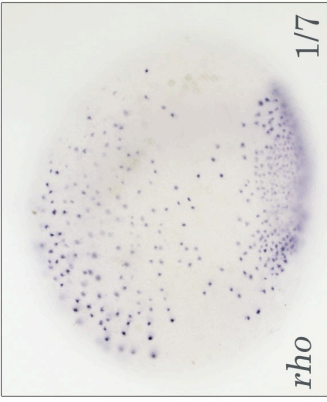
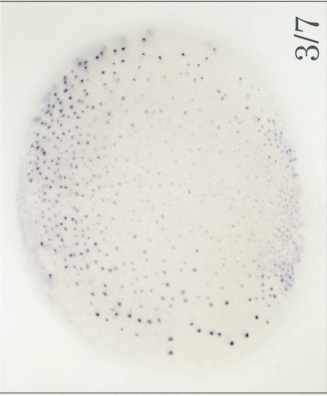
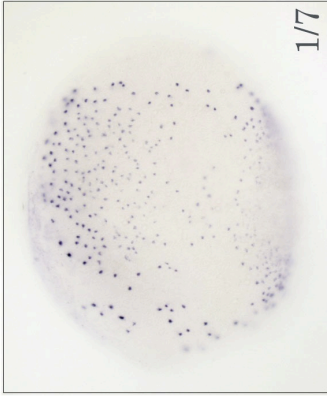
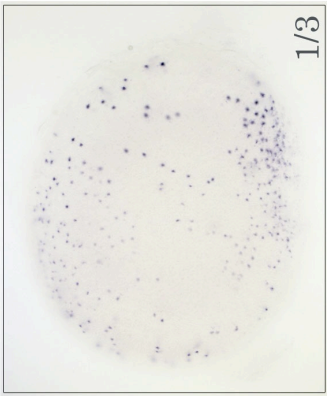
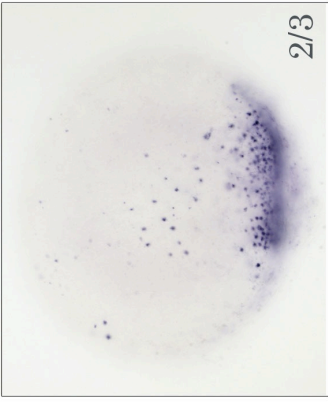
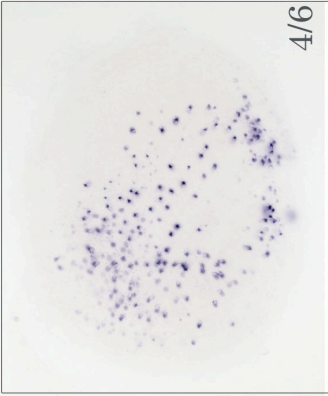
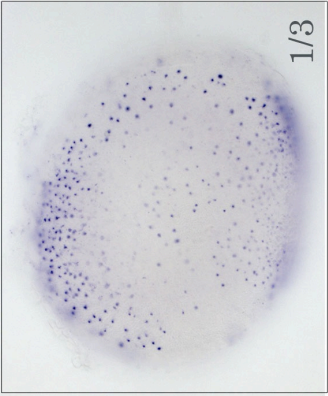
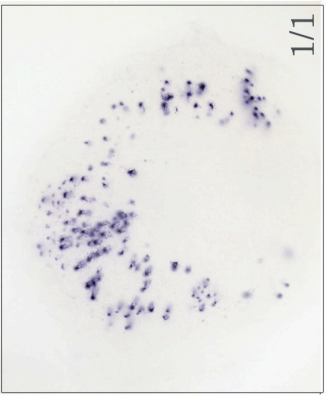
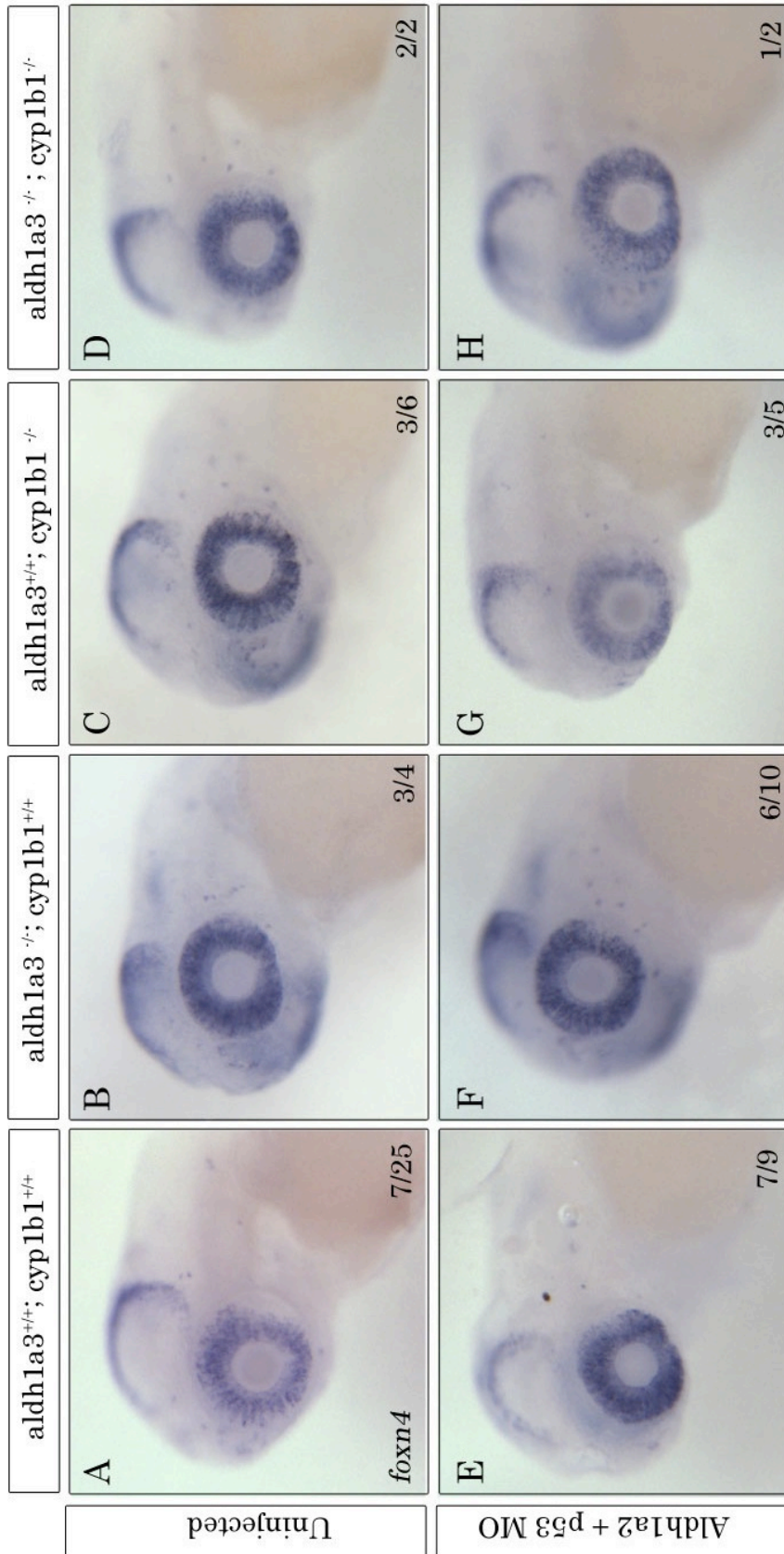
Uninjected	<p><i>aldh1a3^{+/+}; cyp1b1^{+/+}</i></p>  <p><i>rho</i></p> <p>1/7</p>	<p><i>aldh1a3^{-/-}; cyp1b1^{+/+}</i></p>  <p>3/7</p>	<p><i>aldh1a3^{+/+}; cyp1b1^{-/-}</i></p>  <p>1/7</p>	<p><i>aldh1a3^{-/-}; cyp1b1^{-/-}</i></p>  <p>1/3</p>
Aldh1a2 + p53 MO	 <p>2/3</p>	 <p>4/6</p>	 <p>1/3</p>	 <p>1/1</p>

Figure 4.9: Loss of RA synthesis genes results in the upregulation and expansion of *foxn4* expression. Shown are representative dissected eyes from zebrafish embryos following *in situ* hybridization analysis of *foxn4* gene expression at 3 dpf. Preliminary results suggests that, in comparison to wild type (A), loss of one or more RA synthesis gene results in the upregulation and expansion of expression domain of *foxn4* (B-G). Number in each panel represents the proportion of embryos that have overtly expanded expression of *foxn4* within the eye.



5 Evaluating the mutagenic activity of targeted endonucleases containing a *Sharkey* Fok1 cleavage domain variant in zebrafish

A portion of this chapter has been published. Laura M. Pillay, Lyndsay G. Selland, Valerie C. Fleisch, Patricia L. A. Leighton, Caroline S. Cheng, Jakub K. Famulski, R. Gary Ritzel, Lindsey D. March, Hao Wang, W. Ted Allison, and Andrew J. Waskiewicz. 2013. Evaluating the mutagenic activity of targeted endonuclease containing a *Sharkey* FokI cleavage domain variant in zebrafish. *Zebrafish*. 10(3):353-364.

5.1 Introduction

RA signalling within the developing embryo relies on the availability of maternal sources of vitamin A. In the mammalian embryo, retinol is provided from maternal circulation via the placenta, whereas avian, reptilian, amphibian and fish embryos use retinoid stores in the egg yolk. Retinoids in the teleost egg are stored as retinaldehyde and carotenoids. The roles that beta-carotene-metabolizing enzymes play in RA synthesis are yet to be determined. Two enzymes in zebrafish have been implicated in the synthesis of RA from beta-carotene: beta-carotene 15'15' monooxygenase (Bcmo1, also named Bcox, Cmo1, and Bco1) and beta-carotene 9'10' dioxygenase (Bco2a, also named Bcdo2, Bco2, and Cmo2). These two vertebrate carotenoid-oxygenases differ in their metabolism of beta-carotene and in their subcellular localization: BCMO1 is a cytoplasmic protein (Amengual et al., 2011), whereas BCO2a localizes to the mitochondria (Lindqvist and Andersson, 2002). Bcmo1 catalyzes the symmetrical cleavage of beta-carotene into two molecules of retinaldehyde (Lindqvist and Andersson, 2002; Paik et al., 2001; Redmond et al., 2001). Aldh enzymes then generate RA from the resulting retinaldehyde. Bco2a catalyzes an eccentric cleavage of beta-carotenes that results in the production of apo-carotenoids (Amengual et al., 2011; Hu et al., 2006; Mein et al., 2011). Apo-carotenoids may then be synthesized into RA. These products differ from retinoids produced through retinol metabolism and beta-carotene metabolism via Bcmo1.

Previous research has suggested that maternal supplementation of beta-carotene in a vitamin A deficient mouse model is able to support normal embryogenesis (Wassef et al. 2013). When visualized using in situ hybridization, *bcmo1* and *bco2a* mRNA are both expressed in the yolk syncytial layer as early as 14 and 21 somites, respectively (Lampert et al., 2003; Lobo et al., 2012). Bcmo1 knockdown in zebrafish has been previously shown to cause defects in patterning and differentiation during distinct RA-dependent developmental processes, including craniofacial, pectoral fin and

eye development (Lampert et al., 2003). Knockdown of *Bco2a* in zebrafish has demonstrated that *Bco2a* is induced as a response to oxidative stress and prevents apoptosis in blood cells (Lobo et al., 2012). The role of *Bco2a* in RA synthesis is currently unknown. These findings, taken together, suggest that, although retinol is thought to be the primary source of RA, beta-carotene is a viable source of RA during development. Through loss-of function studies of *Bcmo1* and *Bco2a*, we can begin to understand the contributions of enzymes involved in non-canonical RA synthesis in patterning and morphogenesis. We endeavoured to create zebrafish mutants for these genes using Transcription Activator-Like Effector Nuclease (TALEN) technology.

Targeted gene inactivation is a powerful method for the evaluation of gene function. Some technologies, including homologous recombination and RNA interference (RNAi), while shown to be effective in some model organisms, including mouse or *Caenorhabditis elegans*, are not amenable in all model organisms, notably within zebrafish. In the past decade, technologies using synthetic endonucleases have emerged that allow for the manipulation of genes of interest in a diverse range of cell types and organisms. Studies endeavour to create efficient and reliable methods for genome editing. Zinc finger nucleases (ZFNs) and TALENs exploit naturally occurring DNA-binding domains that can recognize many sequences and, when fused with non-specific endonucleases, are able to execute genetic alterations through the generation of double strand DNA breaks. In eukaryote, double strand breaks are repaired by two main mechanisms: homologous recombination (van den Bosch et al., 2002) and non-homologous end-joining (NHEJ) (Barnes, 2001; Lieber, 2010). NHEJ re-joins the broken ends and is often accomplished by loss or gain of some nucleotides, thus generating point mutations, insertions and deletions. Repair of synthetic endonuclease-induced lesions produces frameshift, nonsense or missense mutations, therefore abrogating gene function.

Zinc finger nucleases (ZFNs) selectively target and cleave specific gene sequences, making them a powerful tool for genome manipulation. To date, ZFNs have been successfully used to mutagenize mammalian cell lines (Lee et al., 2010; Lombardo et al., 2007; Maeder et al., 2008; Miller et al., 2007; Moehle et al., 2007; Perez et al., 2008; Porteus, 2006; Urnov et al., 2005; Zou et al., 2011), plants (Lloyd et al., 2005; Sander et al., 2011b; Shukla et al., 2009; Townsend et al., 2009; Wright et al., 2005; Zhang et al., 2010), *Drosophila melanogaster* (Beumer et al., 2006; Bibikova et al., 2002; Bozas et al., 2009), *Caenorhabditis elegans* (Morton et al., 2006), silkworm (Takasu et al., 2010), sea urchin (Ochiai et al., 2010), *Xenopus laevis* (Bibikova et al., 2001), mice (Carbery et al., 2010), rats (Geurts et al., 2009; Moreno et al., 2011), swine (Whyte and Prather; Yang et al.) catfish (Dong et al.), and zebrafish (Ben et al.; Doyon et al., 2008; Foley et al., 2009a; Foley et al., 2009b; Meng et al., 2008; Sander et al.). These synthetic restriction endonucleases are composed of chimeric fusions tandemly linking three or more Cys₂His₂ zinc fingers to the non-specific FokI endonuclease domain (Cathomen and Joung, 2008; Durai et al., 2005; Kim et al., 1996; Porteus and Carroll, 2005). Individual zinc fingers use a seven-amino acid motif to recognize and bind a specific DNA triplet sequence, with possible additional contact to the fourth base on the opposite strand (Figure 1B) (Kim and Berg, 1996; Pavletich and Pabo, 1991). This motif can be modified to generate custom zinc finger domains with novel DNA sequence specificities (Beerli and Barbas, 2002). Each zinc finger recognizes and binds to a specific DNA sequence. When two independent ZFNs bind DNA in a tail-to-tail orientation, with proper spacing (Figure 1A), their FokI endonuclease domains dimerize and generate double-strand DNA breaks (Bibikova et al., 2001; Gupta et al., 2011; Mani et al., 2005). While ZFNs is among the first technologies to provide an efficient and relatively simple platform for inducing site-specific mutations, there are complicating issues regarding their design and application. As zinc-finger modules are not available for all possible nucleotide triplets, not all sequences can be targeted

by ZFNs. ZFN specificity is not easy to predict as sequence specificity of individual zinc-fingers can be influenced by neighbouring domains in the protein (Isalan et al., 1997; Sander et al., 2011b). Further, ZFNs have been associated with cytotoxicity and off-target mutations (Cornu et al., 2008; Pruett-Miller et al., 2008; Radecke et al., 2010).

Transcription activator-like effector nucleases (TALENs) are another technology used for targeted mutagenesis applications. To date, TALENs have been successfully used to mutagenize mammalian cell lines (Cermak et al., 2011; Ding et al., 2013; Hockemeyer et al., 2011; Mussolino et al., 2011; Sakuma et al., 2013; Sanjana et al., 2012; Stroud et al., 2013; Sun et al., 2012), plants (Cermak et al., 2011; Li et al., 2012; Mahfouz et al., 2011; Zhang et al., 2013), yeast (Li et al., 2011b), *Drosophila melanogaster* (Liu et al., 2012; Sakuma et al., 2013), nematodes (Wood et al., 2011), silkworm (Ma et al., 2012; Sajwan et al., 2013), *Xenopus laevis* (Ishibashi et al., 2012; Lei et al., 2012; Sakuma et al., 2013), mice (Menoret et al., 2013; Sung et al., 2013; Wefers et al., 2013), rats (Mashimo et al., 2013; Menoret et al., 2013; Tesson et al., 2011), swine (Carlson et al., 2012) medaka (Ansai et al., 2013), and zebrafish (Bedell et al., 2012; Cade et al., 2012; Dahlem et al., 2012; Gupta et al., 2013; Huang et al., 2011; Moore et al., 2012; Sakuma et al., 2013; Sander et al., 2011a). Similar to ZFNs, TALENs use the catalytic domain of FokI to induce double-strand breaks that are repaired through homologous recombination, or NHEJ to generate insertions and deletions that alter gene function. A TALEN consists of a TAL effector array fused to the FokI endonuclease domain (Christian et al., 2010; Li et al., 2011a) (Figure 2A). TAL effectors recognize and bind to specific DNA sequences through series of repeated modules (Boch and Bonas, 2010; Bogdanove and Voytas, 2011; Deng et al., 2012; Mak et al., 2012). Each module contains two adjacent amino acids (termed a repeat variable di-residue, or RVD) conferring specificity for one of the four DNA basepairs (Boch and Bonas, 2010; Deng et al., 2012; Mak et al., 2012) (Figure 2B). Consequently, TALENs can be engineered to recognize nearly any DNA

sequence, without the requirement for selection assays. Notably, TALENs have been shown to elicit a greater mutation rate than ZFNs in zebrafish (Chen et al., 2013) and because of their high specificity, TALENs produce fewer off-target mutations than ZFNs (Mussolino et al., 2011). However, the somatic mutation rate obtained by using TALENs is still highly variable (<1% to 100%), and depends upon the selected TALEN scaffold, as well as the targeted locus (Bedell et al., 2012).

We sought to improve the efficiency of ZFN and TALEN synthetic targeted endonucleases for use in zebrafish mutagenesis. To achieve this, we examined the activity of both ZFNs and TALENs containing a FokI nuclease variant termed *Sharkey* (Guo et al.). We demonstrate that all tested *Sharkey* ZFNs exhibit greater *in vitro* cleavage of target-site DNA than controls. However, only one of two *Sharkey* ZFNs displays significantly greater activity *in vivo* in zebrafish, producing a higher frequency of insertion/deletion mutations than control ZFNs. As with ZFNs, we demonstrate that *Sharkey* TALENs exhibit greater *in vitro* cleavage of target-site DNA than controls. However, all *Sharkey* TALENs examined fail to produce any insertion/deletion mutations in zebrafish, displaying absent or significantly reduced *in vivo* mutagenic activity in comparison to control TALENs. Notably, embryos injected with *Sharkey* ZFNs and TALENs do not exhibit an increase in toxicity-related defects or mortality.

5.2 Results

5.2.1 Increased efficiency of *Sharkey* FokI nuclease-containing ZFNs *in vitro*

ZFN efficiency is dependent on the affinity and specificity of individual ZFN arrays (Cornu et al., 2008; Urnov et al., 2005), length and identity of the spacer region between ZFN recognition sites (Bibikova et al., 2001; Handel et al., 2009), interaction between FokI nuclease domains (Miller et al., 2007; Szczepek et al., 2007), and catalytic activity of the FokI nuclease domain (Guo et al.). In an attempt to improve the efficiency of our ZFN arrays, we made use

of a FokI nuclease variant termed *Sharkey*. This variant was initially developed and identified through a directed-evolution strategy, and demonstrates greater than fifteen-fold more catalytic activity than wild type FokI nuclease (Guo et al.).

We first wanted to determine if incorporating the *Sharkey* FokI nuclease into our ZFN arrays enhanced their function *in vitro*. To do this, we used our *in vitro* DNA cleavage assay to evaluate the abilities of control versus *Sharkey* FokI nuclease-containing ZFNs to cleave target-site-containing plasmid DNA (Figure 5.3). To compare ZFN cleavage activities, we diluted protein lysates (0.5X or 0.1X). As shown for *prp2* ZFN pairs (Figure 5.3A), samples containing *Sharkey prp2* ZFN protein lysate demonstrate more cleavage of *prp2* ZFN target-site-containing plasmid DNA than samples containing control *prp2* ZFN protein lysate. We observe similar results for *crx* ZFNs (Figure 5.3B). Our results demonstrate that *Sharkey* ZFNs exhibit increased *in vitro* cutting efficiency over control ZFNs. Combined, these data suggest that *Sharkey* FokI nuclease-containing ZFNs cleave DNA more efficiently than control FokI-nuclease containing ZFNs *in vitro*.

5.2.2 *In vivo* mutagenesis by *Sharkey* FokI nuclease-containing ZFNs

Given that *Sharkey* ZFNs function more efficiently than control ZFNs to cleave target-site DNA *in vitro*, we next wanted to determine if *Sharkey* ZFNs possess more *in vivo* mutagenic activity than control ZFNs. To do this, we injected single-cell zebrafish embryos with mRNAs encoding control or *Sharkey* ZFNs, and determined the sequence of target-site genomic DNA. Sequencing results from control versus *Sharkey* ZFN mRNA-injected embryos are summarized in Table 1. For *crx*, embryos injected with *Sharkey* ZFN mRNA exhibit a twenty-six times greater frequency of target-site specific insertion and deletion (indel) mutations than embryos injected with control ZFN mRNA (*Sharkey*, 31.2%, control, 1.2%; Table 5.1). This difference in *crx* indel frequency is statistically significant ($p < 0.0001$). For *prp2*, the difference

in indel frequency between embryos injected with *Sharkey* ZFN mRNA and embryos injected with control ZFN mRNA is not statistically significant (Table 5.1; p-values: *prp2*, 0.738). Combined, these data suggest that *Sharkey* FokI nuclease-containing ZFNs have the capacity to exhibit greater *in vivo* mutagenic activity than control FokI nuclease-containing ZFNs.

5.2.3 Toxicity of *Sharkey* FokI nuclease-containing ZFNs

One concern with using *Sharkey* ZFNs is that increased activity of the FokI nuclease might result in additional off-target effects, thereby increasing the morbidity, and decreasing the survival of injected embryos. We therefore quantified the proportion of embryos that exhibit non-specific developmental defects (referred to as ‘monster’-like), and the mortality rates of embryos injected with mRNAs encoding control or *Sharkey* ZFNs (Figure 5.4). In all cases examined, we failed to observe a significant difference (corrected p-value=1.000 for each) in the mortality rates of embryos injected with control versus *Sharkey* ZFN mRNAs (Figure 5.4). Furthermore, we note that embryos injected with control and *Sharkey* ZFN mRNAs exhibit a comparable proportion of monster-like phenotypes (Figure 5.4; adjusted p-values: *prp2*, 0.202; *crx*, 1.000). Combined, these data suggest that, in comparison to control ZFNs, *Sharkey* ZFNs do not significantly alter the morbidity and survival of zebrafish embryos.

5.2.4 Creation of *bcmo1* and *bco2a* TALENs

We designed pairs of TALENs to target *bcmo1* and *bco2a*. The *bcmo1* TALEN targets within the fourth exon of the gene and is downstream from the start codon (Figure 5.5). The *bco2a* TALEN targets within the second exon and is downstream of the start codon (Figure 5.6). We predicted that the disruption of the coding sequence of the gene would induce a premature stop codon within the gene and thus cause the truncation of the protein before any functional domains.

We injected single-cell zebrafish embryos with either *bcmo1* or *bco2a* TALEN mRNA into wild-type (AB) embryos (P₀). Genomic DNA was isolated from pools of injected embryos to detect for cutting activity of the TALENs. Indels were detected within these genomic DNA pools: 10/180 (5.5%) of the screened embryos contained indels in *bcmo1* and 8/117 (6.8%) of *bco2a* injected embryos contained indels (Table 5.2). A different pool of these injected P₀ were raised to adulthood and were incrossed. The offspring of these crosses were screened via HRM to identify carriers of germline mutations. Although insertions and deletions were detected within injected populations of zebrafish embryos, we failed to identify carriers of germline mutations (Table 5.2). These findings suggest that while indels were detected in TALEN mRNA-injected embryos, mutations were not identified in adult carriers.

5.2.5 Decreased in vivo mutagenesis by Sharkey FokI nuclease-containing TALENs

Given that some *Sharkey* ZFNs may exhibit increased *in vivo* mutagenesis activity in zebrafish when compared to control ZFNs, we next wanted to determine if applying the *Sharkey* FokI nuclease variant to our *WW* domain containing transcription regulator 1 (*wwtr1/taz*) and *homeobox B1b* (*hoxb1b*) TALENs would also increase their activity. To do this, we injected single-cell zebrafish embryos with mRNAs encoding control or *Sharkey* TALENs, and determined the frequency of indel mutations present in target-site genomic DNA using a combination of high-resolution melt curve analysis and sequencing. Results from control versus *Sharkey* TALEN mRNA-injected embryos are summarized in Table 5.4. Embryos injected with control TALENs demonstrate a modest target-site specific indel frequency (Table 5.4; *wwtr1*, 17.2%; *hoxb1b*, 5.9%). Conversely, in each case examined, embryos injected with *Sharkey* TALENs fail to exhibit any target-site specific indel mutations (Table 5.4; *wwtr1*, 0.0%; *hoxb1b*, 0.0%). The difference in *wwtr1* indel formation is statistically significant (p<0.0001). Notably, we fail to observe a significant difference in the mortality rates or monster-like phenotypes of

embryos injected with control versus *Sharkey* TALEN mRNAs (Figure 5.7A, corrected p-value=1.000 for each).

We next wanted to determine if incorporating the *Sharkey* FokI nuclease into our TALENs somehow reduced or destroyed their capacity to cleave target-site DNA. We therefore used our *in vitro* DNA cleavage assay to evaluate the abilities of control versus *Sharkey* FokI nuclease-containing TALENs to cleave target-site-containing plasmid DNA (Figure 5.7B). Notably, protein lysate samples containing *Sharkey wwtr1* TALENs demonstrate more cleavage of *wwtr1* TALEN target-site-containing plasmid DNA than samples containing control *wwtr1* TALENs (Figure 4B). Combined, these results suggest that *Sharkey* FokI nuclease-containing TALENs cleave DNA more efficiently than control FokI-nuclease containing TALENs *in vitro*, but possess absent or reduced *in vivo* mutagenic activity in zebrafish.

5.3 Discussion

Zinc finger nucleases (ZFNs) have been used to generate mutations in organisms that are not amenable to homologous recombination-based genetic modifications (Ben et al.; Doyon et al., 2008; Foley et al., 2009b; Geurts et al., 2009; Meng et al., 2008; Moreno et al.; Sander et al.). The ability for ZFNs to successfully cause mutations within the targeted gene is variable and somewhat low (~50-67%). Thus it is essential to develop techniques that can enhance the efficiency of ZFNs for use in mutagenesis applications.

5.3.1 *Sharkey* FokI nuclease increases ZFN efficiency *in vitro* and *in vivo*

The mutagenesis efficiency of a ZFN is partially dependent on the catalytic activity of its endonuclease domain (Guo et al.). We enhanced the catalytic activity of our ZFNs using the *Sharkey* FokI endonuclease domain variant. We demonstrate that *Sharkey* ZFNs exhibit increased *in vitro* cleavage of target-site DNA over control ZFNs. Our results also suggest that less *Sharkey* ZFN protein is required to elicit site-specific DNA cleavage *in vitro*. More importantly, we demonstrate that, in limited instances, *Sharkey*

ZFNs have the capacity to exhibit greater *in vivo* mutagenic activity than control ZFNs, producing up to a twenty-six-fold increase in the indel mutation frequency of injected zebrafish embryos (Table 5.1). This expands upon previous research in cell culture, which has shown that *Sharkey* ZFNs demonstrate three- to six-fold more mutagenic activity in HEK 293 cells when compared to wild type ZFNs (Guo et al.). Notably, ours is the first study to assess the relative mutagenic activity of control and *Sharkey* ZFNs *in vivo* in embryos. We did not systematically evaluate the off-target cleavage activity of *Sharkey* ZFNs in zebrafish. However, in comparison to control ZFNs, we find that *Sharkey* ZFNs do not increase the frequency of morphological defects, or the mortality of injected embryos. Our overall results suggest that incorporating the *Sharkey* FokI endonuclease domain into ZFNs may be a simple method of enhancing their mutagenic activity *in vivo*. Notably, introducing double-strand DNA breaks near a desired recombination site can dramatically increase the frequency of homologous recombination in mammalian cells (Choulika et al., 1995; Smith et al., 1995). ZFNs have previously been used in this capacity (Bibikova et al., 2003; Porteus and Baltimore, 2003). Consequently, the enhanced catalytic activity of *Sharkey* ZFNs may also be extremely beneficial for homologous recombination-mediated genome engineering applications.

5.3.2 *TALENs may not cause germline transmitted mutations*

Oviparous animals, including reptiles, fish and birds, store retinoids and carotenoids within their yolks. To obtain a greater understanding of how RA is synthesized through non-canonical pathways, we endeavoured to create TALENs for genes that encode for enzymes implicated in beta-carotene metabolism. TALENs for *bcmo1* and *bco2a* were successfully constructed and shown to induce indels in injected embryos. However, adult carriers of germline-transmitted mutations were not identified. The lack of germline mutations induced by these TALENs suggests that indels observed when

injected embryos were somatic. Variability of mutagenesis rates may come from intrinsic properties of the TALENs proteins, epigenetic environments of genomic loci or other unknown causes. Another possibility that germline transmission was not observed could be that mutations in *bcmo1* or *bco2a* results in embryonic lethality or infertility of adult carriers.

5.3.3 *Sharkey FokI nuclease does not increase the efficiency of TALENs*

TALENs have recently been shown to be up to ten times more mutagenic than ZFNs in zebrafish (Chen et al., 2013). Furthermore, TALENs can be targeted to nearly any DNA sequence, and their modular nature makes them easy to design and assemble. For these reasons, TALENs are quickly becoming the technology of choice for targeted mutagenesis in animal models. As we observed that the use of the *Sharkey* FokI endonuclease variant can increase the mutagenic activity of ZFNs, we sought to determine if this variant could also be applied to TALENs to enhance their catalytic activity. We demonstrate that, although *Sharkey* TALENs exhibit increased *in vitro* cleavage of target-site specific DNA over control TALENs, *Sharkey* TALENs exhibit significantly reduced *in vivo* mutagenic activity in injected zebrafish embryos when compared to control TALENs (Table 5.4). Our overall results suggest that incorporating the *Sharkey* FokI endonuclease domain into TALENs may severely abrogate their *in vivo* mutagenesis function in zebrafish.

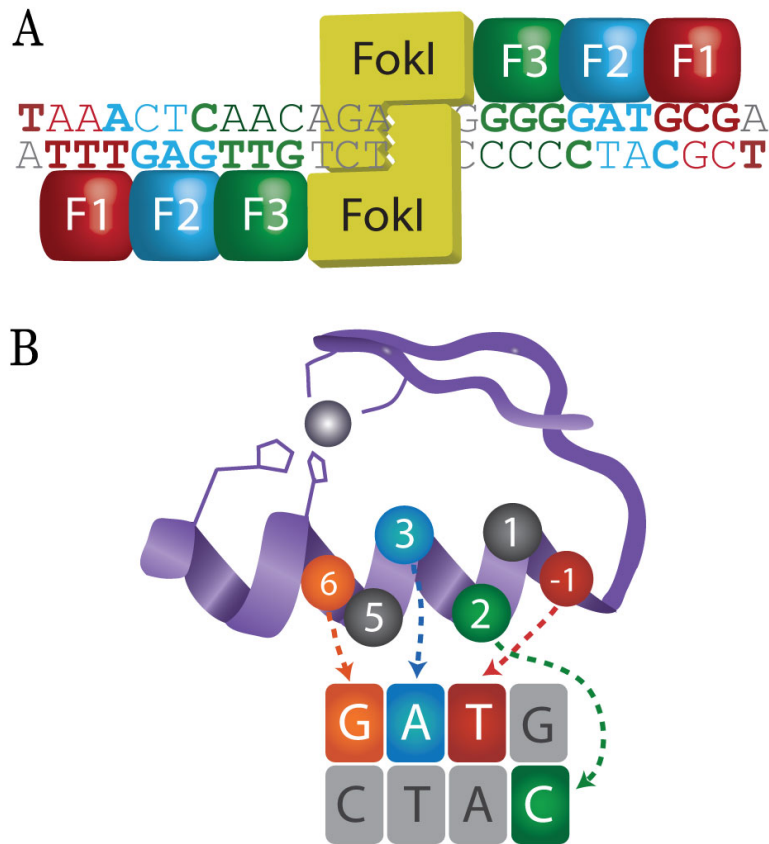


Figure 5.1: Zinc finger nuclease (ZFN) structure and target site recognition. (A) Schematic diagram of ZFN dimer bound to its target. Each ZFN is composed of the non-specific FokI endonuclease domain (Fok1) fused to three zinc fingers (F1, F2 F3) designed to specifically recognize sequences that flank the cleavage sites. Matched colours indicate individual zinc finger recognition sites. Upon sequence-specific binding of the two TALENs, dimerized endonucleases domains generate double-strand DNA breaks. (B) Schematic diagram of an individual zinc finger motif bound to target-site DNA. DNA-binding affinity and specificity is achieved by a seven amino-acid recognition motif. The amino acid side chains -1, 3 and 6 contact a triplet of DNA on the top strand, while the amino acid side chain at position 2 contacts a fourth base on the opposite strand.

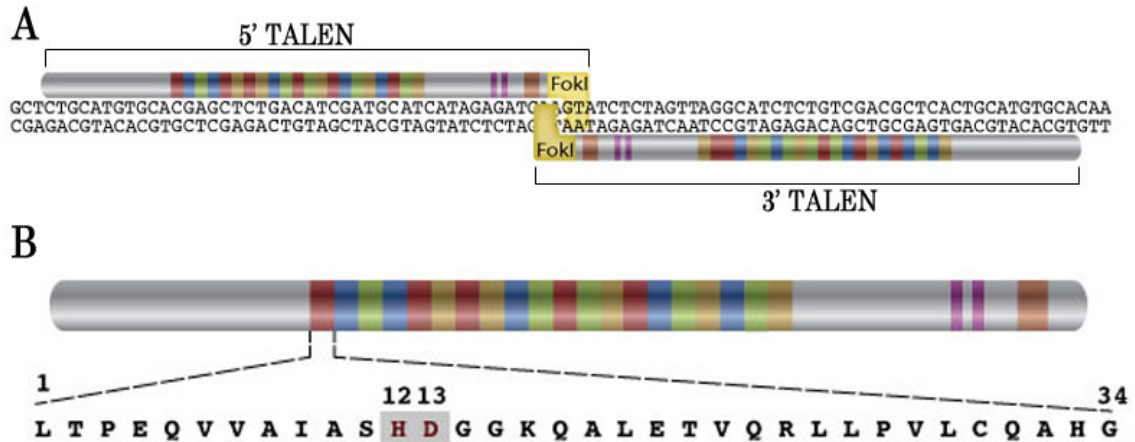


Figure 5.2: Transcription Activator-Like Effector Nuclease (TALEN) structure and target-site recognition. (A) Schematic diagram of TALEN dimer bound to its target. Each TALEN array consists of non-specific FokI endonuclease domain (FokI) fused to 12-27 repeats of highly conserved amino acids termed repeat variable diresidue (RVD) (Twenty RVDs are pictured). Upon sequence-specific binding of the two TALENs, dimerized endonucleases domains generate double-strand DNA breaks. (B) Schematic diagram of an individual TALEN array. A single TAL repeat is expanded with the two hypervariable residues highlighted in grey and red text. The four most common RVDs bind with a particular nucleotide. HD binds to C (pictures) NI binds to A, NG binds to T and NN binds to G (not pictured).

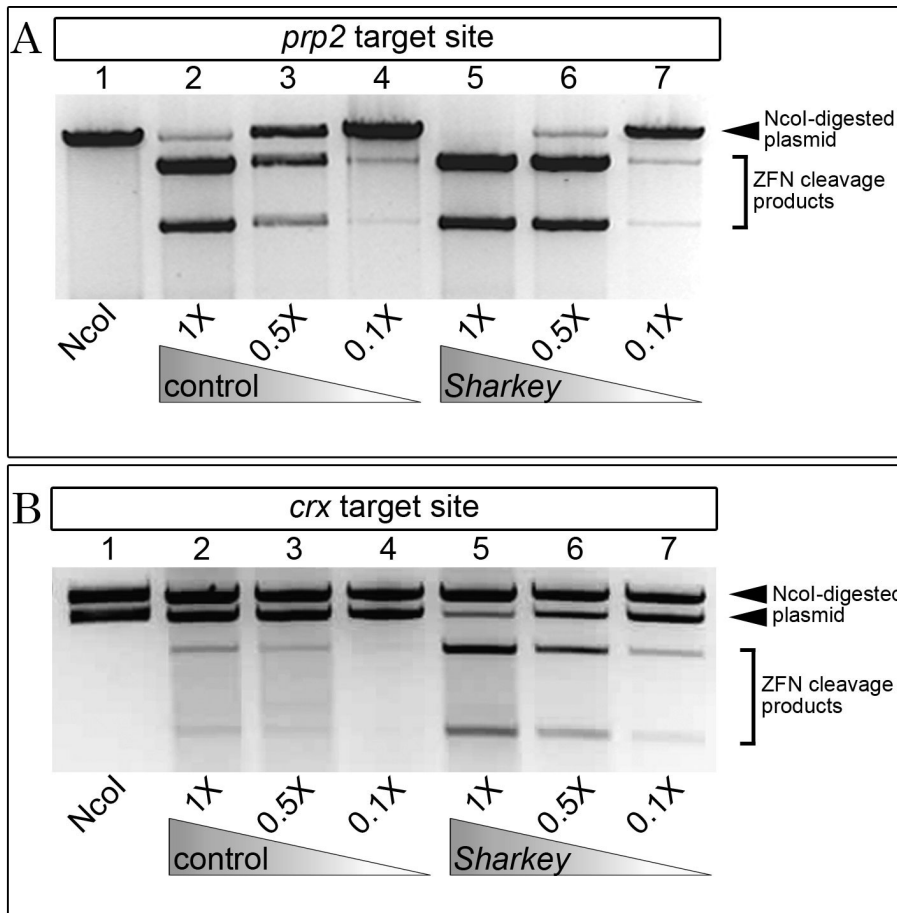


Figure 5.3: *In vitro* comparison of target-site specific DNA cleavage activity between control and *Sharkey* ZFNs. (A, B) Crude protein lysates of ZFN were used at normal concentration or diluted to one-half (0.5X) or one-tenth (0.1X) the amount. Gel electrophoretic analyses of *prp2* (A) and *crx* (B) target-site cleavage products. Incubation with NcoI alone produces a specific cleavage profile (Lane 1; arrowheads). Incubation of NcoI and ZFN crude protein lysates produces two additional cleavage products (brackets), indicating ZFN-mediated cleavage of target-site plasmid. In all cases, *Sharkey* ZFN crude protein lysates exhibit more cleavage of target-site plasmid than control ZFN crude protein lysates.

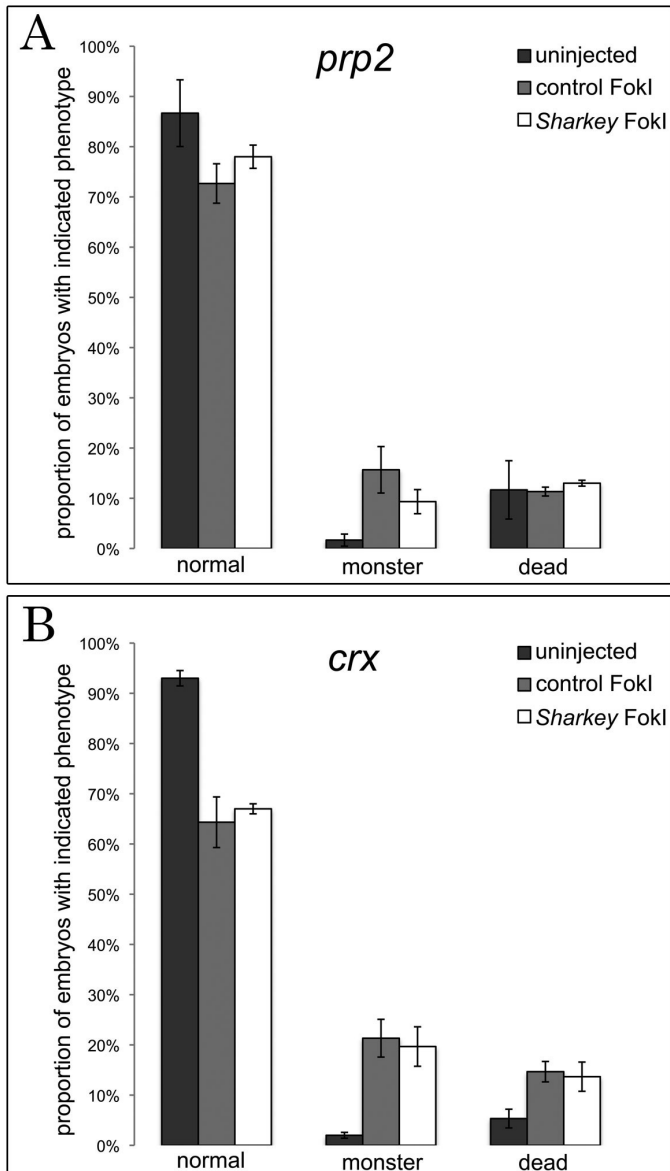


Figure 5.4: Effects of injecting control and *Sharkey* zinc finger nuclease mRNA on embryonic morphology and mortality. Graphs demonstrating the mean proportion of embryos with indicated phenotype at ~24 hpf, following injection of mRNAs encoding control FokI or *Sharkey* FokI *prp2* (A) or *crx* (C) ZFNs. Mean proportion of uninjected wild type embryos with indicated phenotype are also provided. Error bars represent standard error. No statistically significant differences were observed between the proportions of control FokI and *Sharkey* FokI in any category (adjusted *P*-values > 0.05).

GCTCGATTCCCTGAATGGGTGCAGGGAACACTAATACGCAATGGACCCGGCATGTTCTCTG
TTGGAGAGACGACATACAACCATTGGTTTGATGGAATGGCACTTTTGCACAGTTTTCGAA
TTAATAAAG

Figure 5.5: The *bcm1* TALEN binds DNA in coding sequence of the gene. Shown is the sequence of the fourth exon with important features highlighted. TALEN binding site is highlighted in cyan.

CCAAATTAAGTTTTTTCAGCTCAGCGAGCCACCACAAGCAGAACAGC**ATG**TCTTCTATGA
ACCGCCTGAACAGCAGCAAATCTGgtaggttaagacaccattctaactgtagatccacaa
aacttccaatctgaaactcttcttttgctccacagGCTGGAAGAAAACCAGGCCTAAGAA
TAAGGATCAATACTTTACAGATGTTACGGTCTGCCAAGCATTGAGAAGCTGATATGTTT
TGCAGACGAAACCCAGAGCCATT**ACGACCACTATTACAGGT**AACGTCCCTAGCTGGAT
C**AAGGGCAATTCCTCAGG**AACGGACCTGGGAAGTTTGAGATCGGAAGAAGCAG

Figure 5.6: The *bco2a* TALEN binds DNA in coding sequence of the gene. Shown is the sequence of the first two exons and the first intron with important features highlighted. TALEN binding site is highlighted in cyan. Exon (uppercase), intron (lowercase), ATG start codon (bold).

Figure 5.7: Comparison of control and *Sharkey wwtr1* TALENs.

(A) Graph demonstrating the mean proportion of embryos with indicated phenotype at ~ 24 hpf, following injection of mRNAs encoding control FokI or *Sharkey* FokI *wwtr1* TALENs. Mean proportion of uninjected embryos with indicated phenotype is also given. Error bars represent standard error. In no category are proportions of control FokI and *Sharkey* FokI mRNA-injected embryos statistically different from each other (corrected p-value > 0.05 for each). (B) *In vitro* comparison of target-site specific DNA cleavage activity between control and *Sharkey wwtr1* TALENs. TALEN crude protein lysates were used at normal concentration (1X), or were diluted to one-half (0.5X) or one-tenth (0.1X) the amount. Gel-electrophoretic analyses of target-site cleavage products. Incubation with NcoI alone produces a specific cleavage profile (lane 1; arrowhead). Incubation with NcoI and TALEN crude protein lysates produces two additional cleavage products (brackets), indicating TALEN-mediated cleavage of target-site plasmid. *Sharkey* TALEN crude protein lysates (lanes 5-7) exhibit more cleavage of target-site plasmid than control TALEN crude protein lysates (lanes 2-4).

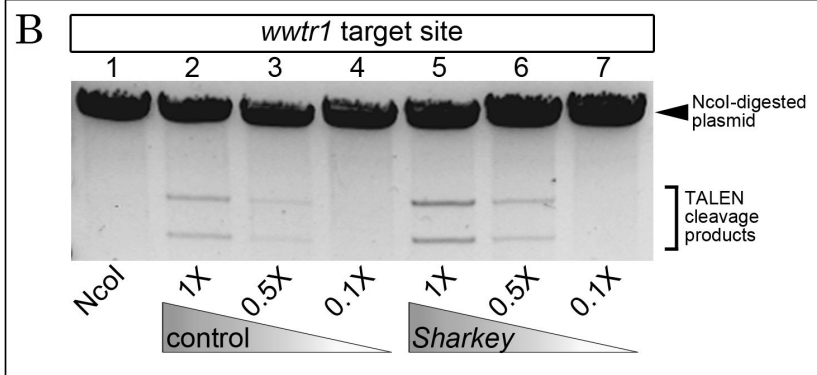
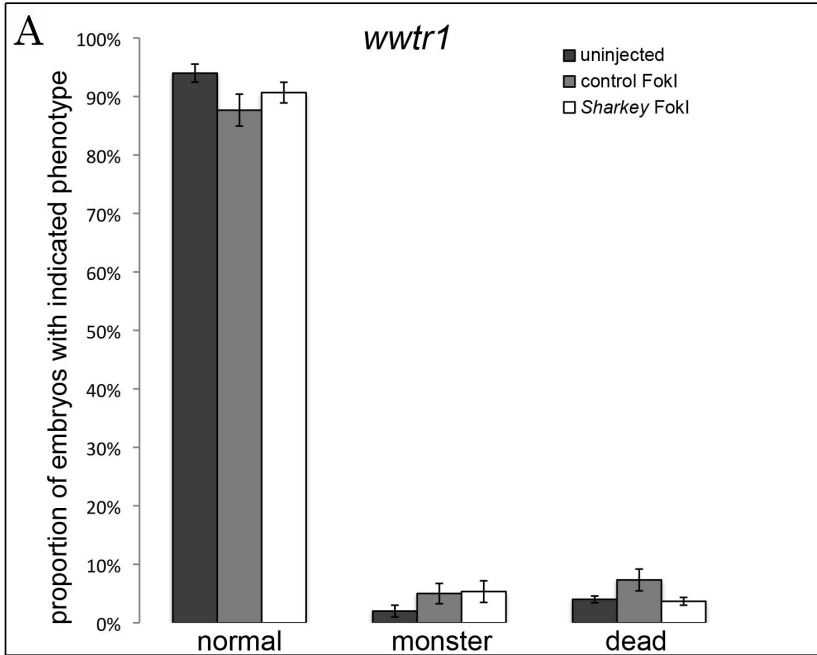


Table 5.1. Analyses of target-site specific mutations present in zebrafish embryos injected with control or *Sharkey* zinc finger nuclease (ZFN) mRNAs.

ZFN	Number of Clones Screened	Number of Indel Mutations	Indel Frequency (%)
<i>prp2</i>	130	6	4.6
<i>prp2</i> (<i>Sharkey</i>)	93	3	3.2
<i>crx</i>	83	1	1.2
<i>crx</i> (<i>Sharkey</i>)	157	49	31.2 ^a

PCR fragments containing the ZFN target-site were amplified, cloned, and sequenced. Data indicates combined frequency of insertions and deletions (indel frequency). ^aIndicates significant difference in indel mutation frequency between embryos injected with *Sharkey* and control ZFNs, as determined by two-tailed Fisher's exact test ($p < 0.0001$).

Table 5.2. Analyses of target-site specific mutations present in zebrafish embryos injected with *bcmo1* or *bco2a* transcription activator-like effector nuclease (TALEN) mRNAs

TALENs	Number of Clones Screened	Number of Indel Mutations	Indel Frequency (%)
<i>bcmo1</i>	180	10	5.5
<i>bco2a</i>	117	8	6.8

PCR fragments containing the ZFN target-site were amplified, cloned, and sequenced. Data indicates combined frequency of insertions and deletions (indel frequency).

Table 5.3. Analyses of target-site specific mutations present in progeny of P0 adults that had been injected with *bcmo1* or *bco2a* transcription activator-like effector nuclease (TALEN) mRNAs.

<i>TALEN</i>	<i>Number of Fish Screened</i>	<i>Number of Indel Mutations</i>	<i>Indel Frequency (%)</i>
<i>bcmo1</i>	54	0	0.0
<i>bco2a</i>	41	0	0.0

PCR fragments containing the TALEN target-site were amplified, cloned, and analyzed through a combination of high-resolution melt curve analysis followed by sequencing. Data indicates combined frequency of insertions and deletions (indel frequency).

Table 5.4. Analyses of target-site specific mutations present in zebrafish embryos injected with control or *Sharkey* transcription activator-like effector nuclease (TALEN) mRNAs.

TALEN	Number of Clones Screened	Number of Indel Mutations	Indel Frequency (%)
<i>wwtr1</i>	81	14	17.2
<i>wwtr1 (Sharkey)</i>	82	0	0.0 ^a
<i>hoxb1b</i>	85	5	5.9
<i>hoxb1b (Sharkey)</i>	44	0	0.0

PCR fragments containing the TALEN target-site were amplified, cloned, and analyzed through a combination of high-resolution melt curve analysis followed by sequencing. Data indicates combined frequency of insertions and deletions (indel frequency). ^aIndicates significant difference in indel mutation frequency between embryos injected with *Sharkey* and control TALENs, as determined by two-tailed Fisher's exact test ($p < 0.0001$).

6 Conclusions and Future Directions

Previous analyses using vertebrate models have identified molecular pathways that govern ocular development. Retinoic acid has been implicated to have functions in eye morphogenesis and photoreceptor differentiation. This pathway is conserved among vertebrates and the critical mammalian genes that regulate eye development have clear orthologs in zebrafish. Using zebrafish as a model organism, we have defined roles of RA synthesis enzymes present within the retina in early eye morphogenesis. We have also obtained preliminary results that reveal a role for retinoic acid signalling in photoreceptor cell fate decisions.

6.1 RA in eye morphogenesis

Previous studies have implicated RA in eye morphogenesis. Loss of RA either through VAD or through the loss of function of RA synthesis genes or signalling genes results in profound eye defects, including anophthalmia, microphthalmia and lack of ventral ocular structures (Lupo et al., 2005; Maden et al., 2007; Sen et al., 2005). Within the zebrafish retina, genes that encode for three RA synthesis enzymes within the retina are localized to discrete domains within the eye: *aldh1a3* is expressed within the ventral retina, *aldh1a2* is expressed within the dorsal retina, and *cyp1b1* is expressed in both dorsal and ventral domains. However, prior to this work, the precise molecular function of these RA synthesis enzymes in regulating eye morphogenesis was unknown. Through targeted ablation of Aldh1a3, Aldh1a2 and Cyp1b1 proteins, we demonstrate functional redundancy among RA synthesis enzymes and that RA generated by remaining enzymes act in a cell-nonautonomous fashion. We observe that RA synthesized by *aldh1a3* in the ventral retina is not sufficient to alter dorsoventral patterning or POM migration. Further, we have elucidated that RA synthesized within the retina is required for the proper closure of the choroid fissure. We also demonstrate that RA synthesized within the ventral domain of the retina is required for RA signalling within the dorsal retina.

aldh1a2 and *aldh1a3* are spatially restricted in the dorsal and ventral retina, respectively (French et al., 2009). It would be expected that each enzyme would synthesize RA that then initiates signalling within its respective domain. Surprisingly, we revealed that loss of *aldh1a3* results in a reduction of RA signalling in both dorsal and ventral domains of the retina. While RA is known to act cell-nonautonomously, it has not been previously documented that RA synthesized within one domain of the retina acts in a different retinal region. Ventrally synthesized RA may initiate signalling in the dorsal retina either directly through the diffusion to neighbouring cells, or indirectly through the regulation of RA synthesis genes within the dorsal eye. It is plausible that RA synthesized within the dorsal and ventral retina directly regulates itself through the suppression of the expression of an upstream synthesis enzyme. Feedback regulation is known to occur in the RA signalling pathway. Endogenous RA has been shown to suppress *Rdh10* expression in *Xenopus* embryos (Strate et al., 2009). Further, observations in zebrafish reveals that endogenous RA induces the expression of the RA degrading enzyme *Cyp26a1* (Dobbs-McAuliffe et al., 2004; Hu et al., 2008). Analysis of expression profiles of *rdh10a* and *cyp26a1* in our RA-depleted model would further our understanding of the spatial and temporal requirements for RA in the retina. To gain a better understanding of how RA regulates RA signalling within the retina, it would be useful to identify downstream transcriptional targets of the RA signalling pathway within the retina. This could be accomplished using RNA-sequencing to compare mRNA expression profiles of dissected heads or eyes of 28 hpf wild type embryos against *aldh1a3*^{-/-} mutants.

As RA synthesis genes are spatially restricted to the dorsal and ventral domains for the retina, it was hypothesized that these defined domains function to initiate or maintain retinal dorsoventral patterning. As mutations with *ALDH1A3* are associated with ventral eye defects in humans, we hypothesized that aberrant ventral retinal patterning result in ventral eye

defects, such as coloboma. Studies in zebrafish and *Xenopus* revealed that exogenous RA results in the ventralization of the eye, manifesting as the expansion of ventral patterning marker, *vax2* (Lupo et al., 2005; Schmitt and Dowling, 1996). We demonstrate that loss of *aldh1a3*, and thus reduction of RA levels within the retina, does not alter dorsoventral patterning. This finding complements murine research revealing that *Raldh1; Raldh3* double mutants have normal dorsoventral patterning (Matt et al., 2005; Matt et al., 2008; Molotkov et al., 2006; See and Clagett-Dame, 2009). While RA does not have a role in the establishment of dorsoventral patterning in the early retina, RA may have a later patterning role in maintaining patterning required for correct retinotectal mapping. A role for RA in the establishment and maintenance of retinotectal mapping was speculated from studies in chick embryos where dominant-negative RA receptors interfere with the expression of topographic guidance molecules EPHRINB2 and EPHB2 (Sen et al., 2005). As RA receptors heterodimerize with RXR receptors that regulate both RA signalling and others (Chawla et al., 2001), the introduction of dominant-negative RA receptors may have wider effects on gene expression. Expression patterns of *ephrinB2* and *ephb2* in mutants for individual and combined RA synthesis genes will provide insight into any role RA has in retinotectal patterning.

Extraocular cells play an important role in eye morphogenesis, notably the closure of choroid fissure. POM, a population of cells derived from cranial neural crest cells, has been previously implicated in mediating the closure of this transient structure (Lupo et al., 2011; Matt et al., 2005; See and Clagett-Dame, 2009). As mutations in *ALDH1A3* have been associated with incidence of MAC, we speculated that ventrally expressed *aldh1a3* would synthesize RA that acts on POM cells in a cell-nonautonomous manner to regulate POM migration. However, we observed that RA synthesized by *aldh1a3* is not sufficient to regulate POM migration. Previous research in mouse has shown that loss of *Raldh1* and *Raldh3* results in defects in POM, whereas *Raldh1* or

Raldh3 mutations yield only mild ocular defects (Matt et al., 2005; Molotkov et al., 2006). As RA enzymes within the eye are capable of functional compensation, it would be of interest to observe if POM dynamics are affected by concomitant reduction of *aldh1a2*, *aldh1a3*, and *cyp11b1*.

Loss-of-function mutations in *ALDH1A3* are associated with human cases of MAC (Aldahmesh et al., 2013; Fares-Taie et al., 2013; Mory et al., 2014; Roos et al., 2014; Yahyavi et al., 2013). We observe that depletion of *Aldh1a2* using morpholino oligonucleotides in zebrafish results in microphthalmia. Our understanding of mechanisms leading to microphthalmia remains incomplete. Microphthalmia could be caused by defects in eye field specification, developmental delay, and/or cellular proliferation or apoptosis. If depletion of *Aldh1a2* causes microphthalmia, it would be of interest to examine markers for proliferation, apoptosis and eye field specification to evaluate for defects in these processes. As morpholinos have been previously documented to activate p53-mediated cell death pathway (Bedell et al., 2011; Gerety and Wilkinson, 2011), the observed phenotype could be attributed to non-specific apoptosis. Alternatively, loss of RA may cause reduction of eye size via p53-dependent apoptosis within ocular tissues. To circumvent potential non-specific apoptotic effects, the acquisition or creation of an *aldh1a2* zebrafish mutant will enable RA depletion in the eye without the use of morpholinos. Further, it would be of interest to rescue eye size and coloboma phenotypes in *Aldh1a2*; *aldh1a3*⁻ morphomutants with exogenous RA treatment. Rescue experiments will ensure that observed phenotypes are specific to *Aldh1a2* depletion and not an artefact of morpholino injection.

Although mutations in *ALDH1A3* are one of the leading causes of MAC, we observe that *aldh1a3* mutant zebrafish do not have coloboma. Depletion of *Aldh1a2*, however, results in an increased incidence of coloboma in both wild type and *aldh1a3*⁻ mutants. This finding demonstrates that RA synthesized by *Aldh1a2* is sufficient to mediate choroid fissure closure whereas RA synthesized by *Aldh1a3* cannot solely fulfill this function. This differs from

observations made in mouse where *Raldh1* and *Raldh3* are each sufficient to control POM migration and invasion into the eye (Molotkov et al., 2006). The mechanism by which RA is required for the proper closure of the choroid fissure is currently unknown. It would be of interest to observe POM cell migration in *Aldh1a2; aldh1a3^{-/-}* zebrafish morphomutants using POM-specific or neural crest markers, such as *eya2* and *crestin*. Alternatively, previous research in mouse has revealed that vitamin A deficient embryos display a persistent fissure (See et al., 2008). As the dissolution of the basement membrane is crucial for the fusion of the choroid fissure, the RA synthesized by *Aldh1a3* and *Aldh1a2* may be responsible for the basal lamina to dissolve in zebrafish. The use of antibody staining against laminin in our *Aldh1a2; aldh1a3^{-/-}* morphomutants will indicate if there are defects in the dissolution of the basement membrane.

Since depletion of RA levels does not cause a fully penetrant coloboma phenotype, RA signalling pathway may not singly act to direct ocular morphogenesis. Instead, possible crosstalk between RA signalling and another signalling pathway(s) likely regulate ocular development in zebrafish. Wnt signalling is established as a regulator of distinct processes in ocular development, including eye field specification, morphogenetic movements, proliferation, differentiation and apoptosis (Fuhrmann, 2008). Cross-regulation of RA signalling and Wnt signalling pathways has been previously found to modulate cartilage development (Yasuhara et al., 2010). Previous studies demonstrated that in mouse Paired-Like Homeodomain 2 (*Pitx2*) mutant embryos, the closure of the choroid fissure is delayed or incomplete. Furthermore, loss of RA in *Raldh1; Raldh3* null mouse embryos causes reduced *Pitx2* expression which in turn decreases the expression of Wnt antagonist, *Dickkopf-related protein 2* (*Dkk2*) (Kumar and Duester, 2010; See and Clagett-Dame, 2009). Taken together, RA synthesized by *Aldh1a2* in the retina may be required to activate *Pitx2* expression within POM, which in turn induces *Dkk2* to suppress Wnt signalling in this tissue. Future work

examining the effects of Wnt signalling in eye morphogenesis and its interactions with RA signalling through the pharmaceutical or genetic inhibition of Wnt signalling will provide insight into the potential crosstalk between these pathways.

aldh1a3, *aldh1a2* and *cyp1b1* are expressed in the dorsal and/or ventral domains of the retina and we observe that they functionally compensate for each other. When these genes are depleted, we observe that RA signalling is markedly reduced but not lost. The residual RA in the retina residual RA may be produced by the small amounts of Aldh1a3, Aldh1a2 and Cyp1b1 remaining after knockdown. Alternatively, the residual RA may be a result of synthesis of RA from an unidentified source. One potential source of RA may be from the metabolism of beta-carotene into RA. In addition to retinol, carotenoids like beta-carotene, are stored in the yolk of oviparous species (Simoes-Costa et al., 2008). *bcmo1* acts tissue-specifically to generate embryonic retinaldehyde and therefore may be an alternate pathway in which RA can be synthesized (Lampert et al., 2003). The contribution of provitamin carotenoids in the maintenance of RA levels has yet to be elucidated. Understanding all of the enzymes that are capable of synthesizing RA will allow the creation of a model devoid of all RA, allowing a greater understanding of the role of this morphogen within vertebrate development.

This, and other studies, has demonstrated that RA acts in a cell-nonautonomous manner to promote proper POM migration and regulation of RA signalling within the dorsal domain of the retina. However, the purpose of strict regionalization of RA synthesizing enzymes within the retina remains unknown. RA synthesis enzymes are regionally restricted through the expression of RA degrading enzymes *cyp26a1* in the nasal and temporal domains of the retina. While murine studies reveal that *Cyp26a1* and *Cyp26c1* function to degrade RA in the central retina in late development (E13.5) (Sakai et al., 2004), no such role has been identified in earlier eye development. It would be of interest to investigate if RA is preferentially degraded along the

nasotemporal axis of the retina and what function an RA-less boundary serves within the retina. This could be accomplished using *giraffe/cyp26a1* zebrafish mutant embryos (Emoto et al., 2005) and analysing *giraffe* mutant embryos for defects in eye morphogenesis, alterations in retinal RA signalling domains, and aberrant expression of genes within the retina and surrounding tissues. As the transgenic *RARE:eGFP* line lacks sensitivity to low concentrations of RA, a more sensitive RA signalling transgenic line, such as the GEPRA reporter (described in 3.3.6) should be used to best visualize the boundaries of RA signalling within the retina.

6.2 RA and retinal neurogenesis

Previous studies have revealed that sustained exposure to high levels of RA causes abnormalities in the photoreceptor mosaic where more rod photoreceptors and red-sensitive cones to be differentiated in lieu of other cone photoreceptor subtypes (Hyatt et al., 1996a; Kelley et al., 1999; Prabhudesai et al., 2005). Our preliminary findings reveal that reduction of RA level through the depletion of *Aldh1a2*, *aldh1a3* and *cyp11b1*, singly or in combination, reveals the loss of UV- and blue- sensitive cones and rod photoreceptors in patches over the retina with a negligible effect on green cones. Further, a greater loss of RA, through the depletion of two or more RA synthesis enzymes results in larger opsin-negative patches within the retina, and thus a greater disruption of the photoreceptor mosaic. Severity of photoreceptor loss is not specific to dorsal and ventral retina suggesting that RA synthesized within the retina is able to diffuse through the entire tissue. It would be of interest to observe how levels of RA are altered when RA synthesis genes are depleted in embryos undergoing retinal neurogenesis. To achieve this, we could use the transgenic *Tg(12x RARE – ef1a:eGFP)* zebrafish line or the more sensitive GEPRA reporter (described in 3.3.6).

While the current study and other studies have suggested that RA influences specific photoreceptor cell fate, the mechanisms through which RA

controls photoreceptor fate remain largely unknown. The aberrations in the photoreceptor mosaic in embryos with reduced RA could be caused by several mechanisms, including but not limited to, loss or gain of other retinal subtypes (addressed in 4.3.2), loss of photoreceptor outer segment, cell death of selective cone photoreceptors, and misregulation of specific photoreceptor genes.

In this study, we observe the expression of opsin mRNAs to examine cone photoreceptor subtypes. Due to genome and tandem duplications, zebrafish have four medium-wave opsins and two long-wave options. Previous research has found that RA affects the expression of *opn1lw1* but not *opn1lw2*, suggesting that RA can regulate differential expression of opsin genes in a tandemly duplicated array (Mitchell et al. 2015). It would be of interest to design assays that will both allow for the observation of all orthologs of a specific opsin gene as well as each individual opsin ortholog. Further, opsins may not represent the presence or absence of the entire photoreceptor. Previous studies in teleost models have shown that knockdown of *bcmo1* which indirectly reduces RA synthesis disrupts photoreceptor morphology and the expression of photoreceptor markers (Biehlmaier et al., 2005; Lampert et al., 2003). Therefore, examination of transverse histological sections of the retina using markers that demarcate the entire photoreceptor would allow us to assess how RA depletion affects photoreceptor morphology.

Retinoids help regulate cell proliferation through the modulation of balance between mitosis and apoptosis (Rogers, 1997; Zakeri and Ahuja, 1997). Previous studies *in vivo* and *in vitro* suggest that RA affects retinal cell fate by modulating proliferation, differentiation and survival during development (Kastner et al., 1994; Kelley et al., 1995; Mendelsohn et al., 1994; Soderpalm et al., 2000; Stenkamp et al., 1993). The observed loss of rods and UV- and blue-sensitive cone photoreceptors could be attributed to increased apoptosis in the retina. To determine if loss of RA induces selective cell death of photoreceptors, it would be of interest to analyze apoptotic markers within the retinas of *Aldh1a2*; *aldh1a3*^{-/-}; *cyp1b1*^{-/-} morphomutants.

One possible mechanism by which RA regulates photoreceptor cell fate decisions is through the activation of intrinsic factors specific to photoreceptors. Previous research in cell culture suggests that RA activates *NRL*, a crucial intrinsic regulator of photoreceptor development and function (Khanna et al., 2006). The genes that RA regulates to mediate photoreceptor cell fate decisions are yet to be fully elucidated and require further analyses. It would therefore be of interest to identify direct and indirect transcriptional targets of RA synthesis genes using RNA-seq. This analysis may provide valuable insights into the genetic pathways that govern photoreceptor cell fate decisions.

Loss of photoreceptor subtypes may be due to the over-differentiation of other retinal cell types, notably horizontal and amacrine cells. Previous studies in cell culture and in zebrafish show that RA promotes rod photoreceptors at the expense of amacrine and horizontal cells. Consistent with this, our preliminary data suggests that loss of RA-synthesis genes causes an increased expression of *foxn4*, a gene that controls the genesis of amacrine and horizontal cells from RPCs (Li et al., 2004). Analysis of amacrine and horizontal cell markers will test the hypothesis that loss of RA causes RPCs to differentiate into amacrine and horizontal cells at the expense of photoreceptors. Additionally, it is unknown how RA regulates the expression of *foxn4*. Previous studies in mouse reveal that transcription factor myeloid ecotropic integration site 1 (Meis1) regulates Foxn4 expression during retinal neurogenesis (Islam et al., 2013). As Meis1 is activated by retinoic acid in mouse limb bud (Mercader et al., 2009), it is plausible that RA promotes amacrine cell fate through the activation of *meis1* and therefore, expression of *foxn4*. Further studies into the expression of *meis1* and its interactions with RA and *foxn4* within the retina will provide insight into this possible model of the RA regulation of amacrine cell fate decision.

Further, all analyses were performed using *in situ* hybridization. This method of analysis optimally requires the embryos to maintain transparent for

optical clarity. As pigmentation commences around 22 hpf within the retinal pigmented epithelium, the production of melanin must be inhibited for observation of gene expression of embryos 24 hpf or older (Karlsson et al., 2001; Kimmel et al., 1995; Millott and Lynn, 1966). We treat the embryos with PTU to block melanogenesis, which has been shown to effectively and reversibly inhibit pigmentation until 120 hpf. Previous research has revealed that PTU interacts with various signalling pathways including insulin-like growth factor and RA (Bohnsack et al., 2011). While our observed photoreceptor phenotypes are consistent with the current literature, these phenotypes may be exacerbated by concurrent PTU treatment. Alternate strategies for gene expression analysis without the use of PTU or other strategies to maintain transparency of zebrafish embryos need to be used to corroborate observations from *in situ* analysis. These strategies include using transgenic reporters for photoreceptors where gene expression can be observed in pigmented embryos. Alternatively, we could use zebrafish strains that have decreased pigmentation, such as *caspar* or *sandy* mutants that lack skin and eye pigmentation (Bohnsack et al., 2011).

6.3 Analyses of targeted endonucleases containing *Sharkey* FokI

ZFNs and TALENs enable the generation of mutations in organisms where homologous recombination-based genetic modifications are not amenable. Both ZFNs and TALENs are composed of a DNA-binding array fused to the non-specific nuclease domain of FokI. In an effort to improve the mutagenesis efficiency of these targeted endonucleases, we enhanced their catalytic activity using the *Sharkey* FokI nuclease domain variant. All construct tested display increased DNA cleavage activity *in vitro*. We demonstrate in zebrafish that the substitution of the wild type FokI for the *Sharkey* FokI variant in ZFN arrays may cause a marked increase in mutagenesis frequency *in vitro*. However, we demonstrate that TALENs containing the *Sharkey* FokI variant exhibit absent or severely reduced *in vivo*

mutagenic activity in zebrafish. Our overall results suggest that incorporating the *Sharkey* FokI endonuclease domain into TALENs may severely abrogate their *in vivo* mutagenesis function in zebrafish. Additionally, *Sharkey* FokI domain incorporation into ZFNs or TALENs does not generate increased toxicity-related defects of mortality. These data suggest that *Sharkey* ZFNs are an effective alternative to conventional ZFNs, but advise against the use of *Sharkey* TALENs in zebrafish.

Construction of *bcmo1* and *bco2a* TALENs was successful. Although insertions and deletions were detected in embryos injected with TALEN mRNA, these mutations were not detected in the germline. The mutagenesis rates of TALENs are highly variable (0 – 100%) and may be a result of intrinsic properties of TALENs, the accessibility of the chromatin, or other unknown factors. As factors that decrease efficiency of TALENs are largely unknown, future endeavours to create mutants could explore a newly developed mutagenesis technology, the CRISPR/Cas9 system. The clustered randomly interspersed short palindromic repeats (CRISPR)/Cas9 system has been modified from bacteria for use in the induction of sequence-specific double strand DNA breaks and targeted genome editing (Jinek et al., 2012). This new system requires two components to perform genome editing: a guide RNA and the Cas9 nuclease. The twenty nucleotides at the 5' end of the guide RNA direct Cas9 to a specific target DNA site. The CRISPR/Cas9 system has been used preferentially to ZFN or TALENs because of its ease of assembly, and fewer restraints on the selection of target DNA sites. Because the guide RNAs are smaller than TALEN arrays, several guide RNAs targeting the same gene in different regions can be injected into the embryo simultaneously without toxicity-related defects and lethality. The use of multiple guide RNAs can create larger deletions within the gene or possible cause precise deletion of the entire gene (Cong et al., 2013; Essletzbichler et al., 2014; Zhang et al., 2015). While CRISPRs induce off-target effects at high frequencies, the CRISPR/Cas9 system is being adapted to reduce off-target cleavage (Ran et al.,

2013). As both systems use very different mechanisms of DNA sequence recognition and creation of double strand breaks, it is possible that in some cases where one system fails or is inefficient, the other might work better (Auer et al., 2014; Hwang et al., 2013).

Because screening for mutations can be time-consuming and expensive, it would be of interest to improve Cas9 cutting efficiency. Cas9 engineering via directed evolution or rational design might improve the efficiency and precision of the CRISPR/Cas9 system. In addition to directed evolution strategies to develop a nuclease with greater cutting efficiency, other adaptations can be made to enhance the CRISPR/Cas9 system. Previous studies have generated a synthetic chimeric protein by fusing catalytically inactive Cas9 with the catalytic domain of FokI endonuclease (Aouida et al., 2015). This modified system uses the a pair of guide RNAs to guide the Cas9 and FokI fusion variants to the sense and antisense DNA strands to facilitate dimerization of the FokI domains and the creation of a double strand break. This Cas9/FokI nuclease variant has been demonstrated to improve specificity of genome editing. As *Sharkey*FokI improves ZFN cutting efficiency *in vivo*, it would be of interest to investigate if *Sharkey*FokI would also improve the cutting efficiency of the novel Cas9/FokI fusion.

References

- Abouzeid, H., Favez, T., Schmid, A., Agosti, C., Youssef, M., Marzouk, I., El Shakankiry, N., Bayoumi, N., Munier, F.L., Schorderet, D.F., 2014. Mutations in ALDH1A3 represent a frequent cause of microphthalmia/anophthalmia in consanguineous families. *Hum Mutat* 35, 949-953.
- Adler, R., Canto-Soler, M.V., 2007. Molecular mechanisms of optic vesicle development: complexities, ambiguities and controversies. *Dev Biol* 305, 1-13.
- Adler, R., Raymond, P.A., 2008. Have we achieved a unified model of photoreceptor cell fate specification in vertebrates? *Brain Res* 1192, 134-150.
- Aldahmesh, M.A., Khan, A.O., Hijazi, H., Alkuraya, F.S., 2013. Mutations in ALDH1A3 cause microphthalmia. *Clin Genet* 84, 128-131.
- Alexa, K., Choe, S.K., Hirsch, N., Etheridge, L., Laver, E., Sagerstrom, C.G., 2009. Maternal and zygotic *aldh1a2* activity is required for pancreas development in zebrafish. *PLoS One* 4, e8261.
- Allison, W.T., Barthel, L.K., Skebo, K.M., Takechi, M., Kawamura, S., Raymond, P.A., 2010. Ontogeny of cone photoreceptor mosaics in zebrafish. *J Comp Neurol* 518, 4182-4195.
- Altshuler, D., Cepko, C., 1992. A temporally regulated, diffusible activity is required for rod photoreceptor development in vitro. *Development* 114, 947-957.
- Alvarez-Delfin, K., Morris, A.C., Snelson, C.D., Gamse, J.T., Gupta, T., Marlow, F.L., Mullins, M.C., Burgess, H.A., Granato, M., Fadool, J.M., 2009. *Tbx2b* is required for ultraviolet photoreceptor cell specification during zebrafish retinal development. *Proc Natl Acad Sci U S A* 106, 2023-2028.
- Amengual, J., Gouranton, E., van Helden, Y.G., Hessel, S., Ribot, J., Kramer, E., Kiec-Wilk, B., Razny, U., Lietz, G., Wyss, A., Dembinska-Kiec, A., Palou, A., Keijer, J., Landrier, J.F., Bonet, M.L., von Lintig, J., 2011. Beta-carotene reduces body adiposity of mice via BCMO1. *PLoS One* 6, e20644.
- Ansai, S., Sakuma, T., Yamamoto, T., Ariga, H., Uemura, N., Takahashi, R., Kinoshita, M., 2013. Efficient targeted mutagenesis in medaka using custom-designed transcription activator-like effector nucleases. *Genetics* 193, 739-749.
- Aouida, M., Eid, A., Ali, Z., Cradick, T., Lee, C., Deshmukh, H., Atef, A., AbuSamra, D., Gadhoom, S.Z., Merzaban, J., Bao, G., Mahfouz, M., 2015. Efficient fdCas9 Synthetic Endonuclease with Improved Specificity for Precise Genome Engineering. *PLoS One* 10, e0133373.
- Asai-Coakwell, M., March, L., Dai, X.H., Duval, M., Lopez, I., French, C.R., Famulski, J., De Baere, E., Francis, P.J., Sundaresan, P., Sauve, Y., Koenekoop, R.K., Berry, F.B., Allison, W.T., Waskiewicz, A.J., Lehmann, O.J., 2013. Contribution of growth differentiation factor 6-dependent cell survival to early-onset retinal dystrophies. *Hum Mol Genet* 22, 1432-1442.

- Auer, T.O., Duroure, K., De Cian, A., Concordet, J.P., Del Bene, F., 2014. Highly efficient CRISPR/Cas9-mediated knock-in in zebrafish by homology-independent DNA repair. *Genome Res* 24, 142-153.
- Baehr, W., Wu, S.M., Bird, A.C., Palczewski, K., 2003. The retinoid cycle and retina disease. *Vision Res* 43, 2957-2958.
- Barbieri, A.M., Broccoli, V., Bovolenta, P., Alfano, G., Marchitello, A., Mocchetti, C., Crippa, L., Bulfone, A., Marigo, V., Ballabio, A., Banfi, S., 2002. Vax2 inactivation in mouse determines alteration of the eye dorsal-ventral axis, misrouting of the optic fibres and eye coloboma. *Development* 129, 805-813.
- Barishak, Y.R., 1992. *Embryology of the Eye and Its Adnexae*. Karger.
- Barnes, D.E., 2001. Non-homologous end joining as a mechanism of DNA repair. *Curr Biol* 11, R455-457.
- Bedell, V.M., Wang, Y., Campbell, J.M., Poshusta, T.L., Starker, C.G., Krug, R.G., 2nd, Tan, W., Penheiter, S.G., Ma, A.C., Leung, A.Y., Fahrenkrug, S.C., Carlson, D.F., Voytas, D.F., Clark, K.J., Essner, J.J., Ekker, S.C., 2012. In vivo genome editing using a high-efficiency TALEN system. *Nature* 491, 114-118.
- Bedell, V.M., Westcot, S.E., Ekker, S.C., 2011. Lessons from morpholino-based screening in zebrafish. *Brief Funct Genomics* 10, 181-188.
- Beerli, R.R., Barbas, C.F., 3rd, 2002. Engineering polydactyl zinc-finger transcription factors. *Nat Biotechnol* 20, 135-141.
- Begemann, G., Schilling, T.F., Rauch, G.J., Geisler, R., Ingham, P.W., 2001. The zebrafish neckless mutation reveals a requirement for raldh2 in mesodermal signals that pattern the hindbrain. *Development* 128, 3081-3094.
- Ben, J., Elworthy, S., Ng, A.S., van Eeden, F., Ingham, P.W., 2011. Targeted mutation of the talpid3 gene in zebrafish reveals its conserved requirement for ciliogenesis and Hedgehog signalling across the vertebrates. *Development* 138, 4969-4978.
- Bermejo, E., Martinez-Frias, M.L., 1998. Congenital eye malformations: clinical-epidemiological analysis of 1,124,654 consecutive births in Spain. *Am J Med Genet* 75, 497-504.
- Beumer, K., Bhattacharyya, G., Bibikova, M., Trautman, J.K., Carroll, D., 2006. Efficient gene targeting in *Drosophila* with zinc-finger nucleases. *Genetics* 172, 2391-2403.
- Bibikova, M., Beumer, K., Trautman, J.K., Carroll, D., 2003. Enhancing gene targeting with designed zinc finger nucleases. *Science* 300, 764.
- Bibikova, M., Carroll, D., Segal, D.J., Trautman, J.K., Smith, J., Kim, Y.G., Chandrasegaran, S., 2001. Stimulation of homologous recombination through targeted cleavage by chimeric nucleases. *Mol Cell Biol* 21, 289-297.
- Bibikova, M., Golic, M., Golic, K.G., Carroll, D., 2002. Targeted chromosomal cleavage and mutagenesis in *Drosophila* using zinc-finger nucleases. *Genetics* 161, 1169-1175.

- Biehlmaier, O., Lampert, J.M., von Lintig, J., Kohler, K., 2005. Photoreceptor morphology is severely affected in the beta,beta-carotene-15,15'-oxygenase (bcox) zebrafish morphant. *Eur J Neurosci* 21, 59-68.
- Blackshaw, S., Snyder, S.H., 1999. Encephalopsin: a novel mammalian extraretinal opsin discretely localized in the brain. *J Neurosci* 19, 3681-3690.
- Blentic, A., Gale, E., Maden, M., 2003. Retinoic acid signalling centres in the avian embryo identified by sites of expression of synthesising and catabolising enzymes. *Dev Dyn* 227, 114-127.
- Boch, J., Bonas, U., 2010. Xanthomonas AvrBs3 family-type III effectors: discovery and function. *Annu Rev Phytopathol* 48, 419-436.
- Bogdanove, A.J., Voytas, D.F., 2011. TAL effectors: customizable proteins for DNA targeting. *Science* 333, 1843-1846.
- Bohnsack, B.L., Gallina, D., Kahana, A., 2011. Phenothiourea sensitizes zebrafish cranial neural crest and extraocular muscle development to changes in retinoic acid and IGF signaling. *PLoS One* 6, e22991.
- Bohnsack, B.L., Kahana, A., 2013. Thyroid hormone and retinoic acid interact to regulate zebrafish craniofacial neural crest development. *Dev Biol* 373, 300-309.
- Bozas, A., Beumer, K.J., Trautman, J.K., Carroll, D., 2009. Genetic analysis of zinc-finger nuclease-induced gene targeting in *Drosophila*. *Genetics* 182, 641-651.
- Brzezinski, J.A., Reh, T.A., 2015. Photoreceptor cell fate specification in vertebrates. *Development* 142, 3263-3273.
- Cade, L., Reyon, D., Hwang, W.Y., Tsai, S.Q., Patel, S., Khayter, C., Joung, J.K., Sander, J.D., Peterson, R.T., Yeh, J.R., 2012. Highly efficient generation of heritable zebrafish gene mutations using homo- and heterodimeric TALENs. *Nucleic Acids Res* 40, 8001-8010.
- Cai, X., Conley, S.M., Naash, M.I., 2009. RPE65: role in the visual cycle, human retinal disease, and gene therapy. *Ophthalmic Genet* 30, 57-62.
- Cai, Z., Tao, C., Li, H., Ladher, R., Gotoh, N., Feng, G.S., Wang, F., Zhang, X., 2013. Deficient FGF signaling causes optic nerve dysgenesis and ocular coloboma. *Development* 140, 2711-2723.
- Cammas, L., Romand, R., Fraulob, V., Mura, C., Dolle, P., 2007. Expression of the murine retinol dehydrogenase 10 (Rdh10) gene correlates with many sites of retinoid signalling during embryogenesis and organ differentiation. *Dev Dyn* 236, 2899-2908.
- Cammas, L., Trenszt, F., Jellali, A., Ghyselinck, N.B., Roux, M.J., Dolle, P., 2010. Retinoic acid receptor (RAR)-alpha is not critically required for mediating retinoic acid effects in the developing mouse retina. *Invest Ophthalmol Vis Sci* 51, 3281-3290.
- Carbery, I.D., Ji, D., Harrington, A., Brown, V., Weinstein, E.J., Liaw, L., Cui, X., 2010. Targeted genome modification in mice using zinc-finger nucleases. *Genetics* 186, 451-459.

- Carlson, D.F., Tan, W., Lillico, S.G., Stverakova, D., Proudfoot, C., Christian, M., Voytas, D.F., Long, C.R., Whitelaw, C.B., Fahrenkrug, S.C., 2012. Efficient TALEN-mediated gene knockout in livestock. *Proc Natl Acad Sci U S A* 109, 17382-17387.
- Cathomen, T., Joung, J.K., 2008. Zinc-finger nucleases: the next generation emerges. *Mol Ther* 16, 1200-1207.
- Centanin, L., Wittbrodt, J., 2014. Retinal neurogenesis. *Development* 141, 241-244.
- Cepko, C.L., 1999. The roles of intrinsic and extrinsic cues and bHLH genes in the determination of retinal cell fates. *Curr Opin Neurobiol* 9, 37-46.
- Cepko, C.L., Austin, C.P., Yang, X., Alexiades, M., Ezzeddine, D., 1996. Cell fate determination in the vertebrate retina. *Proc Natl Acad Sci U S A* 93, 589-595.
- Cermak, T., Doyle, E.L., Christian, M., Wang, L., Zhang, Y., Schmidt, C., Baller, J.A., Somia, N.V., Bogdanove, A.J., Voytas, D.F., 2011. Efficient design and assembly of custom TALEN and other TAL effector-based constructs for DNA targeting. *Nucleic Acids Res* 39, e82.
- Chambers, D., Wilson, L., Maden, M., Lumsden, A., 2007. RALDH-independent generation of retinoic acid during vertebrate embryogenesis by CYP1B1. *Development* 134, 1369-1383.
- Chang, J.H., McCluskey, P.J., Wakefield, D., 2006a. Toll-like receptors in ocular immunity and the immunopathogenesis of inflammatory eye disease. *Br J Ophthalmol* 90, 103-108.
- Chang, L., Blain, D., Bertuzzi, S., Brooks, B.P., 2006b. Uveal coloboma: clinical and basic science update. *Curr Opin Ophthalmol* 17, 447-470.
- Chapman, D.L., Garvey, N., Hancock, S., Alexiou, M., Agulnik, S.I., Gibson-Brown, J.J., Cebra-Thomas, J., Bollag, R.J., Silver, L.M., Papaioannou, V.E., 1996. Expression of the T-box family genes, *Tbx1-Tbx5*, during early mouse development. *Dev Dyn* 206, 379-390.
- Chassaing, N., Golzio, C., Odent, S., Lequeux, L., Vigouroux, A., Martinovic-Bouriel, J., Tiziano, F.D., Masini, L., Piro, F., Maragliano, G., Delezoide, A.L., Attie-Bitach, T., Manouvrier-Hanu, S., Etchevers, H.C., Calvas, P., 2009. Phenotypic spectrum of STRA6 mutations: from Matthew-Wood syndrome to non-lethal anophthalmia. *Hum Mutat* 30, E673-681.
- Chavarria-Soley, G., Sticht, H., Aklillu, E., Ingelman-Sundberg, M., Pasutto, F., Reis, A., Rautenstrauss, B., 2008. Mutations in CYP1B1 cause primary congenital glaucoma by reduction of either activity or abundance of the enzyme. *Hum Mutat* 29, 1147-1153.
- Chawla, A., Repa, J.J., Evans, R.M., Mangelsdorf, D.J., 2001. Nuclear receptors and lipid physiology: opening the X-files. *Science* 294, 1866-1870.
- Chen, S., Oikonomou, G., Chiu, C.N., Niles, B.J., Liu, J., Lee, D.A., Antoshechkin, I., Prober, D.A., 2013. A large-scale in vivo analysis reveals that TALENs are significantly more mutagenic than ZFNs generated using context-dependent assembly. *Nucleic Acids Res* 41, 2769-2778.

- Chhetri, J., Jacobson, G., Gueven, N., 2014. Zebrafish--on the move towards ophthalmological research. *Eye (Lond)* 28, 367-380.
- Chinen, A., Hamaoka, T., Yamada, Y., Kawamura, S., 2003. Gene duplication and spectral diversification of cone visual pigments of zebrafish. *Genetics* 163, 663-675.
- Choulika, A., Perrin, A., Dujon, B., Nicolas, J.F., 1995. Induction of homologous recombination in mammalian chromosomes by using the I-SceI system of *Saccharomyces cerevisiae*. *Mol Cell Biol* 15, 1968-1973.
- Chow, R.L., Lang, R.A., 2001. Early eye development in vertebrates. *Annu Rev Cell Dev Biol* 17, 255-296.
- Christian, M., Cermak, T., Doyle, E.L., Schmidt, C., Zhang, F., Hummel, A., Bogdanove, A.J., Voytas, D.F., 2010. Targeting DNA double-strand breaks with TAL effector nucleases. *Genetics* 186, 757-761.
- Chung, D.C., Traboulsi, E.I., 2009. Leber congenital amaurosis: clinical correlations with genotypes, gene therapy trials update, and future directions. *J AAPOS* 13, 587-592.
- Cong, L., Ran, F.A., Cox, D., Lin, S., Barretto, R., Habib, N., Hsu, P.D., Wu, X., Jiang, W., Marraffini, L.A., Zhang, F., 2013. Multiplex genome engineering using CRISPR/Cas systems. *Science* 339, 819-823.
- Cornu, T.I., Thibodeau-Beganny, S., Guhl, E., Alwin, S., Eichtinger, M., Joung, J.K., Cathomen, T., 2008. DNA-binding specificity is a major determinant of the activity and toxicity of zinc-finger nucleases. *Mol Ther* 16, 352-358.
- Cremers, F.P., van den Hurk, J.A., den Hollander, A.I., 2002. Molecular genetics of Leber congenital amaurosis. *Hum Mol Genet* 11, 1169-1176.
- D'Ambrosio, D.N., Clugston, R.D., Blamer, W.S., 2011. Vitamin A metabolism: an update. *Nutrients* 3, 63-103.
- Dahlem, T.J., Hoshijima, K., Jurynek, M.J., Gunther, D., Starker, C.G., Locke, A.S., Weis, A.M., Voytas, D.F., Grunwald, D.J., 2012. Simple methods for generating and detecting locus-specific mutations induced with TALENs in the zebrafish genome. *PLoS Genet* 8, e1002861.
- den Hollander, A.I., Roepman, R., Koeneke, R.K., Cremers, F.P., 2008. Leber congenital amaurosis: genes, proteins and disease mechanisms. *Prog Retin Eye Res* 27, 391-419.
- Deng, D., Yan, C., Pan, X., Mahfouz, M., Wang, J., Zhu, J.K., Shi, Y., Yan, N., 2012. Structural basis for sequence-specific recognition of DNA by TAL effectors. *Science* 335, 720-723.
- Ding, Q., Lee, Y.K., Schaefer, E.A., Peters, D.T., Veres, A., Kim, K., Kuperwasser, N., Motola, D.L., Meissner, T.B., Hendriks, W.T., Trevisan, M., Gupta, R.M., Moisan, A., Banks, E., Friesen, M., Schinzel, R.T., Xia, F., Tang, A., Xia, Y., Figueroa, E., Wann, A., Ahfeldt, T., Daheron, L., Zhang, F., Rubin, L.L., Peng, L.F., Chung, R.T., Musunuru, K., Cowan, C.A., 2013. A TALEN Genome-Editing System for Generating Human Stem Cell-Based Disease Models. *Cell Stem Cell* 12, 238-251.

- Dobbs-McAuliffe, B., Zhao, Q., Linney, E., 2004. Feedback mechanisms regulate retinoic acid production and degradation in the zebrafish embryo. *Mech Dev* 121, 339-350.
- Doerre, G., Malicki, J., 2002. Genetic analysis of photoreceptor cell development in the zebrafish retina. *Mech Dev* 110, 125-138.
- Dong, Z., Ge, J., Li, K., Xu, Z., Liang, D., Li, J., Jia, W., Li, Y., Dong, X., Cao, S., Wang, X., Pan, J., Zhao, Q., 2011. Heritable targeted inactivation of myostatin gene in yellow catfish (*Pelteobagrus fulvidraco*) using engineered zinc finger nucleases. *PLoS One* 6, e28897.
- Dowling, J.E., Wald, G., 1958. Vitamin a Deficiency and Night Blindness. *Proc Natl Acad Sci U S A* 44, 648-661.
- Doyon, Y., McCammon, J.M., Miller, J.C., Faraji, F., Ngo, C., Katibah, G.E., Amora, R., Hocking, T.D., Zhang, L., Rebar, E.J., Gregory, P.D., Urnov, F.D., Amacher, S.L., 2008. Heritable targeted gene disruption in zebrafish using designed zinc-finger nucleases. *Nat Biotechnol* 26, 702-708.
- Dupe, V., Matt, N., Garnier, J.M., Chambon, P., Mark, M., Ghyselinck, N.B., 2003. A newborn lethal defect due to inactivation of retinaldehyde dehydrogenase type 3 is prevented by maternal retinoic acid treatment. *Proc Natl Acad Sci U S A* 100, 14036-14041.
- Durai, S., Mani, M., Kandavelou, K., Wu, J., Porteus, M.H., Chandrasegaran, S., 2005. Zinc finger nucleases: custom-designed molecular scissors for genome engineering of plant and mammalian cells. *Nucleic Acids Res* 33, 5978-5990.
- Durston, A.J., Timmermans, J.P., Hage, W.J., Hendriks, H.F., de Vries, N.J., Heideveld, M., Nieuwkoop, P.D., 1989. Retinoic acid causes an anteroposterior transformation in the developing central nervous system. *Nature* 340, 140-144.
- Ekker, S.C., Ungar, A.R., Greenstein, P., von Kessler, D.P., Porter, J.A., Moon, R.T., Beachy, P.A., 1995. Patterning activities of vertebrate hedgehog proteins in the developing eye and brain. *Curr Biol* 5, 944-955.
- Emoto, Y., Wada, H., Okamoto, H., Kudo, A., Imai, Y., 2005. Retinoic acid-metabolizing enzyme *Cyp26a1* is essential for determining territories of hindbrain and spinal cord in zebrafish. *Dev Biol* 278, 415-427.
- Essletzbichler, P., Konopka, T., Santoro, F., Chen, D., Gapp, B.V., Kralovics, R., Brummelkamp, T.R., Nijman, S.M., Burckstummer, T., 2014. Megabase-scale deletion using CRISPR/Cas9 to generate a fully haploid human cell line. *Genome Res* 24, 2059-2065.
- Fadool, J.M., 2003. Development of a rod photoreceptor mosaic revealed in transgenic zebrafish. *Dev Biol* 258, 277-290.
- Fan, X., Molotkov, A., Manabe, S., Donmoyer, C.M., Deltour, L., Foglio, M.H., Cuenca, A.E., Blaner, W.S., Lipton, S.A., Duester, G., 2003. Targeted disruption of *Aldh1a1* (*Raldh1*) provides evidence for a complex mechanism of retinoic acid synthesis in the developing retina. *Mol Cell Biol* 23, 4637-4648.

- Fares-Taie, L., Gerber, S., Chassaing, N., Clayton-Smith, J., Hanein, S., Silva, E., Serey, M., Serre, V., Gerard, X., Baumann, C., Plessis, G., Demeer, B., Bretillon, L., Bole, C., Nitschke, P., Munnich, A., Lyonnet, S., Calvas, P., Kaplan, J., Ragge, N., Rozet, J.M., 2013. ALDH1A3 mutations cause recessive anophthalmia and microphthalmia. *Am J Hum Genet* 92, 265-270.
- Fitzpatrick, D.R., van Heyningen, V., 2005. Developmental eye disorders. *Curr Opin Genet Dev* 15, 348-353.
- Fleisch, V.C., Neuhauss, S.C., 2006. Visual behavior in zebrafish. *Zebrafish* 3, 191-201.
- Foley, J.E., Maeder, M.L., Pearlberg, J., Joung, J.K., Peterson, R.T., Yeh, J.R., 2009a. Targeted mutagenesis in zebrafish using customized zinc-finger nucleases. *Nat Protoc* 4, 1855-1867.
- Foley, J.E., Yeh, J.R., Maeder, M.L., Reyon, D., Sander, J.D., Peterson, R.T., Joung, J.K., 2009b. Rapid mutation of endogenous zebrafish genes using zinc finger nucleases made by Oligomerized Pool ENgineering (OPEN). *PLoS One* 4, e4348.
- Forrest, D., Swaroop, A., 2012. Minireview: the role of nuclear receptors in photoreceptor differentiation and disease. *Mol Endocrinol* 26, 905-915.
- French, C.R., Erickson, T., French, D.V., Pilgrim, D.B., Waskiewicz, A.J., 2009. Gdf6a is required for the initiation of dorsal-ventral retinal patterning and lens development. *Dev Biol* 333, 37-47.
- Fuhrmann, S., 2008. Wnt signaling in eye organogenesis. *Organogenesis* 4, 60-67.
- Fuhrmann, S., Levine, E.M., Reh, T.A., 2000. Extraocular mesenchyme patterns the optic vesicle during early eye development in the embryonic chick. *Development* 127, 4599-4609.
- Gage, P.J., Qian, M., Wu, D., Rosenberg, K.I., 2008. The canonical Wnt signaling antagonist DKK2 is an essential effector of PITX2 function during normal eye development. *Dev Biol* 317, 310-324.
- Gage, P.J., Rhoades, W., Prucka, S.K., Hjalt, T., 2005. Fate maps of neural crest and mesoderm in the mammalian eye. *Invest Ophthalmol Vis Sci* 46, 4200-4208.
- Gerety, S.S., Wilkinson, D.G., 2011. Morpholino artifacts provide pitfalls and reveal a novel role for pro-apoptotic genes in hindbrain boundary development. *Dev Biol* 350, 279-289.
- Gerth-Kahlert, C., Williamson, K., Ansari, M., Rainger, J.K., Hingst, V., Zimmermann, T., Tech, S., Guthoff, R.F., van Heyningen, V., Fitzpatrick, D.R., 2013. Clinical and mutation analysis of 51 probands with anophthalmia and/or severe microphthalmia from a single center. *Mol Genet Genomic Med* 1, 15-31.
- Geurts, A.M., Cost, G.J., Freyvert, Y., Zeitler, B., Miller, J.C., Choi, V.M., Jenkins, S.S., Wood, A., Cui, X., Meng, X., Vincent, A., Lam, S., Michalkiewicz, M., Schilling, R., Foeckler, J., Kalloway, S., Weiler, H., Menoret, S., Anegon, I., Davis, G.D., Zhang, L., Rebar, E.J., Gregory,

- P.D., Urnov, F.D., Jacob, H.J., Buelow, R., 2009. Knockout rats via embryo microinjection of zinc-finger nucleases. *Science* 325, 433.
- Grandel, H., Lun, K., Rauch, G.J., Rhinn, M., Piotrowski, T., Houart, C., Sordino, P., Kuchler, A.M., Schulte-Merker, S., Geisler, R., Holder, N., Wilson, S.W., Brand, M., 2002. Retinoic acid signalling in the zebrafish embryo is necessary during pre-segmentation stages to pattern the anterior-posterior axis of the CNS and to induce a pectoral fin bud. *Development* 129, 2851-2865.
- Gregory-Evans, C.Y., Williams, M.J., Halford, S., Gregory-Evans, K., 2004. Ocular coloboma: a reassessment in the age of molecular neuroscience. *J Med Genet* 41, 881-891.
- Gu, X., Xu, F., Wang, X., Gao, X., Zhao, Q., 2005. Molecular cloning and expression of a novel CYP26 gene (*cyp26d1*) during zebrafish early development. *Gene Expr Patterns* 5, 733-739.
- Guillemot, F., Cepko, C.L., 1992. Retinal fate and ganglion cell differentiation are potentiated by acidic FGF in an in vitro assay of early retinal development. *Development* 114, 743-754.
- Guo, J., Gaj, T., Barbas, C.F., 3rd, 2010. Directed evolution of an enhanced and highly efficient FokI cleavage domain for zinc finger nucleases. *J Mol Biol* 400, 96-107.
- Gupta, A., Hall, V.L., Kok, F.O., Shin, M., McNulty, J.C., Lawson, N.D., Wolfe, S.A., 2013. Targeted Chromosomal Deletions and Inversions in Zebrafish. *Genome Res*.
- Gupta, A., Meng, X., Zhu, L.J., Lawson, N.D., Wolfe, S.A., 2011. Zinc finger protein-dependent and -independent contributions to the in vivo off-target activity of zinc finger nucleases. *Nucleic Acids Res* 39, 381-392.
- Gurmu, F., Hussein, S., Laing, M., 2014. The potential of orange-fleshed sweet potato to prevent vitamin A deficiency in Africa. *Int J Vitam Nutr Res* 84, 65-78.
- Hale, F., 1933. Pigs born without eye balls. *J Hered* 24, 105-106.
- Hale, F., 1935. The relation of vitamin A to anophthalmos in pigs. *Amer. J. Ophthalmol* 18, 1087-1093.
- Hale, F., 1937. The relationship of maternal vitamin A deficiency to microphthalmia in pigs. *Tex State J Med* 33, 228-332.
- Hale, L.A., Tallafuss, A., Yan, Y.L., Dudley, L., Eisen, J.S., Postlethwait, J.H., 2006. Characterization of the retinoic acid receptor genes *raraa*, *rarab* and *rarg* during zebrafish development. *Gene Expr Patterns* 6, 546-555.
- Halilagic, A., Zile, M.H., Studer, M., 2003. A novel role for retinoids in patterning the avian forebrain during presomite stages. *Development* 130, 2039-2050.
- Handel, E.M., Alwin, S., Cathomen, T., 2009. Expanding or restricting the target site repertoire of zinc-finger nucleases: the inter-domain linker as a major determinant of target site selectivity. *Mol Ther* 17, 104-111.
- Harada, T., Harada, C., Parada, L.F., 2007. Molecular regulation of visual system development: more than meets the eye. *Genes Dev* 21, 367-378.

- Haskell, G.T., LaMantia, A.S., 2005. Retinoic acid signaling identifies a distinct precursor population in the developing and adult forebrain. *J Neurosci* 25, 7636-7647.
- Hernandez, R.E., Putzke, A.P., Myers, J.P., Margaretha, L., Moens, C.B., 2007. Cyp26 enzymes generate the retinoic acid response pattern necessary for hindbrain development. *Development* 134, 177-187.
- Hockemeyer, D., Wang, H., Kiani, S., Lai, C.S., Gao, Q., Cassady, J.P., Cost, G.J., Zhang, L., Santiago, Y., Miller, J.C., Zeitler, B., Cherone, J.M., Meng, X., Hinkley, S.J., Rebar, E.J., Gregory, P.D., Urnov, F.D., Jaenisch, R., 2011. Genetic engineering of human pluripotent cells using TALE nucleases. *Nat Biotechnol* 29, 731-734.
- Holder, N., Hill, J., 1991. Retinoic acid modifies development of the midbrain-hindbrain border and affects cranial ganglion formation in zebrafish embryos. *Development* 113, 1159-1170.
- Hu, K.Q., Liu, C., Ernst, H., Krinsky, N.I., Russell, R.M., Wang, X.D., 2006. The biochemical characterization of ferret carotene-9',10'-monooxygenase catalyzing cleavage of carotenoids in vitro and in vivo. *J Biol Chem* 281, 19327-19338.
- Hu, M., Easter, S.S., 1999. Retinal neurogenesis: the formation of the initial central patch of postmitotic cells. *Dev Biol* 207, 309-321.
- Hu, P., Tian, M., Bao, J., Xing, G., Gu, X., Gao, X., Linney, E., Zhao, Q., 2008. Retinoid regulation of the zebrafish cyp26a1 promoter. *Dev Dyn* 237, 3798-3808.
- Huang, P., Xiao, A., Zhou, M., Zhu, Z., Lin, S., Zhang, B., 2011. Heritable gene targeting in zebrafish using customized TALENs. *Nat Biotechnol* 29, 699-700.
- Hung, R.J., Boffetta, P., Brennan, P., Malaveille, C., Hautefeuille, A., Donato, F., Gelatti, U., Spaliviero, M., Placidi, D., Carta, A., Scotto di Carlo, A., Porru, S., 2004. GST, NAT, SULT1A1, CYP1B1 genetic polymorphisms, interactions with environmental exposures and bladder cancer risk in a high-risk population. *Int J Cancer* 110, 598-604.
- Hutson, L.D., Jurynek, M.J., Yeo, S.Y., Okamoto, H., Chien, C.B., 2003. Two divergent slit1 genes in zebrafish. *Dev Dyn* 228, 358-369.
- Hwang, W.Y., Fu, Y., Reyon, D., Maeder, M.L., Tsai, S.Q., Sander, J.D., Peterson, R.T., Yeh, J.R., Joung, J.K., 2013. Efficient genome editing in zebrafish using a CRISPR-Cas system. *Nat Biotechnol* 31, 227-229.
- Hyatt, G.A., Schmitt, E.A., Fadool, J.M., Dowling, J.E., 1996a. Retinoic acid alters photoreceptor development in vivo. *Proc Natl Acad Sci U S A* 93, 13298-13303.
- Hyatt, G.A., Schmitt, E.A., Marsh-Armstrong, N., McCaffery, P., Drager, U.C., Dowling, J.E., 1996b. Retinoic acid establishes ventral retinal characteristics. *Development* 122, 195-204.
- Imdad, A., Yakoob, M.Y., Sudfeld, C., Haider, B.A., Black, R.E., Bhutta, Z.A., 2011. Impact of vitamin A supplementation on infant and childhood mortality. *BMC Public Health* 11 Suppl 3, S20.

- Isalan, M., Choo, Y., Klug, A., 1997. Synergy between adjacent zinc fingers in sequence-specific DNA recognition. *Proc Natl Acad Sci U S A* 94, 5617-5621.
- Ishibashi, S., Cliffe, R., Amaya, E., 2012. Highly efficient bi-allelic mutation rates using TALENs in *Xenopus tropicalis*. *Biol Open* 1, 1273-1276.
- Islam, M.M., Li, Y., Luo, H., Xiang, M., Cai, L., 2013. Meis1 regulates Foxn4 expression during retinal progenitor cell differentiation. *Biol Open* 2, 1125-1136.
- Jinek, M., Chylinski, K., Fonfara, I., Hauer, M., Doudna, J.A., Charpentier, E., 2012. A programmable dual-RNA-guided DNA endonuclease in adaptive bacterial immunity. *Science* 337, 816-821.
- Kannan, R., Sreekumar, P.G., Hinton, D.R., 2015. Alpha crystallins in the retinal pigment epithelium and implications for the pathogenesis and treatment of age-related macular degeneration. *Biochim Biophys Acta*.
- Karlsson, J., von Hofsten, J., Olsson, P.E., 2001. Generating transparent zebrafish: a refined method to improve detection of gene expression during embryonic development. *Mar Biotechnol (NY)* 3, 522-527.
- Kastner, P., Grondona, J.M., Mark, M., Gansmuller, A., LeMeur, M., Decimo, D., Vonesch, J.L., Dolle, P., Chambon, P., 1994. Genetic analysis of RXR alpha developmental function: convergence of RXR and RAR signaling pathways in heart and eye morphogenesis. *Cell* 78, 987-1003.
- Kaur, K., Mandal, A.K., Chakrabarti, S., 2011. Primary Congenital Glaucoma and the Involvement of CYP1B1. *Middle East Afr J Ophthalmol* 18, 7-16.
- Kawaguchi, R., Yu, J., Honda, J., Hu, J., Whitelegge, J., Ping, P., Wiita, P., Bok, D., Sun, H., 2007. A membrane receptor for retinol binding protein mediates cellular uptake of vitamin A. *Science* 315, 820-825.
- Kelley, M.W., Turner, J.K., Reh, T.A., 1994. Retinoic acid promotes differentiation of photoreceptors in vitro. *Development* 120, 2091-2102.
- Kelley, M.W., Turner, J.K., Reh, T.A., 1995. Regulation of proliferation and photoreceptor differentiation in fetal human retinal cell cultures. *Invest Ophthalmol Vis Sci* 36, 1280-1289.
- Kelley, M.W., Williams, R.C., Turner, J.K., Creech-Kraft, J.M., Reh, T.A., 1999. Retinoic acid promotes rod photoreceptor differentiation in rat retina in vivo. *Neuroreport* 10, 2389-2394.
- Kettleborough, R.N., Busch-Nentwich, E.M., Harvey, S.A., Dooley, C.M., de Bruijn, E., van Eeden, F., Sealy, I., White, R.J., Herd, C., Nijman, I.J., Fenyves, F., Mehroke, S., Scahill, C., Gibbons, R., Wali, N., Carruthers, S., Hall, A., Yen, J., Cuppen, E., Stemple, D.L., 2013. A systematic genome-wide analysis of zebrafish protein-coding gene function. *Nature* 496, 494-497.
- Khanna, H., Akimoto, M., Siffron-Fernandez, S., Friedman, J.S., Hicks, D., Swaroop, A., 2006. Retinoic acid regulates the expression of photoreceptor transcription factor NRL. *J Biol Chem* 281, 27327-27334.

- Kiefer, C., Hessel, S., Lampert, J.M., Vogt, K., Lederer, M.O., Breithaupt, D.E., von Lintig, J., 2001. Identification and characterization of a mammalian enzyme catalyzing the asymmetric oxidative cleavage of provitamin A. *J Biol Chem* 276, 14110-14116.
- Kim, C.A., Berg, J.M., 1996. A 2.2 Å resolution crystal structure of a designed zinc finger protein bound to DNA. *Nat Struct Biol* 3, 940-945.
- Kim, Y.G., Cha, J., Chandrasegaran, S., 1996. Hybrid restriction enzymes: zinc finger fusions to Fok I cleavage domain. *Proc Natl Acad Sci U S A* 93, 1156-1160.
- Kimmel, C.B., Ballard, W.W., Kimmel, S.R., Ullmann, B., Schilling, T.F., 1995. Stages of embryonic development of the zebrafish. *Dev Dyn* 203, 253-310.
- Koenekoop, R.K., Lopez, I., den Hollander, A.I., Allikmets, R., Cremers, F.P., 2007. Genetic testing for retinal dystrophies and dysfunctions: benefits, dilemmas and solutions. *Clin Experiment Ophthalmol* 35, 473-485.
- Koeppen, B.M., 2008. *Berne and Levy Physiology*, 6th Edition. Elsevier.
- Koshiba-Takeuchi, K., Takeuchi, J.K., Matsumoto, K., Momose, T., Uno, K., Hoepker, V., Ogura, K., Takahashi, N., Nakamura, H., Yasuda, K., Ogura, T., 2000. Tbx5 and the retinotectum projection. *Science* 287, 134-137.
- Kralova, J., Czerny, T., Spanielova, H., Ratajova, V., Kozmik, Z., 2002. Complex regulatory element within the gammaE- and gammaF-crystallin enhancers mediates Pax6 regulation and is required for induction by retinoic acid. *Gene* 286, 271-282.
- Kudoh, T., Wilson, S.W., Dawid, I.B., 2002. Distinct roles for Fgf, Wnt and retinoic acid in posteriorizing the neural ectoderm. *Development* 129, 4335-4346.
- Kumar, M., Agarwal, T., Kaur, P., Kumar, M., Khokhar, S., Dada, R., 2013. Molecular and structural analysis of genetic variations in congenital cataract. *Mol Vis* 19, 2436-2450.
- Kumar, S., Duester, G., 2010. Retinoic acid signaling in perioptic mesenchyme represses Wnt signaling via induction of Pitx2 and Dkk2. *Dev Biol* 340, 67-74.
- Lagnado, L., 1998. Retinal processing: amacrine cells keep it short and sweet. *Curr Biol* 8, R598-600.
- Lampert, J.M., Holzschuh, J., Hessel, S., Driever, W., Vogt, K., von Lintig, J., 2003. Provitamin A conversion to retinal via the beta,beta-carotene-15,15'-oxygenase (bcox) is essential for pattern formation and differentiation during zebrafish embryogenesis. *Development* 130, 2173-2186.
- Langenberg, T., Kahana, A., Wszalek, J.A., Halloran, M.C., 2008. The eye organizes neural crest cell migration. *Dev Dyn* 237, 1645-1652.
- Larison, K.D., Bremiller, R., 1990. Early onset of phenotype and cell patterning in the embryonic zebrafish retina. *Development* 109, 567-576.

- Le, H.G., Dowling, J.E., Cameron, D.J., 2012. Early retinoic acid deprivation in developing zebrafish results in microphthalmia. *Vis Neurosci* 29, 219-228.
- Lee, H.J., Kim, E., Kim, J.S., 2010. Targeted chromosomal deletions in human cells using zinc finger nucleases. *Genome Res* 20, 81-89.
- Lee, J., Gross, J.M., 2007. Laminin beta1 and gamma1 containing laminins are essential for basement membrane integrity in the zebrafish eye. *Invest Ophthalmol Vis Sci* 48, 2483-2490.
- Lei, Y., Guo, X., Liu, Y., Cao, Y., Deng, Y., Chen, X., Cheng, C.H., Dawid, I.B., Chen, Y., Zhao, H., 2012. Efficient targeted gene disruption in *Xenopus* embryos using engineered transcription activator-like effector nucleases (TALENs). *Proc Natl Acad Sci U S A* 109, 17484-17489.
- Lemke, G., Reber, M., 2005. Retinotectal mapping: new insights from molecular genetics. *Annu Rev Cell Dev Biol* 21, 551-580.
- Li, L., Piatek, M.J., Atef, A., Piatek, A., Wibowo, A., Fang, X., Sabir, J.S., Zhu, J.K., Mahfouz, M.M., 2012. Rapid and highly efficient construction of TALE-based transcriptional regulators and nucleases for genome modification. *Plant Mol Biol* 78, 407-416.
- Li, S., Mo, Z., Yang, X., Price, S.M., Shen, M.M., Xiang, M., 2004. Foxn4 controls the genesis of amacrine and horizontal cells by retinal progenitors. *Neuron* 43, 795-807.
- Li, T., Huang, S., Jiang, W.Z., Wright, D., Spalding, M.H., Weeks, D.P., Yang, B., 2011a. TAL nucleases (TALNs): hybrid proteins composed of TAL effectors and FokI DNA-cleavage domain. *Nucleic Acids Res* 39, 359-372.
- Li, T., Huang, S., Zhao, X., Wright, D.A., Carpenter, S., Spalding, M.H., Weeks, D.P., Yang, B., 2011b. Modularly assembled designer TAL effector nucleases for targeted gene knockout and gene replacement in eukaryotes. *Nucleic Acids Res* 39, 6315-6325.
- Li, Z., Joseph, N.M., Easter, S.S., Jr., 2000. The morphogenesis of the zebrafish eye, including a fate map of the optic vesicle. *Dev Dyn* 218, 175-188.
- Lieber, M.R., 2010. The mechanism of double-strand DNA break repair by the nonhomologous DNA end-joining pathway. *Annu Rev Biochem* 79, 181-211.
- Lindqvist, A., Andersson, S., 2002. Biochemical properties of purified recombinant human beta-carotene 15,15'-monooxygenase. *J Biol Chem* 277, 23942-23948.
- Liu, J., Li, C., Yu, Z., Huang, P., Wu, H., Wei, C., Zhu, N., Shen, Y., Chen, Y., Zhang, B., Deng, W.M., Jiao, R., 2012. Efficient and specific modifications of the *Drosophila* genome by means of an easy TALEN strategy. *J Genet Genomics* 39, 209-215.
- Livesey, F.J., Cepko, C.L., 2001. Vertebrate neural cell-fate determination: lessons from the retina. *Nat Rev Neurosci* 2, 109-118.
- Lloyd, A., Plaisier, C.L., Carroll, D., Drews, G.N., 2005. Targeted mutagenesis using zinc-finger nucleases in *Arabidopsis*. *Proc Natl Acad Sci U S A* 102, 2232-2237.

- Lobo, G.P., Isken, A., Hoff, S., Babino, D., von Lintig, J., 2012. BCDO2 acts as a carotenoid scavenger and gatekeeper for the mitochondrial apoptotic pathway. *Development* 139, 2966-2977.
- Lohnes, D., Mark, M., Mendelsohn, C., Dolle, P., Dierich, A., Gorry, P., Gansmuller, A., Chambon, P., 1994. Function of the retinoic acid receptors (RARs) during development (I). Craniofacial and skeletal abnormalities in RAR double mutants. *Development* 120, 2723-2748.
- Lombardo, A., Genovese, P., Beausejour, C.M., Colleoni, S., Lee, Y.L., Kim, K.A., Ando, D., Urnov, F.D., Galli, C., Gregory, P.D., Holmes, M.C., Naldini, L., 2007. Gene editing in human stem cells using zinc finger nucleases and integrase-defective lentiviral vector delivery. *Nat Biotechnol* 25, 1298-1306.
- Loudig, O., Maclean, G.A., Dore, N.L., Luu, L., Petkovich, M., 2005. Transcriptional co-operativity between distant retinoic acid response elements in regulation of Cyp26A1 inducibility. *Biochem J* 392, 241-248.
- Luo, D.G., Xue, T., Yau, K.W., 2008. How vision begins: an odyssey. *Proc Natl Acad Sci U S A* 105, 9855-9862.
- Lupo, G., Gestri, G., O'Brien, M., Denton, R.M., Chandraratna, R.A., Ley, S.V., Harris, W.A., Wilson, S.W., 2011. Retinoic acid receptor signaling regulates choroid fissure closure through independent mechanisms in the ventral optic cup and periocular mesenchyme. *Proc Natl Acad Sci U S A* 108, 8698-8703.
- Lupo, G., Liu, Y., Qiu, R., Chandraratna, R.A., Barsacchi, G., He, R.Q., Harris, W.A., 2005. Dorsoventral patterning of the *Xenopus* eye: a collaboration of Retinoid, Hedgehog and FGF receptor signaling. *Development* 132, 1737-1748.
- Ma, N., Liao, B., Zhang, H., Wang, L., Shan, Y., Xue, Y., Huang, K., Chen, S., Zhou, X., Chen, Y., Pei, D., Pan, G., 2013. Transcription activator-like effector nuclease (TALEN)-mediated gene correction in integration-free beta-thalassemia induced pluripotent stem cells. *J Biol Chem* 288, 34671-34679.
- Ma, S., Zhang, S., Wang, F., Liu, Y., Xu, H., Liu, C., Lin, Y., Zhao, P., Xia, Q., 2012. Highly efficient and specific genome editing in silkworm using custom TALENs. *PLoS One* 7, e45035.
- Maden, M., 2002. Retinoid signalling in the development of the central nervous system. *Nat Rev Neurosci* 3, 843-853.
- Maden, M., Blentic, A., Reijntjes, S., Seguin, S., Gale, E., Graham, A., 2007. Retinoic acid is required for specification of the ventral eye field and for Rathke's pouch in the avian embryo. *Int J Dev Biol* 51, 191-200.
- Maeder, M.L., Thibodeau-Beganny, S., Osiak, A., Wright, D.A., Anthony, R.M., Eichtinger, M., Jiang, T., Foley, J.E., Winfrey, R.J., Townsend, J.A., Unger-Wallace, E., Sander, J.D., Muller-Lerch, F., Fu, F., Pearlberg, J., Gobel, C., Dassie, J.P., Pruett-Miller, S.M., Porteus, M.H., Sgroi, D.C., Iafrate, A.J., Dobbs, D., McCray, P.B., Jr., Cathomen, T., Voytas, D.F., Joung, J.K., 2008. Rapid "open-source" engineering of customized zinc-

- finger nucleases for highly efficient gene modification. *Mol Cell* 31, 294-301.
- Mahfouz, M.M., Li, L., Shamimuzzaman, M., Wibowo, A., Fang, X., Zhu, J.K., 2011. De novo-engineered transcription activator-like effector (TALE) hybrid nuclease with novel DNA binding specificity creates double-strand breaks. *Proc Natl Acad Sci U S A* 108, 2623-2628.
- Mak, A.N., Bradley, P., Bogdanove, A.J., Stoddard, B.L., 2012. TAL effectors: function, structure, engineering and applications. *Curr Opin Struct Biol* 23, 93-99.
- Mani, M., Kandavelou, K., Dy, F.J., Durai, S., Chandrasegaran, S., 2005. Design, engineering, and characterization of zinc finger nucleases. *Biochem Biophys Res Commun* 335, 447-457.
- Marsh-Armstrong, N., McCaffery, P., Gilbert, W., Dowling, J.E., Drager, U.C., 1994. Retinoic acid is necessary for development of the ventral retina in zebrafish. *Proc Natl Acad Sci U S A* 91, 7286-7290.
- Mashimo, T., Kaneko, T., Sakuma, T., Kobayashi, J., Kunihiro, Y., Voigt, B., Yamamoto, T., Serikawa, T., 2013. Efficient gene targeting by TAL effector nucleases coinjected with exonucleases in zygotes. *Sci Rep* 3, 1253.
- Matt, N., Dupe, V., Garnier, J.M., Dennefeld, C., Chambon, P., Mark, M., Ghyselinck, N.B., 2005. Retinoic acid-dependent eye morphogenesis is orchestrated by neural crest cells. *Development* 132, 4789-4800.
- Matt, N., Ghyselinck, N.B., Pellerin, I., Dupe, V., 2008. Impairing retinoic acid signalling in the neural crest cells is sufficient to alter entire eye morphogenesis. *Dev Biol* 320, 140-148.
- Mayo-Wilson, E., Imdad, A., Herzer, K., Yakoob, M.Y., Bhutta, Z.A., 2011. Vitamin A supplements for preventing mortality, illness, and blindness in children aged under 5: systematic review and meta-analysis. *BMJ* 343, d5094.
- McCaffery, P., Wagner, E., O'Neil, J., Petkovich, M., Drager, U.C., 1999. Dorsal and ventral retinoic territories defined by retinoic acid synthesis, break-down and nuclear receptor expression. *Mech Dev* 85, 203-214.
- McMahon, C., Gestri, G., Wilson, S.W., Link, B.A., 2009. *Lmx1b* is essential for survival of periorbital mesenchymal cells and influences Fgf-mediated retinal patterning in zebrafish. *Dev Biol* 332, 287-298.
- Meeker, N.D., Hutchinson, S.A., Ho, L., Trede, N.S., 2007. Method for isolation of PCR-ready genomic DNA from zebrafish tissues. *Biotechniques* 43, 610, 612, 614.
- Mein, J.R., Dolnikowski, G.G., Ernst, H., Russell, R.M., Wang, X.D., 2011. Enzymatic formation of apo-carotenoids from the xanthophyll carotenoids lutein, zeaxanthin and beta-cryptoxanthin by ferret carotene-9',10'-monooxygenase. *Arch Biochem Biophys* 506, 109-121.
- Mendelsohn, C., Lohnes, D., Decimo, D., Lufkin, T., LeMeur, M., Chambon, P., Mark, M., 1994. Function of the retinoic acid receptors (RARs) during

- development (II). Multiple abnormalities at various stages of organogenesis in RAR double mutants. *Development* 120, 2749-2771.
- Meng, X., Noyes, M.B., Zhu, L.J., Lawson, N.D., Wolfe, S.A., 2008. Targeted gene inactivation in zebrafish using engineered zinc-finger nucleases. *Nat Biotechnol* 26, 695-701.
- Menoret, S., Fontaniere, S., Jantz, D., Tesson, L., Thinard, R., Remy, S., Usal, C., Ouisse, L.H., Fraichard, A., Anegon, I., 2013. Generation of Rag1-knockout immunodeficient rats and mice using engineered meganucleases. *FASEB J* 27, 703-711.
- Mercader, N., Selleri, L., Criado, L.M., Pallares, P., Parras, C., Cleary, M.L., Torres, M., 2009. Ectopic Meis1 expression in the mouse limb bud alters P-D patterning in a Pbx1-independent manner. *Int J Dev Biol* 53, 1483-1494.
- Meyer, A., Van de Peer, Y., 2005. From 2R to 3R: evidence for a fish-specific genome duplication (FSGD). *Bioessays* 27, 937-945.
- Mic, F.A., Molotkov, A., Molotkova, N., Duester, G., 2004. Raldh2 expression in optic vesicle generates a retinoic acid signal needed for invagination of retina during optic cup formation. *Dev Dyn* 231, 270-277.
- Miller, J.C., Holmes, M.C., Wang, J., Guschin, D.Y., Lee, Y.L., Rupniewski, I., Beausejour, C.M., Waite, A.J., Wang, N.S., Kim, K.A., Gregory, P.D., Pabo, C.O., Rebar, E.J., 2007. An improved zinc-finger nuclease architecture for highly specific genome editing. *Nat Biotechnol* 25, 778-785.
- Millott, N., Lynn, W.G., 1966. Ubiquity of melanin and the effect of phenylthiourea. *Nature* 209, 99-101.
- Mitchell, D.M., Stevens, C.B., Frey, R.A., Hunter, S.S., Ashino, R., Kawamura, S., Stenkamp, D.L., 2015. Retinoic Acid Signaling Regulates Differential Expression of the Tandemly-Duplicated Long Wavelength-Sensitive Cone Opsin Genes in Zebrafish. *PLoS Genet* 11, e1005483.
- Moehle, E.A., Rock, J.M., Lee, Y.L., Jouvenot, Y., DeKolver, R.C., Gregory, P.D., Urnov, F.D., Holmes, M.C., 2007. Targeted gene addition into a specified location in the human genome using designed zinc finger nucleases. *Proc Natl Acad Sci U S A* 104, 3055-3060.
- Molotkov, A., Molotkova, N., Duester, G., 2006. Retinoic acid guides eye morphogenetic movements via paracrine signaling but is unnecessary for retinal dorsoventral patterning. *Development* 133, 1901-1910.
- Moore, F.E., Reyon, D., Sander, J.D., Martinez, S.A., Blackburn, J.S., Khayter, C., Ramirez, C.L., Joung, J.K., Langenau, D.M., 2012. Improved somatic mutagenesis in zebrafish using transcription activator-like effector nucleases (TALENs). *PLoS One* 7, e37877.
- Moosajee, M., Gregory-Evans, K., Ellis, C.D., Seabra, M.C., Gregory-Evans, C.Y., 2008. Translational bypass of nonsense mutations in zebrafish *repl1*, *pax2.1* and *lamb1* highlights a viable therapeutic option for untreatable genetic eye disease. *Hum Mol Genet* 17, 3987-4000.

- Morcillo, J., Martinez-Morales, J.R., Trousse, F., Fermin, Y., Sowden, J.C., Bovolenta, P., 2006. Proper patterning of the optic fissure requires the sequential activity of BMP7 and SHH. *Development* 133, 3179-3190.
- Moreno, C., Hoffman, M., Stodola, T.J., Didier, D.N., Lazar, J., Geurts, A.M., North, P.E., Jacob, H.J., Greene, A.S., 2011. Creation and characterization of a renin knockout rat. *Hypertension* 57, 614-619.
- Morton, J., Davis, M.W., Jorgensen, E.M., Carroll, D., 2006. Induction and repair of zinc-finger nuclease-targeted double-strand breaks in *Caenorhabditis elegans* somatic cells. *Proc Natl Acad Sci U S A* 103, 16370-16375.
- Mory, A., Ruiz, F.X., Dagan, E., Yakovtseva, E.A., Kurolap, A., Pares, X., Farres, J., Gershoni-Baruch, R., 2014. A missense mutation in *ALDH1A3* causes isolated microphthalmia/anophthalmia in nine individuals from an inbred Muslim kindred. *Eur J Hum Genet* 22, 419-422.
- Mui, S.H., Hindges, R., O'Leary, D.D., Lemke, G., Bertuzzi, S., 2002. The homeodomain protein *Vax2* patterns the dorsoventral and nasotemporal axes of the eye. *Development* 129, 797-804.
- Mussolino, C., Morbitzer, R., Lutge, F., Dannemann, N., Lahaye, T., Cathomen, T., 2011. A novel TALE nuclease scaffold enables high genome editing activity in combination with low toxicity. *Nucleic Acids Res* 39, 9283-9293.
- Nathans, J., 1999. The evolution and physiology of human color vision: insights from molecular genetic studies of visual pigments. *Neuron* 24, 299-312.
- Nawrocki, L., BreMiller, R., Streisinger, G., Kaplan, M., 1985. Larval and adult visual pigments of the zebrafish, *Brachydanio rerio*. *Vision Res* 25, 1569-1576.
- Nelson, S.M., Park, L., Stenkamp, D.L., 2009. Retinal homeobox 1 is required for retinal neurogenesis and photoreceptor differentiation in embryonic zebrafish. *Dev Biol* 328, 24-39.
- Niederreither, K., Abu-Abed, S., Schuhbaur, B., Petkovich, M., Chambon, P., Dolle, P., 2002a. Genetic evidence that oxidative derivatives of retinoic acid are not involved in retinoid signaling during mouse development. *Nat Genet* 31, 84-88.
- Niederreither, K., Dolle, P., 2008. Retinoic acid in development: towards an integrated view. *Nat Rev Genet* 9, 541-553.
- Niederreither, K., Subbarayan, V., Dolle, P., Chambon, P., 1999. Embryonic retinoic acid synthesis is essential for early mouse post-implantation development. *Nat Genet* 21, 444-448.
- Niederreither, K., Vermot, J., Schuhbaur, B., Chambon, P., Dolle, P., 2000. Retinoic acid synthesis and hindbrain patterning in the mouse embryo. *Development* 127, 75-85.
- Niederreither, K., Vermot, J., Schuhbaur, B., Chambon, P., Dolle, P., 2002b. Embryonic retinoic acid synthesis is required for forelimb growth and anteroposterior patterning in the mouse. *Development* 129, 3563-3574.

- Novitch, B.G., Wichterle, H., Jessell, T.M., Sockanathan, S., 2003. A requirement for retinoic acid-mediated transcriptional activation in ventral neural patterning and motor neuron specification. *Neuron* 40, 81-95.
- Obata, H., Kaji, Y., Yamada, H., Kato, M., Tsuru, T., Yamashita, H., 1999. Expression of transforming growth factor-beta superfamily receptors in rat eyes. *Acta Ophthalmol Scand* 77, 151-156.
- Ochiai, H., Fujita, K., Suzuki, K., Nishikawa, M., Shibata, T., Sakamoto, N., Yamamoto, T., 2010. Targeted mutagenesis in the sea urchin embryo using zinc-finger nucleases. *Genes Cells* 15, 875-885.
- Online Mendelian Inheritance in Man, O., 2015. McKusick-Nathans Institute of Genetic Medicine, John Hopkins University, Baltimore, MD.
- Onwochei, B.C., Simon, J.W., Bateman, J.B., Couture, K.C., Mir, E., 2000. Ocular colobomata. *Surv Ophthalmol* 45, 175-194.
- Ozeki, H., Ogura, Y., Hirabayashi, Y., Shimada, S., 2000. Apoptosis is associated with formation and persistence of the embryonic fissure. *Curr Eye Res* 20, 367-372.
- Paik, J., During, A., Harrison, E.H., Mendelsohn, C.L., Lai, K., Blaner, W.S., 2001. Expression and characterization of a murine enzyme able to cleave beta-carotene. The formation of retinoids. *J Biol Chem* 276, 32160-32168.
- Pavletich, N.P., Pabo, C.O., 1991. Zinc finger-DNA recognition: crystal structure of a Zif268-DNA complex at 2.1 Å. *Science* 252, 809-817.
- Pennimpede, T., Cameron, D.A., MacLean, G.A., Li, H., Abu-Abed, S., Petkovich, M., 2010. The role of CYP26 enzymes in defining appropriate retinoic acid exposure during embryogenesis. *Birth Defects Res A Clin Mol Teratol* 88, 883-894.
- Perez, E.E., Wang, J., Miller, J.C., Jouvenot, Y., Kim, K.A., Liu, O., Wang, N., Lee, G., Bartsevich, V.V., Lee, Y.L., Guschin, D.Y., Rupniewski, I., Waite, A.J., Carpenito, C., Carroll, R.G., Orange, J.S., Urnov, F.D., Rebar, E.J., Ando, D., Gregory, P.D., Riley, J.L., Holmes, M.C., June, C.H., 2008. Establishment of HIV-1 resistance in CD4+ T cells by genome editing using zinc-finger nucleases. *Nat Biotechnol* 26, 808-816.
- Perrault, I., Rozet, J.M., Gerber, S., Ghazi, I., Leowski, C., Ducroq, D., Souied, E., Dufier, J.L., Munnich, A., Kaplan, J., 1999. Leber congenital amaurosis. *Mol Genet Metab* 68, 200-208.
- Perz-Edwards, A., Hardison, N.L., Linney, E., 2001. Retinoic acid-mediated gene expression in transgenic reporter zebrafish. *Dev Biol* 229, 89-101.
- Philip, S., Castro, L.F., da Fonseca, R.R., Reis-Henriques, M.A., Vasconcelos, V., Santos, M.M., Antunes, A., 2012. Adaptive evolution of the Retinoid X receptor in vertebrates. *Genomics* 99, 81-89.
- Pittlik, S., Domingues, S., Meyer, A., Begemann, G., 2008. Expression of zebrafish *aldh1a3* (*raldh3*) and absence of *aldh1a1* in teleosts. *Gene Expr Patterns* 8, 141-147.

- Plasilova, M., Stoilov, I., Sarfarazi, M., Kadasi, L., Ferakova, E., Ferak, V., 1999. Identification of a single ancestral CYP1B1 mutation in Slovak Gypsies (Roms) affected with primary congenital glaucoma. *J Med Genet* 36, 290-294.
- Porteus, M.H., 2006. Mammalian gene targeting with designed zinc finger nucleases. *Mol Ther* 13, 438-446.
- Porteus, M.H., Baltimore, D., 2003. Chimeric nucleases stimulate gene targeting in human cells. *Science* 300, 763.
- Porteus, M.H., Carroll, D., 2005. Gene targeting using zinc finger nucleases. *Nat Biotechnol* 23, 967-973.
- Prabhudesai, S.N., Cameron, D.A., Stenkamp, D.L., 2005. Targeted effects of retinoic acid signaling upon photoreceptor development in zebrafish. *Dev Biol* 287, 157-167.
- Prokudin, I., Simons, C., Grigg, J.R., Storen, R., Kumar, V., Phua, Z.Y., Smith, J., Flaherty, M., Davila, S., Jamieson, R.V., 2014. Exome sequencing in developmental eye disease leads to identification of causal variants in GJA8, CRYGC, PAX6 and CYP1B1. *Eur J Hum Genet* 22, 907-915.
- Pruett-Miller, S.M., Connelly, J.P., Maeder, M.L., Joung, J.K., Porteus, M.H., 2008. Comparison of zinc finger nucleases for use in gene targeting in mammalian cells. *Mol Ther* 16, 707-717.
- Quigley, H.A., Broman, A.T., 2006. The number of people with glaucoma worldwide in 2010 and 2020. *Br J Ophthalmol* 90, 262-267.
- Radecke, S., Radecke, F., Cathomen, T., Schwarz, K., 2010. Zinc-finger nuclease-induced gene repair with oligodeoxynucleotides: wanted and unwanted target locus modifications. *Mol Ther* 18, 743-753.
- Ran, F.A., Hsu, P.D., Lin, C.Y., Gootenberg, J.S., Konermann, S., Trevino, A.E., Scott, D.A., Inoue, A., Matoba, S., Zhang, Y., Zhang, F., 2013. Double nicking by RNA-guided CRISPR Cas9 for enhanced genome editing specificity. *Cell* 154, 1380-1389.
- Raymond, S.M., Jackson, I.J., 1995. The retinal pigmented epithelium is required for development and maintenance of the mouse neural retina. *Curr Biol* 5, 1286-1295.
- Redmond, T.M., Gentleman, S., Duncan, T., Yu, S., Wiggert, B., Gantt, E., Cunningham, F.X., Jr., 2001. Identification, expression, and substrate specificity of a mammalian beta-carotene 15,15'-dioxygenase. *J Biol Chem* 276, 6560-6565.
- Robinson, J., Schmitt, E.A., Harosi, F.I., Reece, R.J., Dowling, J.E., 1993. Zebrafish ultraviolet visual pigment: absorption spectrum, sequence, and localization. *Proc Natl Acad Sci U S A* 90, 6009-6012.
- Rochette-Egly, C., Germain, P., 2009. Dynamic and combinatorial control of gene expression by nuclear retinoic acid receptors (RARs). *Nucl Recept Signal* 7, e005.
- Rogers, M.B., 1997. Life-and-death decisions influenced by retinoids. *Curr Top Dev Biol* 35, 1-46.

- Roos, L., Fang, M., Dali, C., Jensen, H., Christoffersen, N., Wu, B., Zhang, J., Xu, R., Harris, P., Xu, X., Gronskov, K., Tumer, Z., 2014. A homozygous mutation in a consanguineous family consolidates the role of ALDH1A3 in autosomal recessive microphthalmia. *Clin Genet* 86, 276-281.
- Ross, S.A., McCaffery, P.J., Drager, U.C., De Luca, L.M., 2000. Retinoids in embryonal development. *Physiol Rev* 80, 1021-1054.
- Sajwan, S., Takasu, Y., Tamura, T., Uchino, K., Sezutsu, H., Zurovec, M., 2013. Efficient disruption of endogenous Bombyx gene by TAL effector nucleases. *Insect Biochem Mol Biol* 43, 17-23.
- Sakai, Y., Meno, C., Fujii, H., Nishino, J., Shiratori, H., Saijoh, Y., Rossant, J., Hamada, H., 2001. The retinoic acid-inactivating enzyme CYP26 is essential for establishing an uneven distribution of retinoic acid along the antero-posterior axis within the mouse embryo. *Genes Dev* 15, 213-225.
- Sakuma, T., Hosoi, S., Woltjen, K., Suzuki, K.I., Kashiwagi, K., Wada, H., Ochiai, H., Miyamoto, T., Kawai, N., Sasakura, Y., Matsuura, S., Okada, Y., Kawahara, A., Hayashi, S., Yamamoto, T., 2013. Efficient TALEN construction and evaluation methods for human cell and animal applications. *Genes Cells*.
- Salbreux, G., Barthel, L.K., Raymond, P.A., Lubensky, D.K., 2012. Coupling mechanical deformations and planar cell polarity to create regular patterns in the zebrafish retina. *PLoS Comput Biol* 8, e1002618.
- Sandell, L.L., Sanderson, B.W., Moiseyev, G., Johnson, T., Mushegian, A., Young, K., Rey, J.P., Ma, J.X., Staehling-Hampton, K., Trainor, P.A., 2007. RDH10 is essential for synthesis of embryonic retinoic acid and is required for limb, craniofacial, and organ development. *Genes Dev* 21, 1113-1124.
- Sander, J.D., Cade, L., Khayter, C., Reyon, D., Peterson, R.T., Joung, J.K., Yeh, J.R., 2011a. Targeted gene disruption in somatic zebrafish cells using engineered TALENs. *Nat Biotechnol* 29, 697-698.
- Sander, J.D., Dahlborg, E.J., Goodwin, M.J., Cade, L., Zhang, F., Cifuentes, D., Curtin, S.J., Blackburn, J.S., Thibodeau-Beganny, S., Qi, Y., Pierick, C.J., Hoffman, E., Maeder, M.L., Khayter, C., Reyon, D., Dobbs, D., Langenau, D.M., Stupar, R.M., Giraldez, A.J., Voytas, D.F., Peterson, R.T., Yeh, J.R., Joung, J.K., 2011b. Selection-free zinc-finger-nuclease engineering by context-dependent assembly (CoDA). *Nat Methods* 8, 67-69.
- Sander, J.D., Yeh, J.R., Peterson, R.T., Joung, J.K., 2011c. Engineering zinc finger nucleases for targeted mutagenesis of zebrafish. *Methods Cell Biol* 104, 51-58.
- Sanjana, N.E., Cong, L., Zhou, Y., Cunniff, M.M., Feng, G., Zhang, F., 2012. A transcription activator-like effector toolbox for genome engineering. *Nat Protoc* 7, 171-192.
- Schmitt, E.A., Dowling, J.E., 1994. Early eye morphogenesis in the zebrafish, *Brachydanio rerio*. *J Comp Neurol* 344, 532-542.

- Schmitt, E.A., Dowling, J.E., 1996. Comparison of topographical patterns of ganglion and photoreceptor cell differentiation in the retina of the zebrafish, *Danio rerio*. *J Comp Neurol* 371, 222-234.
- Schmitt, E.A., Dowling, J.E., 1999. Early retinal development in the zebrafish, *Danio rerio*: light and electron microscopic analyses. *J Comp Neurol* 404, 515-536.
- See, A.W., Clagett-Dame, M., 2009. The temporal requirement for vitamin A in the developing eye: mechanism of action in optic fissure closure and new roles for the vitamin in regulating cell proliferation and adhesion in the embryonic retina. *Dev Biol* 325, 94-105.
- See, A.W., Kaiser, M.E., White, J.C., Clagett-Dame, M., 2008. A nutritional model of late embryonic vitamin A deficiency produces defects in organogenesis at a high penetrance and reveals new roles for the vitamin in skeletal development. *Dev Biol* 316, 171-190.
- Sen, J., Harpavat, S., Peters, M.A., Cepko, C.L., 2005. Retinoic acid regulates the expression of dorsoventral topographic guidance molecules in the chick retina. *Development* 132, 5147-5159.
- Shimada, T., 2006. Xenobiotic-metabolizing enzymes involved in activation and detoxification of carcinogenic polycyclic aromatic hydrocarbons. *Drug Metab Pharmacokinet* 21, 257-276.
- Shimozono, S., Iimura, T., Kitaguchi, T., Higashijima, S., Miyawaki, A., 2013. Visualization of an endogenous retinoic acid gradient across embryonic development. *Nature* 496, 363-366.
- Shukla, V.K., Doyon, Y., Miller, J.C., DeKolver, R.C., Moehle, E.A., Worden, S.E., Mitchell, J.C., Arnold, N.L., Gopalan, S., Meng, X., Choi, V.M., Rock, J.M., Wu, Y.Y., Katibah, G.E., Zhifang, G., McCaskill, D., Simpson, M.A., Blakeslee, B., Greenwalt, S.A., Butler, H.J., Hinkley, S.J., Zhang, L., Rebar, E.J., Gregory, P.D., Urnov, F.D., 2009. Precise genome modification in the crop species *Zea mays* using zinc-finger nucleases. *Nature* 459, 437-441.
- Simoës-Costa, M.S., Azambuja, A.P., Xavier-Neto, J., 2008. The search for non-chordate retinoic acid signaling: lessons from chordates. *J Exp Zool B Mol Dev Evol* 310, 54-72.
- Sive, H.L., Draper, B.W., Harland, R.M., Weintraub, H., 1990. Identification of a retinoic acid-sensitive period during primary axis formation in *Xenopus laevis*. *Genes Dev* 4, 932-942.
- Skalicky, S.E., White, A.J., Grigg, J.R., Martin, F., Smith, J., Jones, M., Donaldson, C., Smith, J.E., Flaherty, M., Jamieson, R.V., 2013. Microphthalmia, anophthalmia, and coloboma and associated ocular and systemic features: understanding the spectrum. *JAMA Ophthalmol* 131, 1517-1524.
- Smith, G.R., Amundsen, S.K., Dabert, P., Taylor, A.F., 1995. The initiation and control of homologous recombination in *Escherichia coli*. *Philos Trans R Soc Lond B Biol Sci* 347, 13-20.

- Smolen, G.A., Schott, B.J., Stewart, R.A., Diederichs, S., Muir, B., Provencher, H.L., Look, A.T., Sgroi, D.C., Peterson, R.T., Haber, D.A., 2007. A Rap GTPase interactor, RADIL, mediates migration of neural crest precursors. *Genes Dev* 21, 2131-2136.
- Soderpalm, A.K., Fox, D.A., Karlsson, J.O., van Veen, T., 2000. Retinoic acid produces rod photoreceptor selective apoptosis in developing mammalian retina. *Invest Ophthalmol Vis Sci* 41, 937-947.
- Stenkamp, D.L., 2007. Neurogenesis in the fish retina. *Int Rev Cytol* 259, 173-224.
- Stenkamp, D.L., Adler, R., 1993. Photoreceptor differentiation of isolated retinal precursor cells includes the capacity for photomechanical responses. *Proc Natl Acad Sci U S A* 90, 1982-1986.
- Stenkamp, D.L., Frey, R.A., Mallory, D.E., Shupe, E.E., 2002. Embryonic retinal gene expression in sonic-you mutant zebrafish. *Dev Dyn* 225, 344-350.
- Stenkamp, D.L., Gregory, J.K., Adler, R., 1993. Retinoid effects in purified cultures of chick embryo retina neurons and photoreceptors. *Invest Ophthalmol Vis Sci* 34, 2425-2436.
- Stenkamp, D.L., Hisatomi, O., Barthel, L.K., Tokunaga, F., Raymond, P.A., 1996. Temporal expression of rod and cone opsins in embryonic goldfish retina predicts the spatial organization of the cone mosaic. *Invest Ophthalmol Vis Sci* 37, 363-376.
- Stevens, C.B., Cameron, D.A., Stenkamp, D.L., 2011. Plasticity of photoreceptor-generating retinal progenitors revealed by prolonged retinoic acid exposure. *BMC Dev Biol* 11, 51.
- Stoilov, I., Akarsu, A.N., Sarfarazi, M., 1997. Identification of three different truncating mutations in cytochrome P4501B1 (CYP1B1) as the principal cause of primary congenital glaucoma (Buphthalmos) in families linked to the GLC3A locus on chromosome 2p21. *Hum Mol Genet* 6, 641-647.
- Strate, I., Min, T.H., Iliev, D., Pera, E.M., 2009. Retinol dehydrogenase 10 is a feedback regulator of retinoic acid signalling during axis formation and patterning of the central nervous system. *Development* 136, 461-472.
- Strauss, O., 2005. The retinal pigment epithelium in visual function. *Physiol Rev* 85, 845-881.
- Stroud, D.A., Formosa, L.E., Wijeyeratne, X.W., Nguyen, T.N., Ryan, M.T., 2013. Gene knockout using transcription activator-like effector nucleases (TALENs) reveals that human NDUFA9 protein is essential for stabilizing the junction between membrane and matrix arms of complex I. *J Biol Chem* 288, 1685-1690.
- Sun, N., Liang, J., Abil, Z., Zhao, H., 2012. Optimized TAL effector nucleases (TALENs) for use in treatment of sickle cell disease. *Mol Biosyst* 8, 1255-1263.
- Sung, Y.H., Baek, I.J., Kim, D.H., Jeon, J., Lee, J., Lee, K., Jeong, D., Kim, J.S., Lee, H.W., 2013. Knockout mice created by TALEN-mediated gene targeting. *Nat Biotechnol* 31, 23-24.

- Swaroop, A., Kim, D., Forrest, D., 2010. Transcriptional regulation of photoreceptor development and homeostasis in the mammalian retina. *Nat Rev Neurosci* 11, 563-576.
- Szcepek, M., Brondani, V., Buchel, J., Serrano, L., Segal, D.J., Cathomen, T., 2007. Structure-based redesign of the dimerization interface reduces the toxicity of zinc-finger nucleases. *Nat Biotechnol* 25, 786-793.
- Szel, A., Lukats, A., Fekete, T., Szepessy, Z., Rohlich, P., 2000. Photoreceptor distribution in the retinas of subprimate mammals. *J Opt Soc Am A Opt Image Sci Vis* 17, 568-579.
- Takasu, Y., Kobayashi, I., Beumer, K., Uchino, K., Sezutsu, H., Sajwan, S., Carroll, D., Tamura, T., Zurovec, M., 2010. Targeted mutagenesis in the silkworm *Bombyx mori* using zinc finger nuclease mRNA injection. *Insect Biochem Mol Biol* 40, 759-765.
- Tanwar, M., Dada, T., Sihota, R., Dada, R., 2010. Mitochondrial DNA analysis in primary congenital glaucoma. *Mol Vis* 16, 518-533.
- Terrell, A.M., Anand, D., Smith, S.F., Dang, C.A., Waters, S.M., Pathania, M., Beebe, D.C., Lachke, S.A., 2015. Molecular characterization of mouse lens epithelial cell lines and their suitability to study RNA granules and cataract associated genes. *Exp Eye Res* 131, 42-55.
- Tesson, L., Usal, C., Menoret, S., Leung, E., Niles, B.J., Remy, S., Santiago, Y., Vincent, A.I., Meng, X., Zhang, L., Gregory, P.D., Anegon, I., Cost, G.J., 2011. Knockout rats generated by embryo microinjection of TALENs. *Nat Biotechnol* 29, 695-696.
- Thisse, C., Thisse, B., 2008. High-resolution in situ hybridization to whole-mount zebrafish embryos. *Nat Protoc* 3, 59-69.
- Tini, M., Otulakowski, G., Breitman, M.L., Tsui, L.C., Giguere, V., 1993. An everted repeat mediates retinoic acid induction of the gamma F-crystallin gene: evidence of a direct role for retinoids in lens development. *Genes Dev* 7, 295-307.
- Townsend, J.A., Wright, D.A., Winfrey, R.J., Fu, F., Maeder, M.L., Joung, J.K., Voytas, D.F., 2009. High-frequency modification of plant genes using engineered zinc-finger nucleases. *Nature* 459, 442-445.
- UNICEF, 2011. *The State of the World's Children, Children in the Urban World*.
- Urnov, F.D., Miller, J.C., Lee, Y.L., Beausejour, C.M., Rock, J.M., Augustus, S., Jamieson, A.C., Porteus, M.H., Gregory, P.D., Holmes, M.C., 2005. Highly efficient endogenous human gene correction using designed zinc-finger nucleases. *Nature* 435, 646-651.
- van den Bosch, M., Lohman, P.H., Pastink, A., 2002. DNA double-strand break repair by homologous recombination. *Biol Chem* 383, 873-892.
- Varga, Z.M., Wegner, J., Westerfield, M., 1999. Anterior movement of ventral diencephalic precursors separates the primordial eye field in the neural plate and requires cyclops. *Development* 126, 5533-5546.
- Vasiliou, V., Gonzalez, F.J., 2008. Role of CYP1B1 in glaucoma. *Annu Rev Pharmacol Toxicol* 48, 333-358.

- Verma, A.S., Fitzpatrick, D.R., 2007. Anophthalmia and microphthalmia. *Orphanet J Rare Dis* 2, 47.
- von Lintig, J., Vogt, K., 2000. Filling the gap in vitamin A research. Molecular identification of an enzyme cleaving beta-carotene to retinal. *J Biol Chem* 275, 11915-11920.
- Wang, H., Kesinger, J.W., Zhou, Q., Wren, J.D., Martin, G., Turner, S., Tang, Y., Frank, M.B., Centola, M., 2008. Identification and characterization of zebrafish ocular formation genes. *Genome* 51, 222-235.
- Warkany, J., 1944. Congenital malformations induced by vitamin A deficiency. *J Pediatr* 25, 476-480.
- Warkany, J., Schraffenberger, E., 1946. Congenital malformations induced in rats by maternal vitamin A deficiency; defects of the eye. *Arch Ophthalmol* 35, 150-169.
- Watanabe, T., Raff, M.C., 1992. Diffusible rod-promoting signals in the developing rat retina. *Development* 114, 899-906.
- Waxman, J.S., Yelon, D., 2007. Comparison of the expression patterns of newly identified zebrafish retinoic acid and retinoid X receptors. *Dev Dyn* 236, 587-595.
- Waxman, J.S., Yelon, D., 2011. Zebrafish retinoic acid receptors function as context-dependent transcriptional activators. *Dev Biol* 352, 128-140.
- Wefers, B., Meyer, M., Ortiz, O., Hrabe de Angelis, M., Hansen, J., Wurst, W., Kuhn, R., 2013. Direct production of mouse disease models by embryo microinjection of TALENs and oligodeoxynucleotides. *Proc Natl Acad Sci U S A* 110, 3782-3787.
- West, K.P., Jr., 2002. Extent of vitamin A deficiency among preschool children and women of reproductive age. *J Nutr* 132, 2857S-2866S.
- Westerfield, M., 2007. *The zebrafish book. A guide for the laboratory use of zebrafish (Danio rerio)*. 5 ed. University of Oregon Press, Eugene, OR.
- White, J.A., Guo, Y.D., Baetz, K., Beckett-Jones, B., Bonasoro, J., Hsu, K.E., Dilworth, F.J., Jones, G., Petkovich, M., 1996. Identification of the retinoic acid-inducible all-trans-retinoic acid 4-hydroxylase. *J Biol Chem* 271, 29922-29927.
- White, R.J., Schilling, T.F., 2008. How degrading: Cyp26s in hindbrain development. *Dev Dyn* 237, 2775-2790.
- White, T., Lu, T., Metlapally, R., Katowitz, J., Kherani, F., Wang, T.Y., Tran-Viet, K.N., Young, T.L., 2008. Identification of STRA6 and SKI sequence variants in patients with anophthalmia/microphthalmia. *Mol Vis* 14, 2458-2465.
- WHO, 1996. Indicators for assessing vitamin A deficiency and their application in monitoring and evaluating intervention programmes. . World Health Organization, Geneva.
- WHO, 2009. Global prevalence of vitamin A deficiency in populations at risk 1995 - 2005. WHO Global Database on Vitamin A Deficiency. World Health Organization, Geneva.

- Whyte, J.J., Prather, R.S., 2012. CELL BIOLOGY SYMPOSIUM: Zinc finger nucleases to create custom-designed modifications in the swine (*Sus scrofa*) genome. *J Anim Sci* 90, 1111-1117.
- Williams, A.L., Bohnsack, B.L., 2015. Neural crest derivatives in ocular development: discerning the eye of the storm. *Birth Defects Res C Embryo Today* 105, 87-95.
- Williamson, K.A., FitzPatrick, D.R., 2014. The genetic architecture of microphthalmia, anophthalmia and coloboma. *Eur J Med Genet* 57, 369-380.
- Wilson, J.G., Roth, C.B., Warkany, J., 1953. An analysis of the syndrome of malformations induced by maternal vitamin A deficiency. Effects of restoration of vitamin A at various times during gestation. *Am J Anat* 92, 189-217.
- Wong, G.K., Baudet, M.L., Norden, C., Leung, L., Harris, W.A., 2012. Slit1b-Robo3 signaling and N-cadherin regulate apical process retraction in developing retinal ganglion cells. *J Neurosci* 32, 223-228.
- Woo, K., Fraser, S.E., 1995. Order and coherence in the fate map of the zebrafish nervous system. *Development* 121, 2595-2609.
- Wood, A.J., Lo, T.W., Zeitler, B., Pickle, C.S., Ralston, E.J., Lee, A.H., Amora, R., Miller, J.C., Leung, E., Meng, X., Zhang, L., Rebar, E.J., Gregory, P.D., Urnov, F.D., Meyer, B.J., 2011. Targeted genome editing across species using ZFNs and TALENs. *Science* 333, 307.
- Wright, D.A., Townsend, J.A., Winfrey, R.J., Jr., Irwin, P.A., Rajagopal, J., Lonosky, P.M., Hall, B.D., Jondle, M.D., Voytas, D.F., 2005. High-frequency homologous recombination in plants mediated by zinc-finger nucleases. *Plant J* 44, 693-705.
- Yahyavi, M., Abouzeid, H., Gawdat, G., de Preux, A.S., Xiao, T., Bardakjian, T., Schneider, A., Choi, A., Jorgenson, E., Baier, H., El Sada, M., Schorderet, D.F., Slavotinek, A.M., 2013. ALDH1A3 loss of function causes bilateral anophthalmia/microphthalmia and hypoplasia of the optic nerve and optic chiasm. *Hum Mol Genet* 22, 3250-3258.
- Yang, D., Yang, H., Li, W., Zhao, B., Ouyang, Z., Liu, Z., Zhao, Y., Fan, N., Song, J., Tian, J., Li, F., Zhang, J., Chang, L., Pei, D., Chen, Y.E., Lai, L., 2011. Generation of PPARgamma mono-allelic knockout pigs via zinc-finger nucleases and nuclear transfer cloning. *Cell Res* 21, 979-982.
- Yashiro, K., Zhao, X., Uehara, M., Yamashita, K., Nishijima, M., Nishino, J., Saijoh, Y., Sakai, Y., Hamada, H., 2004. Regulation of retinoic acid distribution is required for proximodistal patterning and outgrowth of the developing mouse limb. *Dev Cell* 6, 411-422.
- Yasuhara, R., Yuasa, T., Williams, J.A., Byers, S.W., Shah, S., Pacifici, M., Iwamoto, M., Enomoto-Iwamoto, M., 2010. Wnt/beta-catenin and retinoic acid receptor signaling pathways interact to regulate chondrocyte function and matrix turnover. *J Biol Chem* 285, 317-327.
- Zakeri, Z.F., Ahuja, H.S., 1997. Cell death/apoptosis: normal, chemically induced, and teratogenic effect. *Mutat Res* 396, 149-161.

- Zhang, F., Maeder, M.L., Unger-Wallace, E., Hoshaw, J.P., Reyon, D., Christian, M., Li, X., Pierick, C.J., Dobbs, D., Peterson, T., Joung, J.K., Voytas, D.F., 2010. High frequency targeted mutagenesis in *Arabidopsis thaliana* using zinc finger nucleases. *Proc Natl Acad Sci U S A* 107, 12028-12033.
- Zhang, L., Jia, R., Palange, N.J., Satheka, A.C., Togo, J., An, Y., Humphrey, M., Ban, L., Ji, Y., Jin, H., Feng, X., Zheng, Y., 2015. Large genomic fragment deletions and insertions in mouse using CRISPR/Cas9. *PLoS One* 10, e0120396.
- Zhang, X.M., Yang, X.J., 2001. Regulation of retinal ganglion cell production by Sonic hedgehog. *Development* 128, 943-957.
- Zhang, Y., Zhang, F., Li, X., Baller, J.A., Qi, Y., Starker, C.G., Bogdanove, A.J., Voytas, D.F., 2013. Transcription activator-like effector nucleases enable efficient plant genome engineering. *Plant Physiol* 161, 20-27.
- Zhou, C.J., Molotkov, A., Song, L., Li, Y., Pleasure, D.E., Pleasure, S.J., Wang, Y.Z., 2008. Ocular coloboma and dorsoventral neuroretinal patterning defects in *Lrp6* mutant eyes. *Dev Dyn* 237, 3681-3689.
- Zou, J., Sweeney, C.L., Chou, B.K., Choi, U., Pan, J., Wang, H., Doney, S.N., Cheng, L., Malech, H.L., 2011. Oxidase-deficient neutrophils from X-linked chronic granulomatous disease iPS cells: functional correction by zinc finger nuclease-mediated safe harbor targeting. *Blood* 117, 5561-5572.

Appendix 1: Identification of RA-responsive genes in the zebrafish eye

A1.1 Introduction

Proper eye development requires precise coordination of morphological movements and spatial and temporal expression of genes. Many genes and signalling pathways have been associated in several different processes in eye development. Numerous reports, including findings within this study, have found that RA is essential in regulating several processes within eye development, including choroid fissure closure, maintenance of eye size and retinal neurogenesis (Hyatt et al., 1996a; Hyatt et al., 1996b; Kelley et al., 1994; Kelley et al., 1999; Khanna et al., 2006; Matt et al., 2005; Matt et al., 2008; Mitchell et al., 2015; Molotkov et al., 2006; Prabhudesai et al., 2005; Sen et al., 2005; Stenkamp and Adler, 1993; Stevens et al., 2011; Williams and Bohnsack, 2015). Previous microarray analysis revealed that high levels of RA significantly alter the expression of transcription factors and components of signalling pathways in dissected eyes of 75 hpf zebrafish embryos (Mitchell et al., 2015). In our previous study, we observed that reduction of the ventrally expressed RA synthesis gene, *aldh1a3*, reduces RA signalling in both dorsal and ventral domains of the eye. Regulatory mechanisms for ocular processes have been investigated but are yet to be fully elucidated. We performed an RNA-sequencing (RNA-seq) analysis of mRNA transcripts expressed in dissected heads of *aldh1a3^{-/-}; cyp1b1^{-/-}* zebrafish embryos. Our original goal was to identify a gene (or a suite of genes) that regulate(s) RA signalling in the dorsal retina in 48 hpf zebrafish embryos. Interestingly, however, this preliminary RNA-seq analysis revealed that lens development, neural crest migration and neuron differentiation and migration are affected by depleted levels of RA through the loss of *aldh1a3* and *cyp1b1*.

A1.2 Results and Discussion

We wanted to identify eye-specific genes that are regulated by a RA levels in zebrafish. Preliminary RNA-seq analysis of dissected heads of *aldh1a3^{-/-}; cyp1b1^{-/-}* mutants in comparison to wild type embryos identified a

list of 934 differentially expressed sequences: 60.5% were known sequences and 39.5% were unknown, potentially novel sequences. Analysis of the genes was performed using gene ontology clustering software DAVID. A summary of this analysis, listing biological and molecular processes of interest, found changes in genes that regulate lens development neural crest migration and neuron morphogenesis (Figure A1.1). Other broader categories overrepresented in the differentially expressed list included metabolic processes and ion channel activity. Notably metal ion homeostasis was also affected within RA-depleted embryos; this could be attributed to the loss of *cyp1b1* as CYP enzymes play an important role in detoxification (Hung et al., 2004; Shimada, 2006).

Twenty-two genes differentially expressed in RA-depleted embryos encode for crystallins. All crystallins were downregulated in *aldh1a3*^{-/-}; *cyp1b1*^{-/-} mutants (Table A1.2). Crystallins are the predominant structural proteins in the lens that are required for the transparency of the structure. In addition to lens structure, previous research has found that the family of α -crystallins protect photoreceptors and the cells that compose the RPE from oxidative stress injury (Kannan et al., 2015). Previously, lens crystallins, though not the specific crystallin genes detected in this analysis, were identified as RA signalling targets (Kralova et al., 2002).

Loss of *aldh1a3* and *cyp1b1* caused differential expression of genes implicated with neural projections, *slit1b* and roundabout homolog 3 (*robo3*). *slit1b* is upregulated in our assay whereas its receptor *robo3* was downregulated (Table A1.2). Slit1b-Robo3 signalling is required for retinal ganglion cells to detach from the neuroepithelium. (Hutson et al., 2003; Wong et al., 2012). This finding suggests that RA may play a role in the innervation of RGC axons to the brain as neuroepithelial detachment is crucial for RGC neurogenesis and neuronal migration (Wong et al., 2012).

Analysis of RNA-seq data indicated the downregulation of only one gene involved in photoreceptor function, *rho* (Table A1.2). Interestingly,

encephalopsin, an extraocular opsin that is localized in the brain and implicated in central nervous system photosensitivity (Blackshaw and Snyder, 1999), was also downregulated as a result of RA depletion. These findings suggest that *Aldh1a3* and/or *Cyp1b1* enzymes could affect the synthesis of 11-*cis* retinal or the expression of opsins.

activin receptor 2a (acvr2a) and *rap GTPase interactor (radil)* are differentially expressed in *aldh1a3^{-/-}; cyp1b1^{-/-}* mutants. *radil* is a regulator of neural crest migration during vertebrate embryogenesis (Table A1.2)(Smolen et al., 2007). *acvr2a* is expressed in cranial neural crest cells, and later in the cornea, the lens and the inner segments of photoreceptors (Obata et al., 1999). Depletion of *acvr2a* causes absent or aberrant migration of neural crest cell streams. Interestingly, *dkk2* is downregulated in *aldh1a3^{-/-}; cyp1b1^{-/-}* mutants. *dkk2* is an antagonist of canonical Wnt signalling. Previous studies revealed that *dkk2* is an essential downstream target of *Pitx2* in neural crest during eye development. *Dkk2*-deficient mice have development defects within the mesenchyme, cornea and ocular blood vessels. Further, RA and Wnt signalling are speculated to act combinatorially or synergistically to regulate *Pitx2* expression in mouse (Gage et al., 2008). Although it is unknown if *radil* and *acvr2a* are expressed in POM, these findings suggest previous research that RA has a role in the migration of a subpopulation of neural crest cells (POM).

This preliminary analysis established suspected roles of RA in ocular development as well as shedding light on new processes. As this RNA-sequencing has only been performed once, we endeavour to repeat this analysis. Future work would be to validate the genes found within this analysis using quantitative PCR. Further, it would be of interest to look at differential gene expression in embryos depleted of *aldh1a3*, *cyp1b1* and *aldh1a2* and at different time points. By 48 hpf, eye morphogenesis is near completion and retinal neurogenesis has just initiated. As eye development is dynamic over a relatively long period of time, analysis of differential gene

expression at earlier or later time points would provide insight into genes and pathways required for proper eye development. An earlier time point would elucidate processes involved in early eye morphogenesis, including dorsoventral patterning, and maintenance of eye size whereas later time points elucidate genes and pathways required for retinal cell fate decisions and retinal neurogenesis.

Table A1.1: RNA-seq analysis of gene expression in zebrafish embryo heads at 48hpf. Comparison was performed between wild type embryos and *aldh1a3^{-/-}*; *cyp1b1^{-/-}* embryos. Gene ontology (GO analysis) with selected GO categories shown.

Term	Number of genes within cluster	P-value
Beta and gamma crystallin	22	1.4E-19
Neuron projection morphogenesis	5	4.7E-2
Neural crest cell migration	3	9.1E-2
Pattern specification	10	6.1E-2

Table A1.2: Differential expression of eye, photoreceptor and extraocular tissues genes in dissected heads of *aldh1a3*^{-/-}; *cyp11b1*^{-/-} zebrafish embryos at 48 hpf.

Gene	Log2 fold change	Function/expression in developing eye (if known)	References
<i>acvr2a</i>	2.26905	Neural crest migration	(Obata et al., 1999)
<i>cryba1b</i>	-2.63385	Lens development	(Wang et al., 2008)
<i>cryba4</i>	-2.55457	Lens development	(Kumar et al., 2013)
<i>crybb1</i>	-3.0559	Lens development	(Terrell et al., 2015)
<i>crygm2</i> d3	-3.21055	Lens development	(Wang et al., 2008)
<i>dkk2</i>	2.58456	Neural crest migration	(Gage et al., 2008)
<i>opn3</i>	-3.06221	Unknown	(Blackshaw and Snyder, 1999)
<i>radil</i>	-2.05339	Neural crest migration	(Smolen et al., 2007)
<i>rho</i>	-2.32017	Rod opsin	
<i>robo3</i>	-3.07798	Retinal ganglion cell development	(Wong et al., 2012)
<i>slit1b</i>	2.62946	Retinal ganglion cell development	(Wong et al., 2012)